Factors Involved in the Pathogenesis of Human Uveal Melanoma

Kenneth Lai

Discipline of Clinical Ophthalmology and Eye Health

Save Sight Institute

University of Sydney

A Thesis Submitted for the Degree of

Master of Science in Medicine

January 2008

Declaration

I hereby certify this thesis does not contain, without appropriate acknowledgement, any material previously submitted for a degree or diploma in any university. I also certify that this thesis does not contain, to the best of my knowledge, any material previously published or written by another person, except where due reference is made.

Kenneth Lai

Abstract

Background

Uveal melanoma is the most common primary ocular cancer in adults and ~50% of patients will develop metastatic disease within 10 years of diagnosis. Growth and development of uveal melanoma involves both cellular and environmental factors. Cellular factors including metalloproteinases and their inhibitors (MMPs and TIMPs) and CD146, an immunoglobulin superfamily protein, have been suggested to be involved in melanoma growth and invasion. Epidemiological studies have implicated long-term UV exposure as a risk factor for developing uveal melanoma. The role(s) of these factors in the pathogenesis of uveal melanoma were more comprehensively investigated in this thesis.

Methods

The expression and distribution of MMP-9, TIMP-3 and CD146 were examined in paraffin sections of primary uveal melanomas (n=23; 5/23 spindle; 18/23 mixed and epithelioid) and normal eyes (n=3) using immunohistochemistry. The intensity of immunostaining was graded semi-quantitatively (grade 0 to 3) by 2 independent observers. For the *in vitro* studies melanoma cell lines (7 uveal and 3 metastasis-derived) were assessed for CD146 mRNA and protein expression using RT-PCR and immunoblotting respectively.

To assess for the effects of *UV-B* on cell growth and survival, cultures of primary uveal melanocytes (P1-P3) and melanoma cell lines (OCM-1 and OCM-8) were used. Cells were exposed to 0-30 mJ/cm^2 *UV-B*, and cell morphology and growth were examined; cell viability was assessed using an MTT assay. Gelatin zymography was used to assess enzymatic activity for MMPs in conditioned media following *UV-B* treatment.

Results

Moderate to strong ($\geq$ Grade2) cytoplasmic MMP-9 immunolabelling was observed in 74% tumours, with $\geq$ Grade 2 TIMP-3 immunolabelling found in ~50% of tumours. Heterogeneous MMP-9 immunolabelling was observed in tumour vasculature, and intravascular leukocytes also expressed MMP-9. Groups of tumour cells with intense

TIMP-3 immunostaining were seen surrounding tumour vessels in 5/23 tumours, although the vasculature did not express TIMP-3.

Heterogeneous cell membrane and cytoplasmic CD146 expression was observed, with ≥ Grade 2 immunostaining seen in ~70% of tumours. In primary mixed and epithelioid tumour specimens, CD146 immunoreactivity was significantly greater than in spindle cell tumours. The vasculature in tumours, and in the retina and choroid of all melanoma and normal eyes showed intense CD146 immunostaining. All cell lines and uveal melanocytes expressed CD146 mRNA and protein (~130kDa) but levels of protein varied among different cell lines.

UV-B ≥20 mJ/cm^2 was cytotoxic for uveal melanocytes. Cytotoxic doses of 5 to 10 mJ/cm^2 were found for OCM-8 and OCM-1 melanoma cell lines respectively. Low levels of *UV-B* (2.5 and 3.5 mJ/cm^2) significantly reduced melanoma cell viability after 48 hrs, although melanocyte viability was not affected for doses of *UV-B* <10 mJ/cm^2. Conditioned media from melanoma cells and melanocytes displayed pro-MMP-2 activity, independent of *UV-B*. Control and *UV-B* treated OCM-1 cells secreted active MMP-2 up to 72 hrs. Pro-MMP-9 was seen from 36 hrs for control and *UV-B* treated OCM-1 and OCM-8 cells.

Conclusions

The distinct immunostaining patterns observed within uveal melanoma for MMP-9 and TIMP-3 are consistent with their involvement in tumour growth and angiogenesis. In particular, the heterogeneous expression within regions of the tumours, and the localized expression in vasculature emphasises the importance of the tumour microenvironment in the pathogenesis of uveal melanoma.

The present study indicates that while CD146 is important for uveal melanoma growth, its expression may not be essential for invasion and metastasis, consistent with findings in other tumours, including cutaneous melanoma. Interactions between CD146-positive melanoma cells and vasculature, *via* an as yet unidentified ligand, may be important for the haematogenous spread of tumour cells during metastases and requires further investigation.

Decreased survival of uveal melanoma cells, but not melanocytes, following low doses of *UV-B* exposure suggests differences in cellular responses to DNA damage that may be

important in subsequent transformation of melanocytes to melanoma cells. *UV-B* did not induce the production and/or activation of MMP-2 and -9 in melanocytes or melanoma cells, although whether other proteinases may be regulated by *UV-B* in these cells remains to be determined. These observations suggest that the expression of DNA damage response genes such as *p53*, *p21* and *GADD45*, can be regulated following *UV-R* exposure, and may be important for uveal melanoma development, particularly associated with long-term exposure to *UV-B*.

Abbreviations

DMEM - Dulbecco's modified Eagle's medium

cDNA - complementary deoxyribonucleic acid

ECM - extracellular matrix

EDTA - ethylenediamine tetra-acetic acid

FBS - foetal bovine serum

FGF - fibroblast growth factor

GCL - ganglion cell layer

GFAP - glial fibrillary acidic protein

H&E – haemotoxylin and eosin

HUVECs - human umbilical vein endothelial cells

hr - hour

Ig - immunoglobulin

INL - inner nuclear layer

IPL - inner plexiform layer

ITS+3 – insulin, transferrin and selenium

kDa - kilo Dalton

MGM – melanocyte growth medium

mins - minutes

MMP - matrix metalloproteinase

MT – membrane type

MTT - 3-(4,5-dimethylthiazol-2-yl)-2,5-diphenyltetrazolium bromide

MW - molecular weight

NDS - normal donkey serum

NHM – normal human melanocytes

NSS - normal sheep serum

NGS - normal goat serum

NFL - nerve fibre layer

ONL - outer nuclear layer

OPL - outer plexiform layer

PAS - Periodic Acid Schiff

PBS - phosphate buffered saline

PCR- Polymerase Chain Reaction

PR - photoreceptor layer

RGC - retinal ganglion cell

RPE - retinal pigmented epithelium

RPMI - Roswell Park Memorial Institute medium

RT - room temperature

RT-PCR - Reverse Transcription-PCR

SFM - serum free medium

TGF – transforming growth factor

TIMP - tissue inhibitors of metalloproteinase

TTT - transpupillary thermotherapy

UV - ultraviolet

VEGF- vascular endothelial growth factor

Publications & Conference Presentations

Published Papers

Lai K, Conway RM, Crouch R, Madigan MC Expression and Distribution of MMPs and TIMPs in Human Uveal Melanoma. *Exp Eye Res.* 2008 Mar 16 PMID: 18423620.

Lai K, Sharma V, Jager M J, Conway RM, Madigan MC. Expression and Distribution of MUC18 in Human Uveal Melanoma. *Virchows Arch.* 2007 451(5):967-76.

Lai K, Di Girolamo N, Conway RM, Jager MJ, Madigan MC. The Effect of Ultraviolet Radiation on Choroidal Melanocytes and Melanoma Cell Lines: Cell Survival and Matrix Metalloproteinase Production. *Graefes Arch Clin Exp Ophthalmol.* 2007 245(5):715-24.

Published Abstracts

Conway RM, Sharma V, **Lai K**, Jager MJ, Madigan MC (2006) MUC18 (CD146/MelCAM/MCAM) expression in human uveal melanoma. *Invest. Ophthalmol. Vis. Sci.* 2006 47: E-Abstract 2224.

Madigan MC, Sharma V, **Lai K**, Jager MJ, Conway RM. (2006) Expression of MUC18(CD146) in Human Choroidal Melanomas. *Eur J Cancer* Suppl. 4: 31-32 P12.

Madigan MC, **Lai K**, Jager MJ, Crouch R, Conway RM (2004) Expression of MMPs and EMMPRIN in human uveal melanoma. *Exp Eye Res* 79 (Suppl): 124

Lai K, Di Girolamo N, Jager MJ, Conway RM & Madigan MC (2004) Effect of UV-B irradiation on MMP expression in uveal melanoma. *Exp Eye Res* 79 (Suppl): 125.

Madigan MC, **Lai K**, Collier SA, Billson FA, Crouch R, Provis JM, Conway RM (2002). A Role for Matrix Metalloproteinases in Uveal Melanoma? *Differentiation* 70: 377.

Madigan MC, **Lai K**, Crouch R, Billson FA, Madigan MC (2002). Retinal Detachment (RD) Secondary to Choroidal Melanoma: A Role for MMP-2? *Ophthalmic Res* 34 (Suppl 1): 133.

Madigan MC, **Lai K**, Crouch R, Billson FA, Madigan MC (2002). Matrix Metalloproteinases (MMPs) in Uveal Melanoma. *Exp Eye Res 72* (Suppl 2): 23.

Conference Presentations

Lai K, Conway RM, Crouch R, Madigan MC (2007). MMP-9 Immunoreactivity in Normal & Uveal Melanoma-Associated Retinae. *12th Australasian Ophthalmic and Visual Science Meeting, Canberra.*

Lai K, Sharma V, Conway RM, Jager MJ, Madigan MC (2006). Distribution and Expression of MUC18 in Human Uveal Melanoma? *11th Australasian Ophthalmic and Visual Science Meeting, Canberra.*

Lai K, Di Girolamo N, Conway RM, Jager MJ, Madigan MC. (2005). Effects of UV-B Radiation on Choroidal Melanocytes and Melanoma Cell Lines: Cell Survival and Matrix Metalloproteinase Production. *10th Australasian Ophthalmic and Visual Science Meeting, Sydney.*

Madigan MC, **Lai K**, Jager MJ, Conway RM (2004) Expression of MMPs and EMMPRIN in human uveal melanoma. *10th International Congress, Metastasis Research Society, Genoa, Italy.*

Lai K, Conway RM, Crouch R, Billson FA, Madigan MC (2002). A Role for MMPs and TIMPs in Uveal Melanoma? *9th Australasian Ophthalmic and Visual Science Meeting, Sydney.*

Acknowledgements

I would like to thank my supervisor Dr. Michele Madigan, for allowing me the opportunity to undertake this Masters degree. I would also like to thank her for her excellent advice, expertise, encouragement and patience throughout this project.

I would like to thank Dr. R Max Conway and Dr. Nick Girolamo for being my co-supervisors; without their expertise and support this project would not be possible.

I thank Dr. Roger Crouch from SEALS Anatomical Pathology (Prince of Wales Hospital) for providing access to a huge collection of primary uveal melanoma specimens.

I am forever grateful to Dr. Li Wen for her continuous support, advice and encouragement throughout this project, and I want to thank her for her friendship.

I would like to thank Drs. Martine Jager and Mary Hendrix for providing uveal melanoma cell lines for the studies in this thesis. I am also grateful to Dr Jager for her many constructive suggestions that contributed to all my publications.

I thank past and present staff of the Save Sight Institute for the enjoyable experience.

Finally I would like to thank my family and friends, who have always supported every decision I have ever made. This thesis would not have been possible without their support, encouragement and patience – thank you.

List of Figures

List of Tables

Table of Contents

Chapter 1

Introduction

1.1.1 Uveal Melanoma: Introduction

Uveal melanoma, the most common primary eye tumour in adults, is derived from the melanocytes of the uveal tract, consisting of the iris (3%), ciliary body (5-10%) and choroid (~90%). The choroid is the largest part of the uvea and the most common site for uveal melanoma (Jager, et al., 2004). Uveal melanoma is characterized by an unpredictable clinical course (Woll, et al., 1999), it is often undetectable for months to years prior to the occurrence of visual symptoms such as a visual field defect or decreased vision related to retinal detachment (Kanski, 1994).

1.1.2 Uveal Melanoma: Epidemiology

The mean incidence of uveal melanoma is 7-8 per million per year [USA- (Seddon, et al., 1994); Australia- (Vajdic, et al., 2003)]. Uveal melanoma is usually diagnosed between 50 to 75 years of age (Jager, et al., 2004), it is relatively rare in black population, and with a slight male-predominance in the non-Hispanic white population (Hu, et al., 2005). Approximately 10-40% of patients diagnosed with uveal melanoma will develop metastatic disease within 10 years after treatment of the primary tumour (Woll, et al., 1999). Metastasis is most likely to occur hematogeneously via the choroid, allowing uveal melanoma to develop distant metastases, particulary to the liver (60.5%) and lung (24.4%); (Jager, et al., 2004; Rietschel, et al., 2005; Woll, et al., 1999). Development of metastatic disease is associated with a mean survival of 2 months for untreated patients and approximately 5 months for those who receive treatment after diagnosis (Gragoudas, et al., 1991).

1.1.3 Uveal Melanoma: Clinical Features

Iris melanomas are easily visible and tend to be detected at an early age. They are usually smaller in size than ciliary body and choroidal melanomas. Iris melanomas have variable pigmentation but they are usually pale in colour (Fig 1.1.1). Iris melanomas may adopt a nodular or superficial spreading growth pattern and can be circumscribed or diffuse. Malignant iris melanomas often contain prominent and abnormal blood vessels visible clinically (Fig 1.1.1) (Hungerford, 1995).

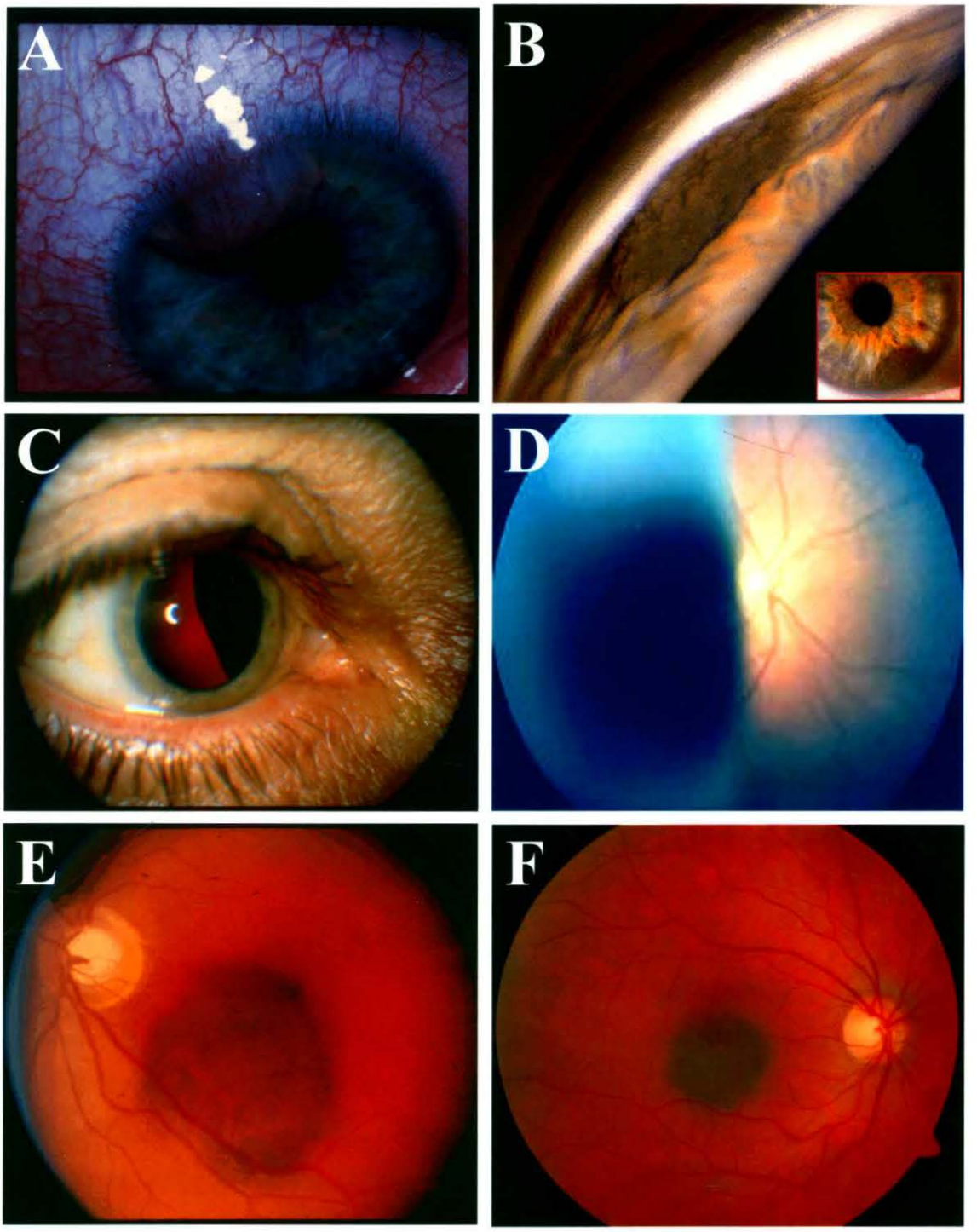

Figure 1.1.1
Clinical features of uveal melanoma.
A. Iris melanoma with prominent blood vessels.[1]
B. Iris melanoma viewed by gonioscopy lens and slit-lamp.[2]
C. Ciliary melanoma in a patient's eye.[3]
D. Fundus image of a large ciliary body melanoma.[4]
E. Fundus image of a large choroidal melanoma with retinal detachment.[1]
F. Fundus image of choroidal naevi.[3]

[1]Image from The David G.Cogan Ophthalmic Pathology Collection (http://cogancollection.nei.nih.gov)
[2]Image from Wake Forest University Baptist Medical centre (www1.wfubmc.edu/eye)
[3]Image from The Liverpool Ocular Oncology Centre (www.eyetumour.com)
[4]Image from Enrique Garcia-Valenzuela *et al* (www.emedicine.com)

Ciliary body melanomas are the most diffcult to detect in the early stage due to their location (Fig 1.1.1). Ciliary body melanomas can be nodular or diffuse, they tend to grow circumferentially around the eye, invading the trabecular meshwork and leading to glaucoma. They usually become noticeable when the patient suffers pain from glaucoma, and visual loss when the tumour grows to invade the choroid, leading to retinal detachment. They are associated with a poor prognosis due to their tendency for late presentation (Hungerford, 1995).

Small choroidal melanomas can be detected during routine sight testing whereas larger lesions may present with loss of visual acuity caused by the tumour itself, retinal detachment or vitreous haemorrhage (Fig 1.1.1). Most choroidal melanomas adopt a nodular growth pattern and develop a unique mushroom shape when Bruch's membrane is ruptured (Fig 1.1.2). Small choroidal melanomas may sometimes be mistaken as choroidal naevi (Fig 1.1.1). Malignant choroidal melanomas are often associated with a thickness of >1.5mm, serous retinal detachment and the presence of orange lipofuscin pigment on the tumour surface (Hungerford, 1995).

1.1.4 Uveal Melanoma Pathology

Gross Pathology

Uveal melanoma can be divided into three groups according to size: small (<3mm height, 5-10mm diameter), medium (3-5mm height, 10-15mm diameter) and large (>5mm height, >15mm diameter) (Shields, et al., 1991). On gross histopathological examination, melanomas may be dome or mushroom shaped with a vertical and/or diffuse growth pattern (Fig 1.1.2) (McLean, et al., 2004; Shields, et al., 1999). Dome-shaped melanoma occurs when the tumour ruptures Bruch's membrane, herniating through the rupture and growing into the subretinal space (McLean, et al., 2004). When the tumour mass in the subretinal space is larger than that in the choroid, a mushroom-shaped melanoma is formed (McLean, et al., 2004). Inward growth displacing Bruch's membrane (vertical growth) is more often seen than lateral growth within the choroid, with no or little displacement of Bruch's membrane (diffuse pattern) (COMS, 1998). Retinal detachment generally occurs secondary to tumour growth, related to serous exudation from the choriocapillaris and the tumour vasculature (Fig 1.1.2). Serous fluid may also track into

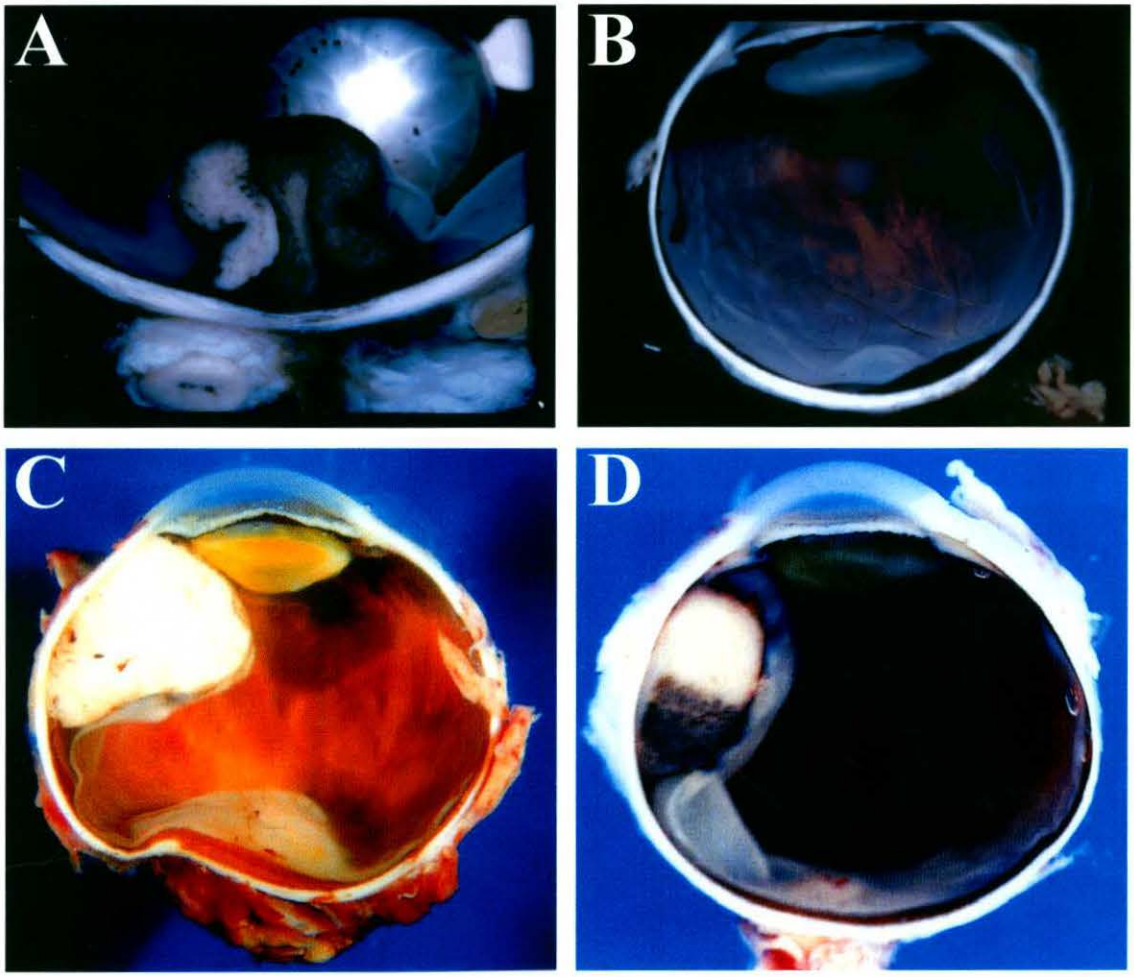

Figure 1.1.2
Gross pathology of uveal melanoma
A. Mushroom-shaped melanoma.[1]
B. Diffuse choroidal melanoma.[1]
C. Non-pigmented uveal melanoma anterior to the equator.[2]
D. Partly pigmented uveal melanoma anterior to the equator.[2]

[1]Images from The David G.Cogan Ophthalmic Pathology Collection (http://cogancollection.nei.nih.gov)
[2]Images from Intraocular Tumors (Shields & Shields, 1999)

the macula region producing clinical macula oedema. Various stages of photoreceptor degeneration, reduction or loss of the outer nuclear layer and outer plexiform layer have been observed associated with retinal detachment secondary to uveal melanoma (Kroll, 1969). Müller cell hypertrophy and gliosis also ocurred in these cases (Kroll, 1969). Similar to cutaneous melanoma, uveal melanoma can be heavily, partially or non-pigmented (Fig 1.1.2) (Shields, et al., 1999).

Microscopic Pathology:

A. Cellular Features

Uveal melanoma may consist of spindle cells, epithelioid cells or combinations of both (mixed cell) (Fig 1.1.3) (Kanski, 1994; McLean, et al., 2004; Shields, et al., 1999). Spindle cells are further divided into spindle A or spindle B depending on their nuclear features. Spindle A cells contain slender nuclei with fine chromatin, the nucleolus is indistinct and the longitudinal infolding of the nuclear membrane often forms a prominent basophilic nuclear line (Kanski, 1994; McLean, et al., 2004). Spindle B cells are round or oval shape and their nuclei are plumper than spindle A cells, the nucleolus being prominent, with poorly differentiated cytoplasmic borders (Kanski, 1994; McLean, et al., 2004). Epithelioid cells are large oval-shaped melanoma cells with a distinct cell membrane, eosinophilic cytoplasm and large round nuclei, which are occasionally multinucleated (Kanski, 1994; McLean, et al., 2004). Extracellular spaces often appear between adjacent epithelioid cells and this loss of cohesion is an important characteristic distinguishing them from spindle cells (McLean, et al., 2004). Their mitotic rate is usually greater than spindle cells and they can also vary in size and shape (polymorphism) as well as pigmentation (COMS, 1998; Kanski, 1994; McLean, et al., 2004). The most common form of uveal melanoma are mixed cell tumours (~50%), followed by spindle cell tumours (~30%), then epithelioid cell tumours (COMS, 1998; McLean, et al., 2004).

An early morphological study suggested that malignant melanoma may arise from pre-existing naevi, and with a relatively flat zone of tumour tissue extending into the adjacent uvea, that was usually more pigmented and composed of more mature cells than the main portion of the tumour (Yanoff, et al., 1967). These naevi cells were located most frequently in the posterior third of the choroid and least frequently in the anterior third of

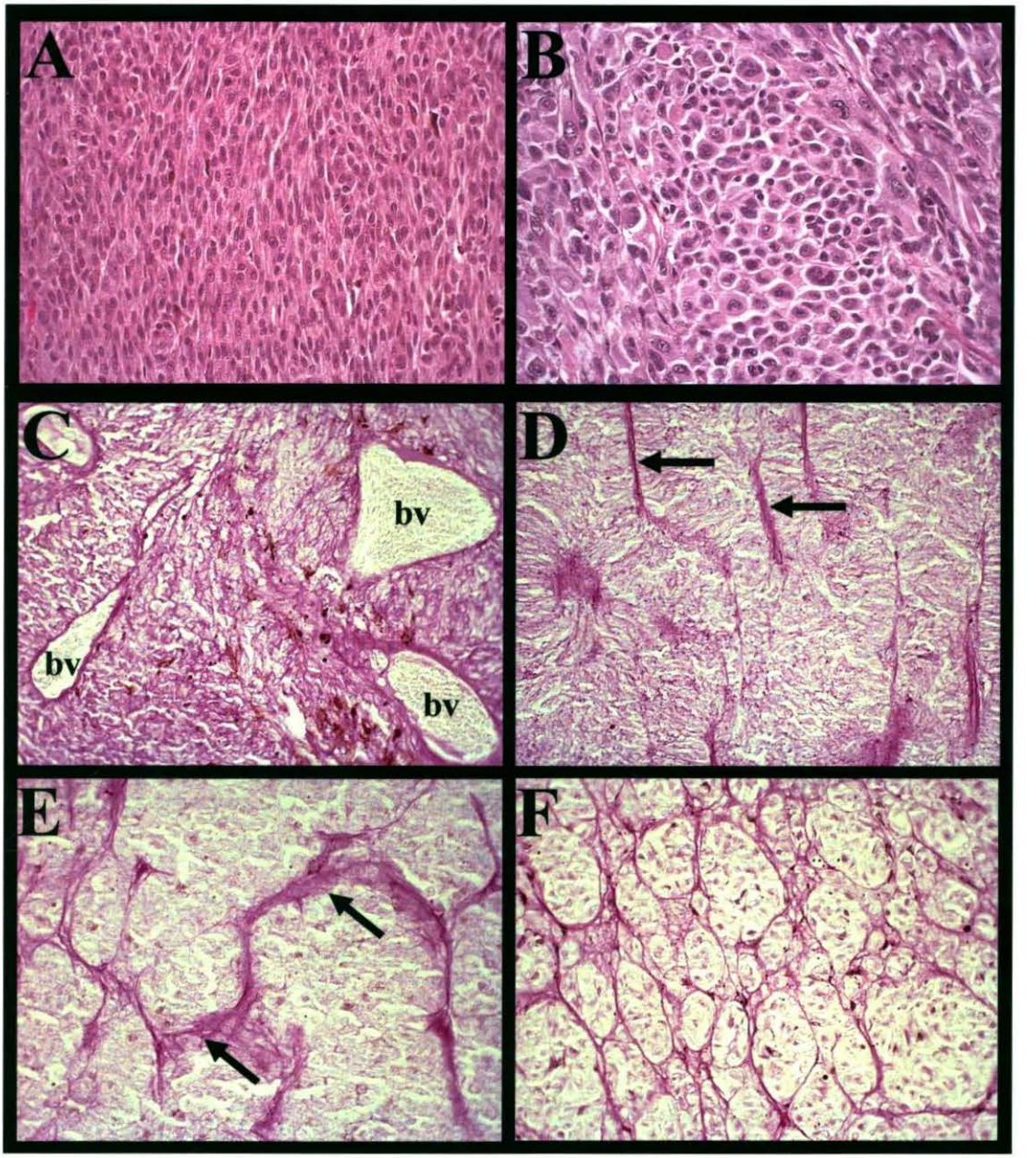

Figure 1.1.3
Cellular features (A & B) and examples of PAS patterns (C – F) in uveal melanoma
A. Spindle cells. (H&E)
B. Epithelioid cells. (H&E)
C. Blood vessels (bv).
D. Parallel channels (arrows).
E. Arcs/incomplete loops (arrows).
F. Networks.

the choroid and ciliary body (Naumann, et al., 1966). The flat zone located at the base of the tumour was later identified as benign-appearing atypical melanocytes (naevus cells), and often displayed slender spindle or plump fusiform cells (Yanoff, et al., 1967).

B. Tumour Microcirculation - Vasculature and Vasculogenic Mimicry

The microcirculation in uveal melanomas is complicated and heterogeneous. Uveal melanomas are highly vascularised and their vessels often arise from the pre-existing choroidal vessels (Folberg, et al., 1993). Additionally the cross sections of uveal melanoma blood vessels are often irregular with acute angles and concave walls, possibily due to compression by adjacent nests of growing tumour cells (Jager, et al., 2004). Tumour vasculature is structurally and functionally different from normal vasculature: the vessels are highly disorganized, tortuous and irregular, with excessive branching and shunts, possibly due to imbalances of angiogenic regulators such as HIF-1 and VEGF (Carmeliet, et al., 2000; Cuenod, et al., 2006). Tumour vessel walls are generally lined by fenestrated endothelial cells and an incomplete basement membrane with widened interendothelial junctions, and are more permeable than normal capillaries, resulting in extravasation of plasma proteins and erythrocytes to the tumour cells, and facilitating their traffic into the bloodstream and subsequent metastases (Carmeliet, et al., 2000; Cuenod, et al., 2006; Hashizume, et al., 2000). The microvascular density and microvascular patterns (see below) of uveal melanoma have been suggested to be associated with poor prognosis but this remains controversial (Al-Jamal, et al., 2003; Chen, et al., 2002; Foss, et al., 1996; Lane, et al., 1997; Makitie, et al., 1999).

Folberg *et al* (1992, 1993) originally observed fibrovascular channels in periodic acid-Schiff (PAS) stained uveal melanoma sections and categorized them into nine morphological patterns: normal vessels, silent with no vessels, straight with randomly distributed vessels, parallel-oriented straight vessels, parallel with cross-linking vessels, arcs, arcs with branching, loops and networks (Fig 1.1.3) (Folberg, et al., 1992, 1993). Most tumours have areas of more than one of these patterns and statistical analysis revealed that cross-linked parallel channels, loops and networks were associated with poor prognosis (Folberg, et al., 1993, 1997; Makitie, et al., 1999). Initially these PAS patterns were believed to be involved in angiogenesis and lined externally by melanoma cells but their basal laminar profiles did not resemble blood vessels (Maniotis, et al., 1999;

Folberg, et al., 2000). *In vitro* studies with aggressive uveal melanoma cell lines indicated that they were capable of generating cellular channels in the absence of endothelial cells, fibroblasts and soluble growth factors including VEGF (Daniels, et al., 1996). These cell lines can also produce type VI collagen, which is believed to contribute to the histogenesis of the PAS patterns (Maniotis, et al., 1999). Maniotis *et al* (1999) termed these phenomenona "vasulogenic mimcry", describing the formation of vasculogenic-like channels by aggressive tumour cells (Maniotis, et al., 1999). These cells express both endothelial and epithelial markers, and form channels independent of angiogenesis, that lined by tumour cells with a basement membrane (Folberg, et al., 2004).

The PAS patterns were later reassessed by other researchers who contended that they were fibrovascular septa, considered insignificant in terms of uveal melanoma prognosis (Foss, et al., 1997; McDonald, et al., 2000). However, several lines of evidence suggested that PAS channels were functional and associated with tumour microcirculation. First, an active circulating network resembling the PAS patterns were detected *in vivo* by indocyanine green angiography in uveal melanoma patients, suggesting these channels are functional (Mueller, et al., 1998). Second, loops and networks are found in hepatic metastases and all secondary metastatic sites from ciliary body and choroidal melanomas, indicating they are associated with tumour aggressiveness rather than the site of dissemination (Folberg, et al., 2000, 2007; Rummelt, et al., 1998). Third, electron and light microscopy studies confirmed that PAS channels were lined externally by tumour cells rather than endothelium (Maniotis, et al., 1999). Finally, a recent study showed that uveal melanoma cells synthesized type I collagen, which was also detected in tumour's PAS patterns, independent of a host stromal response (Lin, et al., 2005). Functionally, vasculogenic mimcry channels have been suggested as a "fluid-conducting network" to accommodate the transport of plasma-derived molecules (i.e oxygen and nutrients) into the tumour lesion, thereby facilitating tumour growth and progression (Clarijs, et al., 2005; Frenkel, et al., 2007). These networks may also be significant for the survival of tumour cells, consistent with the observation that necrosis is generally low in uveal melanoma (less than 2% with >50% necrosis) and absent in areas that contain PAS patterns with low vessel density (Clarijs, et al., 2005; COMS, 1998; Folberg, et al., 2000).

Local Spread

Local spread usually occurs transclerally into the orbit but may also invade the optic nerve (Kanski, et al., 2005). As the choroid does not possess lymphatic vessels, spread to regional lymph nodes is very rare and usually only occurs after the tumour has spread extracellularly into the orbit (Jager, et al., 2004; Lindegaard, et al., 2007).

Distant Spread (Metastases)

Uveal melanoma is interesting in that it tends to spread purely by haematogenous dissemination with a marked tendency to metastasise to the liver (93%), followed by lung (24%), bone (16%), skin or subcutaneous tissue (11%), lymph nodes (10%) and brain (5%) (COMS, 2001; McLean, 1993). Multiple metastases are also common (43%) in these patients (COMS, 2001).

1.1.5 Treatments for Uveal Melanoma

Currently, there are several methods of treatment available for uveal melanoma. The choice of appropiate therapy depends on various clinical factors including the size, location, extent and apparent activity of the tumor, the general health, age and psychological status of the patient, visual acuity of the involved eye as well as the state of the fellow eye (Kanski, 1994; Shields, et al., 1999).

A. Treatment of the Primary Intraocular Tumour

Laser Therapy

Photocoagulation using xenon arc or argon laser may be used to treat small to medium tumours with signs of growth (<6.5 disc diameter/10mm widest length and 3mm thickness) (Kanski, 1994; Shields, et al., 1999). Photocoagulation is used less frequent today as transpupillary thermotherapy (TTT) is now considerd to be more effective (Shields, et al., 1999). TTT involves heating the tumour with infrared light and it appears to be most effective for small tumours in early stage (< 4mm thickness} (Shields, et al.,

1999). However TTT may induce vitreous traction on the retina over the choroidal tumour and lead to retinal tear or even detachment (Browning, et al., 2003). There are also reports showing apparent regression of a choroidal melanoma by TTT, however deeper melanoma cells may remain viable resulting in extra-ocular spread (Forte, et al., 2005; Godfrey, et al., 1999). Therefore all patients require carefull long term follow-up after treatment.

Radiotherapy

Radiotherapy using radioactive plaque or charged particles is the most common treatment modality for medium to large sized melanoma (>10mm diameter) when the involved eye has a reasonable chance of retaining some vision (Damato, 2004; Kanski, 1994; Shields, et al., 1999). COMS has also reported that the survival rate between plaque brachytherapy and enucleation were very similar up to 12 years, hence plaque brachytherapy has been increasingly used for medium sized tumours (COMS, 2006; Diener-West, et al., 2001). Radioactive plaques contain γ- and β-emitting isotopes such as I^{125} and Ru^{106} are sutured to the sclera over the base of the tumour. This faciliates the delivery of a fixed dose of radiation to the tumour while minimizing damage normal tissue (Damato, 2004; Kanski, 1994; Shields, et al., 1999). Side effects of plaque brachytherapy and charged particle therapy include radiation retinopathy (charactersied by microaneurysms, haemorrhages, exudates and occasionally retinal neovascularisation), which can induce irreversible visual impairment in 42% of patients at 5 years (Cruess, et al., 1984; Gunduz, et al., 1999; Kanski, 1994). Other complications of radiotherapy include: cataract, scleral necrosis, hypotony, serous retinal detachment, neovascular glaucoma, radiation optic neuropath etc, all of which may compromise vision. More recently, proton beam radiotherapy is increasingly being used to treat uveal melanoma (Marnitz, et al., 2006). This technique has the advantage of delivering a significant dose of radiation to the tumour, while inducing minimal damage to nearby tissue including optic disc, lens, ciliary body and retina (particularly the macula), with the potential of reducing ocular morbidity (Courdi, et al., 1999).

Surgical Resection

For melanoma located anterior to the ciliary body or in the peripheral choroid, partial lamellar sclerouvectomy (known as transcleral resection or TSR) has been used where the tumour with a rim of healthy choroid is removed under a scleral flap, without disrupting the retina (Kanski, 1994; Shields, et al., 1999). A recent study suggests that TSR preserves vision better than plaque brachytherapy but it has a greater risk of local recurrence (Puusaari, et al., 2007).

Recently endoresection of choroidal melanomas has been reported where by a posteriorly located tumour is resected via an internal approach. Endoresection following irradiation of large uveal melanomas has been shown to be more effective and safer than irradiation alone or enucleation (Bechrakis, et al., 2004).

Enucleation

Enucleation is generally used for large tumours (>15mm) especially when the involved eye becomes symptomatic and/or blind from complications (Kanski, 1994; Shields, et al., 1999). Zimmerman and McLean (1979) (Zimmerman, et al., 1979) suggested that enucleation might seed tumour cells systemically promoting tumour metastasis and reducing the surivival rate from 85% down to 55% after 15 years based on an observation from a hypothetical survival curve. This hypothesis has since been refuted by the large COMS trial in the USA which found no difference in survival for medium sized tumours for enucleation *vs* plaque brachytherapy for up to 12 years after treatment (COMS, 2006; Diener-West, et al., 2001).

B. Treatment of Metastatic Disease

When the tumour has already metastasised, treatments may be limited to resection of solitary metastases, chemotherapy (hepatic and systemic) and immunotherapy, all of which may slightly extend the patient's life (Feldman, et al., 2004; Kanski, 1994).

Resection of Solitary Metastases

Surgical resection of solitary hepatic metastases has been reported to be associated with a longer survival rate than other metastatic therapies, but can only be applied for a minority of patients with limited metastatic disease to the liver (<10%) (Feldman, et al., 2004).

Hepatic Arterial Chemotherapy

Hepatic arterial infusion (HAI) involves direct infusion of chemotherapeutic drugs into the hepatic artery. HAI is commonly administered by a catheter placed adjacent to the hepatic artery via the gastroduodenal artery during laparotomy and connected to a subcutaneously implanted pump. The median survival rate for this treatment is around 15 months and it is limited by its inability to deliver high concentrations of drug to the tumour cells without systemic toxicity (Choti, et al., 1999; Feldman, et al., 2004).

Hepatic artery chemoembolization (HACE) combines hepatic artery embolization with simultaneous infusion of chemotherapeutic drugs (Soulen, 1994). Theoretical this treatment allows local embolization in the liver, resulting in necrosis of the tumour area with minimum systemic toxicity (Feldman, et al., 2004). However the criteria for using HACE are highly selective including that the metastases must only be limited to the liver, that the portal venous system is patent so as to tolerate hepatic arterial occlusion, and that no biliary obstruction occurs to affect the liver's dependence on arterial flow (Feldman, et al., 2004).

Transarterial chemoembolization (TACE) in the segmental arteries is another approach to chemotherapy for patients diagnosed with early stage liver metastases, and has been reported to be well tolerated in 12 patients without any relevant side effects (Vogl, et al., 1999, 2006).

Systemic Chemotherapy

Although numerous studies have attempted to develop systemic chemotherapy for disseminated uveal melanoma including fotemustine, gemcitabine plus treosulfan, dacarbazine and cisplatin, these agents are associated with many side-effects and have not been effective in controlling metastases (O'Neill, et al., 2006; Peters, et al., 2006; Pfohler, et al., 2003; Schmittel, et al., 2005). Thus, there is an urgent need for better strategies to treat widespread disseminated disease, and further laboratory and therapeutic trials are mandatory for the development of such treatments.

Immunotherapy

Several studies have attempted to introduce immunotherapy as a possible treatment for metastatic patients but the results to date are poor. Keilholz *et al* (1994) infused interleukin-2 continuously into the splenic artery, as well as intravenously infused lymphokine-activated killer cells into the hepatic artery or portal vein but found no responses. Sato *et al.* (2002) used hepatic artery immunoembolization with granulocyte-macrophage colony-stimulating factor to stimulate the antigen-presenting cells in 12 patients with liver metastases, and reported one complete response, four partial responses, and stable disease in five patients.

1.1.6 Prognostic Factors in Uveal Melanoma

Clinical Factors-Tumour Size

Uveal melanomas have been classified into three groups based on their height and base diameter (Diener-West, et al., 1992). In a meta-analysis on 5-year mortality rates following enucleation, the mortality rate for small tumours (<3mm in height and <10mm in base diameter) was 16%, medium tumours (3-8mm in height and <15mm in base diameter) 32% and large tumours (>8mm in height and >15mm in base diameter) 53% (Diener-West, et al., 1992). However it is difficult to use tumour size as a prognostic feature when the tumours grow in an irregular shape (McLean, et al., 2004).

Clinical Factors-Tumour Location

• Most of the medium to large tumours have been found to be located either entirely or partially posterior to the equator (COMS, 1998). Iris melanoma has the most favorable prognosis while ciliary body melanoma has the worst prognosis (Singh, et al., 2001). Iris melanoma has the lowest 10-year mortality (3-5%) compared to choroidal and ciliary body melanoma. This may be due to iris melanoma being easier to detect in early development (Arentsen, et al., 1975; Shields, et al., 2001; Singh, et al., 2001). In a case study of 3,432 choroidal and ciliary body melanoma, the 15-year mortality was about 46%, at least 10 times greater than iris melanoma (McLean, et al., 1982; Singh, et al., 2001).

Histopathological Factors-Cell Type

Spindle cell tumours have the best prognosis, mixed cell tumours have an intermediate prognosis and epithelioid cell tumours have the worst prognosis (Kanski, 1994; McLean, et al., 1982, 2004). In a study with 3,432 cases of uveal melanoma, the 15-year mortality of patients with mixed-cell tumours was three times higher (60%) than patients with spindle cell tumors (20%) (McLean, et al., 1982, 2004).

Histopathological Factors-Vascular Patterns

Statistical analysis has indicated that patients with tumours in the absence of loops, networks, arcs or parallel with cross-linking vessels have approximately 80% 20-year survival rate and tumours with these patterns will reduce down to about 40% (Folberg, et al., 1993). McLean *et al* (1997) later simplified the classification into three categories – presence of loops, presence of equivocal loops and absence of vascular loops, and found that the survival rate of patients decreased from 67.5% to 33.8% at 15 years when vascular loops were present in the tumours.

Histopathological Factors- Mitotic Rate

The prognostic value of the mitotic rate was introduced by McLean *et al* (1977). They recommended using 40 HPFs (High Power Fields) to determine the mitotic rate in uveal melanoma due to the low number of mitotic figures (McLean, et al., 1977). In a case

study with 217 uveal melanomas, tumours with low frequency or mitotic rate (0-1 per HPF) were shown to have a better prognosis (15% mortality) compared to tumours with high mitotic rate (9-48 per HDF) (56% mortality) in 6 years (McLean, et al., 1977). Consistent with these findings, the mitotic rate was also significantly higher in epithelioid cell tumours than in spindle cell and mixed cell tumours (COMS, 1998)

Immunological Factors

Several studies have shown that tumour-infiltrating macrophages and lymphocytes may be associated with a poor prognosis in uveal melanoma patients (Makitie, et al., 2001; Whelchel, et al., 1993). Expression of human leukocyte antigens (HLA class I and II), important for immune recognition of tumour cells, has also been associated with uveal melanoma metastases and poor prognosis (Ericsson, et al., 2001; Jager, et al., 2004; Krishnakumar, et al., 2004). This contrasts with other tumours such as cutaneous melanoma, breast carcinoma and small cell lung carcinoma where HLA expression is associated with better survival (Concha, et al., 1991; Kikuchi, et al., 2007; van Duinen, et al., 1988). HLA class I expression may be protective for disseminated melanoma cells by blocking natural killer (NK) cell cytolysis, especially in the liver (Blom, et al., 1997; Ma, et al., 1995).

Cytological Factors

Cytogenetic studies reveal that uveal melanoma is often characterised by clonal abnormalities such as loss of material from the long arm of chromosome 1 (1q) (33%), monosomy 3 (56%), gain and loss of material in chromosome 6q (78% and 39% respectively), trisomy 8 (44%) and gain of material in chromosome 8q (78%) (Aalto, et al., 2001; Dahlenfors, et al., 1993; Horsman, et al., 1993; Hughes, et al., 2005; Kilic, et al., 2006; Prescher, et al., 1990, 1995; Prescher, et al., 1996; Sandinha, et al., 2004; Scholes, et al., 2003; Singh, et al., 1994; Sisley, et al., 1992; Tschentscher, et al., 2000; Wiltshire, et al., 1993). Abnormalities in chromosome 3 are found almost exclusively in uveal melanoma associated with metastases, and two tumour suppressor genes are proposed to correlate with these aberrations (Prescher, et al., 1996; Tschentscher, et al., 2001; White, et al., 1998). Gene expression profiling revealed that the presence or absence of monosomy 3 defined two distinct uveal melanoma types (Tschentscher, et al., 2003).

Furthermore, gene expression profiling has identified two distinct groups of primary uveal melanomas - low-grade (group 1) and high-grade (group 2) - where monosomy 3 is associated with group 2 (more aggressive) tumours (Onken, et al., 2004). Abnormalities of both chromosome 3 and 8 often co-exist in the same tumour and are correlated with poor prognosis (Prescher, et al., 1996; Sisley, et al., 1997), whereas an abnormality in chromosome 6 may be associated with a better prognosis, even when associated with chromosome 3 and 8 aberrations (Baggetto, et al., 2005; Onken, et al., 2004; White, et al., 1998). The mechanisms underlying the possible protective effect of an abnormality in chromsome 6 in uveal melanoma remain to be investigated.

There are several techniques to assess the nonrandom chromosomal abnormalities in uveal melanoma including standard cytogenetics with cultured tumour cells (Horsman, et al., 1993; Prescher, et al., 1995; Singh, et al., 1994; Sisley, et al., 1990, 1992; Tschentscher, et al., 2001), comparative genomic hybridization and microsatellite analysis with fresh and paraffin embedded tissue (Aalto, et al., 2001; Hughes, et al., 2005; Scholes, et al., 2003; Tschentscher, et al., 2000, 2001), fluorescence *in situ* hybridization (FISH) with fresh tissue and stained slides prepared from tumour cells (Wiltshire, et al., 1993) and chromosome *in situ* hybridization (CISH) with formalin or glutaraldehyde fixed tissue (Sandinha, et al., 2004). Recently high-density single nucleotide polymorphism (SNP) mapping array with fresh tissue has been shown to be more sensitive in detecting chromosome 3 aberrations and monosomy than FISH (Young, et al., 2007).

1.2 Matrix Metalloproteinases (MMPs) and Tissue Inhibitors of Metalloproteinases (TIMPs)

MMPs are a family of enzymes responsible for the degradation of extracellular matrix (ECM) constituents including collagen, laminin and proteoglycans. These enzymes are important for embryogenesis, wound healing, ECM remodelling as well as tumour invasion and angiogenesis. MMPs can be secreted, stored or anchored to the membrane by a transmembrane domain (membrane-type [MT-] MMPs), and are generally subdivided into distinct classes based on their structural differences. MMPs can be inhibited by TIMPs, hence their imbalance often results in various pathological processes including tumour development and metastases.

Molecular Structure of MMPs

MMPs are synthesized as pro-enzymes and secreted as inactive pro-MMPs in most cases. The general structure of MMPs consists of five domain motifs: signal peptide, propeptide domain (~80 amino acids), metalloproteinase catalytic domain (~170 amino acids), hinge region and a hemopexin domain (~200 amino acids) (Fig 1.2.1) (Nagase, et al., 2006; Visse, et al., 2003).

The propeptide domain has a specific sequence including cysteine that maintains the latency of pro-MMPs by binding zinc ion. The catalytic domain contains a zinc binding motif and conserved methionine (Bode, et al., 1992; Dhanaraj, et al., 1996). In MMPs, the catalytic domain contains additional zinc and calcium ions for stability and expression of enzymatic activity (Nagase, et al., 1999). The C-terminal hemopexin-like domain (PEX) is critical for collagenases to cleave collagen, however, the catalytic domain is required to maintain proteolytic activity towards other substrates (Bode, 1995; Clark, et al., 1989).

Types of MMPs and TIMPs

MMPs were originally subdivided into collagenases, gelatinases, stromelysins and matrilysins based on their specificity for ECM components. More recently MMPs have been observed to share common substrates and can also be grouped according to their structural differences (Table 1.2.1, Table 1.2.3, Fig 1.2.1) (Egeblad, et al., 2002; Nagase, et al., 2006). There are eight distinct structural classes of MMPs identified so far: five are secreted and three are membrane-type MMPs (Fig 1.2.1) (Egeblad, et al., 2002).

Collagenases (MMP-1, -8, -13 and -18 in Xenopus) (Table 1.2.1, Table 1.2.3, Fig 1.2.1) cleave several types of collagens, ECM molecules and soluble proteins (Egeblad, et al., 2002; Nagase, et al., 2006; Stamenkovic, 2000). MMP-1 is broadly expressed in various normal cells including fibroblasts, macrophages, endothelial cells, epithelial cells as well as in tumour cells from colorectal, oesophageal and gastric carcinomas (Brinckerhoff, et al., 2000; Inoue, et al., 1999; Murray, et al., 1996, 1998). MMP-1 has been reported to be associated with a poor prognosis in colorectal, oesophageal and

Figure 1.2 Simplified Domain Structure of MMPs

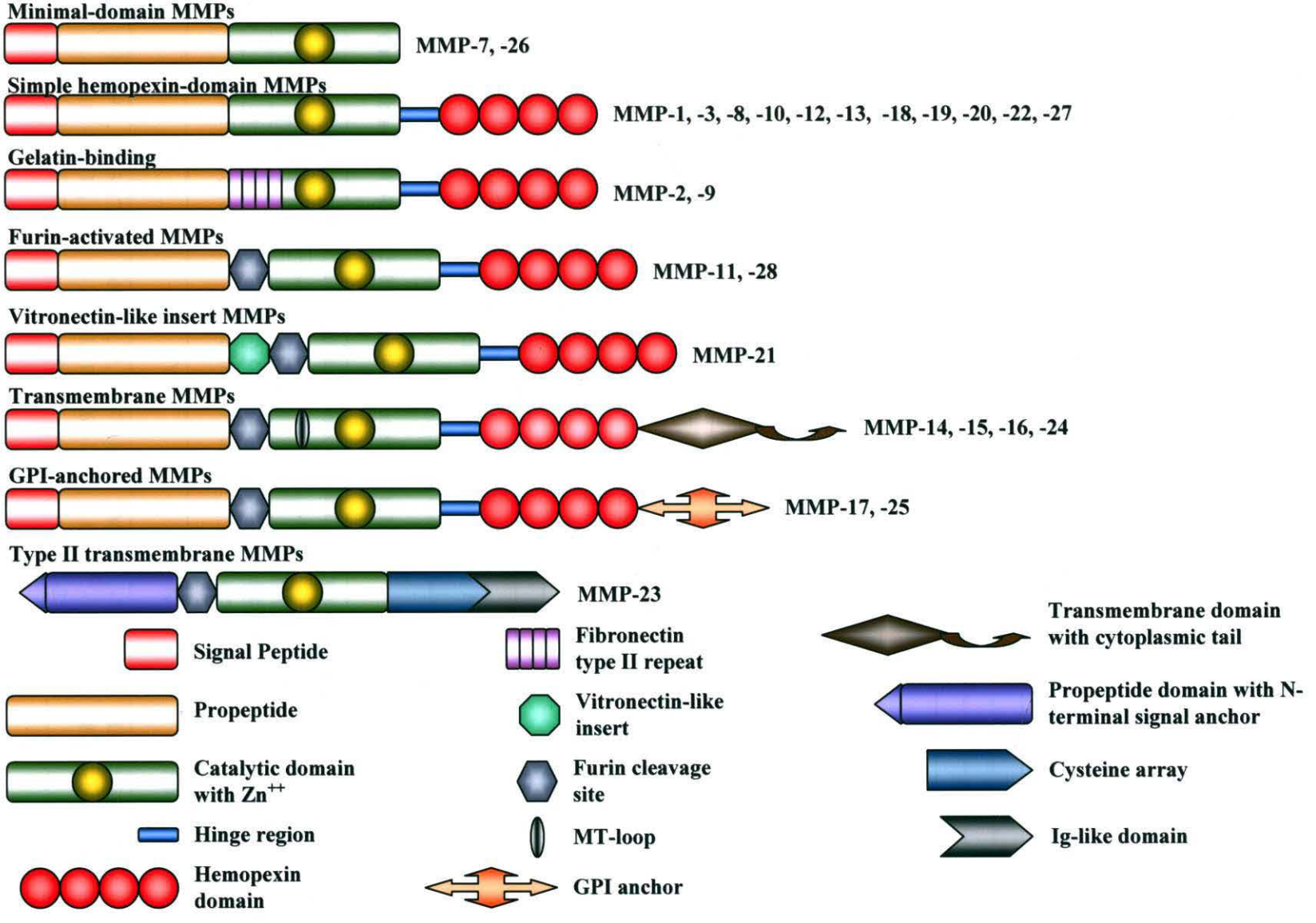

*Adapted from Egeblad and Werb (2002). Nat Rev Cancer, 2(3): 161-74

Table 1.2.1 Classification of Matrix Metalloproteinases (MMPs)		
Structural class	**MMP**	**Common name(s)**
Minimal-domain	7	Matrilysin, Matrin, PUMP1, Small uterine metalloproteinase
	26	Matrilysin-2, Endometase
Simple hemopexin-domain	1	Collagenase-1, Interstitial collagenase, fibroblast collagenase, Tissue collagenase
	3	Stromelysin-1, Transin-1, Proteoglycanase, Procollagenase-activating protein
	8	Collagenase-2, Neutrophil collagenase, PMN collagenase, Granulocyte collagenase
	10	Stromelysin-2, Transin-2
	12	Metalloelastase, Macrophage elastase, macrophage metalloelastase
	13	Collagenase-3
	18	Collagenase-4 (Xenopus)
	19	RASI-I
	20	Enamelysin
	22	CMMP (Chicken)
	27	None
Gelatin-binding	2	Gelatinase A, 72-kDa gelatinase, 72-kDa type IV collagenase, neutrophil gelatinase
	9	Gelatinase B, 92-kDa gelatinase, 92-kDa type IV gelatinase
Furin-activated secreted	11	Stromelysin-3
	28	Epilysin
Vitronectin-like insert	21	XMMP (Xenopus)
Transmembrane	14	MT1-MMP, MT-MMP1
	15	MT2-MMP, MT-MMP2
	16	MT3-MMP, MT-MMP3
	24	MT5-MMP, MT-MMP5
GPI-anchored	17	MT4-MMP, MT-MMP4
	25	MT6-MMP, MT-MMP6, Leukolysin
Type II transmembrane	23	Cysteine array MMP (CA-MMP), Femalysin, MIFR

***Adapted from Egeblad and Werb (2002). Nat Rev Cancer 2(3): 161-74.**

Table 1.2.2 Properties of Tissue Inhibitors of Metalloproteinases (TIMPs)				
	TIMP-1	**TIMP-2**	**TIMP-3**	**TIMP-4**
Expression	inducible	mainly constitutive	inducible	unknown
Main form	diffusible secreted	diffusible secreted	ECM-associated	diffusible secreted
MMP-2 activation	No	Yes	No	No
MMPs inhibited	MMP-1, -2, -3, -7, -8, -9, -10, -11, -12, -13, -17, -19, -25, -26,	MMP-1, -2, -3, -7, -8, -9, -10, -13, -14, -16, -17, -19, -24, -25, -26	MMP-1, -2, -3, -9, -13, -14. -16, -17, -19, -25, -26	MMP-1, -2, -3, -8, -9, -14, -19

***Adapted from Egeblad and Werb (2002). Nat Rev Cancer 2(3): 161-74.**

gastric cancers (Inoue, et al., 1999; Murray, et al., 1996, 1998), although high expression of MMP-1 in human metastastic cutaneous melanoma cells has been reported to be correlated with a favourable treatment response (Nikkola, et al., 2001). A recent study suggested that MMP-1 activated protease activated receptor 1 (PAR-1) and promoted growth and invasion of breast carcinoma cells (Boire, et al., 2005). Cleavage products of MMP-1, -8 and -13 can be rapidly denatured to gelatin and further degraded by gelatinases (MMP-2 and -9) (Stamenkovic, 2000). MMP-8 has been reported to be expressed in neural crest cells during early development as well as in cutaneous melanoma cells (Giambernardi, et al., 2001).

Gelatinases (MMP-2 and -9) (Table 1.2.1, Table 1.2.3, Fig 1.2.1) preferentially degrade collagens but they can also digest laminins (Egeblad, et al., 2002; Nagase, et al., 2006; Stamenkovic, 2000). Increased MMP-2 expression has been detected in various human cancers including carcinoma of the colon, pancreas, prostate, bladder, skin, breast and ovary (Yu, et al., 1996). Activated MMP-2 is strongly associated with tumour cell invasion and metastasis in several human cancers including colorectal, pancreatic and cervical cancers (Koshiba, et al., 1997; Sheu, et al., 2003; Waas, et al., 2002; Yu, et al., 1996). Furthermore MMP-2 is also proposed as a prognostic marker of uveal melanoma (see next section) (Vaisanen, et al., 1999). MMP-9 expression is often low or absent in normal tissue, however, it can be induced in wound healing and tumour invasion (Egeblad, et al., 2002; Stamenkovic, 2000).

Stromelysins (MMP-3, -10 and -11) (Table 1.2.1, Table 1.2.3, Fig 1.2.1) are predominantly expressed by normal epithelium but can also be found in carcinomas (Stamenkovic, 2000). MMP-3 is involved in mammary epithelial cell apoptosis and alveolar formation (Nagase, et al., 2006). MMP-11 was originally identified in the stromal cells surrounding invasive breast carcinomas and it cleaves IGFBP, α2-macroglobulin and α1-proteinase inhibitor (Table 1.2.2) (Basset, et al., 1990; Egeblad, et al., 2002). Although MMP-12 (macrophage metalloelastase) doesn't belong to stromelysin subgroup, it is structurally similar to MMP-3 and -10 (Fig 1.2.1) (Egeblad, et al., 2002). MMP-28 (epilysin) shares a common structural class with MMP-11 and it is broadly expressed in both normal and fetal tissue (Fig 1.2.1) (Egeblad, et al., 2002; Lohi, et al., 2000; Marchenko, et al., 2001). MMP-28 has been observed in several carcinomas including

Table 1.2.3 Matrix Metalloproteinases (MMPs) and their substrates	
MMP	Substrate(s)
1	Collagens (type I-III, VII, VIII, X, XI), gelatins, aggrecan, brevican, entactin/nidogen, fibronectin, IGFBP, laminin, link protein, myelin basic protein, tenascin, vitronectin, α1-antichymotrypsin, α2-macroglobulin, α1-proteinase inhibitor, C1q, casein, CXCL12, fibrin, fibrinogen, IL-1β, L-selectin, pro-TNF-α, pro-MMP-2, -9
2	Collagens (type I, III-V, VII, X, XI), gelatins, aggrecan, brevican, decorin, elastin, entactin/nidogen, fibrillin, fibronectin, fibulins, IGFBP, laminin, link protein, myelin basic protein, osteonectin, tenascin, vitronectin, α1-antichymotrypsin, α1-proteinase inhibitor, ADAMTS-1, C1q, CCL7, CXCL12, endothelin, FGFR1, fibrin, fibrinogen, galectin-3, IL-1β, pro-MMP-9, MMP-13, plasminogen, substance P, latent TGFβ, pro-TNFα
3	Collagens (type III-V, VII, IX-XI), gelatins, aggrecan, brevican, decorin, elastin, entactin/nidogen, fibrillin, fibronectin, IGFP, link protein, myelin basic protein, osteonectin, osteopontin, perlecan, tenascin, vitronectin, α1-antichymotrypsin, α2-macroglobulin, α1-proteinase inhibitor, C1q, casein, CXCL12, E-cadherin, fibrin, fibrinogen, pro-HB-EGF, IL-1β, L-selectin, pro-MMP-1, -7, -8, -9, -13, NC1 fragment of collagen XVIII, PAI-1, plasminogen, substance P, T kininogen, pro-TNF-α, uPA
7	Collagens (type I, IV), gelatins, aggrecan, brevican, decorin, elastin, entactin/nidogen, fibronectin, fibulins, laminin, link protein, myelin basic protein, osteonectin, osteopontin, tenascin, vitronectin, α1-proteinase inhibitor, casein, E-cadherin, FAS ligand, fibrinogen, pro-HB-EGF, β4 integrin, pro-MMP-1, -2, -9, plasminogen, pro-TNF-α
8	Collagens (type I-III), aggrecan, brevican, α2-macroglobulin. α1-proteinase inhibitor. ADAMTS-1. C1q, fibrinogen, substance P
9	Collagens (type IV, V, XI, XIV), gelatins, aggrecan, decorin, elastin, fibrillin, IGFBP3, laminin, link protein, myelin basic protein, osteonectin, vitronectin, α2-macroglobulin, α1-proteinase inhibitor, casein, C1q, CXCL1, CXCL4, CXCL7-precursor, CXCL12, endothelin, fibrin, fibrinogen, galectin-3, IL-1β, IL-8/CXCL8, IL-2Rα, c-kit ligand, pro-MMP-2, NC1 fragment of collagen XVIII, plasminogen, substance P, latent TGF-β, pro-TNF-α
10	Collagens (type III-V), gelatins, aggrecan, brevican, elastin, fibronectin, link protein, casein, fibrinogen, pro-MMP-1, -7, -8, -9
11	IGFBP. α2-macroglobulin, α1-proteinase inhibitor
12	Collagens (type I, IV), gelatins, aggrecan, elastin, entactin/nidogen, fibrillin, fibronectin, laminin, myelin basic protein, vitronectin, α2-macroglobulin, α1-proteinase inhibitor, factor XII, fibrinogen, IgG, NC1 fragment of collagen XVIII, plasminogen, pro-TNF-α
13	Collagens (type I-IV, VI, IX, X, XIV), gelatins, aggrecan, brevican, fibrillin, fibronectin, osteonectin, tenascin, α2-macroglobulin, C1q, casein, CXCL12, factor XII, fibrinogen, pro-MMP-9, NC1 fragment of collagen XVIII

Table 1.2.3 Matrix Metalloproteinases (MMPs) and their substrates (cont.)	
MMP	**Substrate(s)**
14	Collagens (type I-III), gelatins, aggrecan, entactin/nidogen, fibrillin, fibronectin, perlecan, vitronectin, α2-macroglobulin, α1-proteinase inhibitor, CD44, CXCL12, factor XII, fibrin, fibrinogen, αv integrin, pro-MMP-2, -13, tenascin, tissue transglutaminase, pro-TNF-α
15	Aggrecan, entactin/nidogen, fibronectin, laminin, perlecan, tenascin, tissue transglutaminase, ADAMTS-1, pro-MMP-2
16	Collagen III, gelatin, casein, fibronectin, tissue transglutaminase, pro-MMP-2
17	Gelatin, fibrin, fibrinogen, pro-MMP-2, pro-TNF-α
18	Collagen I, gelatins
19	Collagen (type I, IV), gelatins, aggrecan, cartilage oligomeric matrix protein, entactin/nidogen, fibronectin, laminin, tenascin, casein
20	Aggrecan, amelogenin, cartilage oligomeric matrix protein, NC1 fragment of collagen XVIII
21	Unknown
22	Casein, gelatin
23	Unknown
24	Gelatin, fibronectin, pro-MMP-2
25	Collagen type IV, gelatin, fibronectin, fibrinogen, fibrin, pro-MMP-2
26	Collagen type IV, gelatin, fibronectin, fibrinogen, fibrin, vitronectin, α1-proteinase inhibitor, casein, pro-MMP-9
27	Unknown
28	Casein

***Adapted from Egeblad and Werb (2002). Nat Rev Cancer 2(3): 161-74.**

colon adenocarcinoma, ovarian carcinoma and pancreatic adenocarcinoma (Marchenko, et al., 2001).

Matrilysins (MMP-7 and MMP-26) lack of hemopexin domain and structurally classified as minimal-domain MMPs (Table 1.2.1, Table 1.2.3, Fig 1.2.1) (Egeblad, et al., 2002; Nagase, et al., 2006). MMP-7 is mainly stored in secretory epithelial cells of various organs including endometrium, small intestine, breast, pancreas, liver and prostate, as well as tumours including prostate and breast carcinoma (Nagase, et al., 2006; Saarialho-Kere, et al., 1995). MMP-26 is found in the placenta, epithelial conjunctiva cells of the human eye, endometrioid tumours, epithelial tumours and breast cacinoma, suggesting its involvement in normal development and pathology (de Coignac, et al., 2000; Marchenko, et al., 2001, 2004). MMP-26 can cleave fibrinogen in a manner similar to MT1-MMP, and may also participate in angiogenesis involving fibrin formation and degradation (Hiraoka, et al., 1998; Marchenko, et al., 2001). Unlike other MMPs, MMP-26 is mainly stored intracellularly (Marchenko, et al., 2004).

MMP-19 is one of the recently discovered MMP members and structurally belongs to simple hemopexin-domain MMPs (Egeblad, et al., 2002; Pendas, et al., 1997) (Table 1.2.1, Table 1.2.3, Fig 1.2.1). MMP-19 cleaves various ECM components as well as cartilage oligomeric matrix protein (COMP), which found in cartilage and tendons (Table 1.2.2) (Stracke, et al., 2000). MMP-19 is expressed in macrophages, smooth muscle cells and keratinocytes, and MMP-19 mRNA is also upregulated in psoriatic keratinocytes and skin (Suomela, et al., 2003). MMP-19 was strongly expressed in the synovial capillary endothelial cells found in an acutely inflamed tissue, suggesting its involvement during acute inflammation and angiogenesis (Kolb, et al., 1999). Downregulation of MMP-19 in tumour cells and vessels has been reported to be associated with increased breast tumour invasiveness, suggesting that MMP-19 might inhibit malignant transformation, unlike other MMPs (Djonov, et al., 2001).

Apart from secreted MMPs, there are six cell membrane-associated MMPs that are categorized as membrane-type MMPs (MT-MMPs). MT-MMPs can be further divided into two subgroups, the transmemebrane and the glycosylphosphatidyl inositol (GPI)-anchored MT-MMPs (Egeblad, et al., 2002; Nagase, et al., 2006). MT1-, 2-, 3-, and 5-MMPs belong to the transmembrane MT-MMPs, and contain a transmembrane and

cytoplasmic tail domain, while MT4- and MT6-MMP belong to GPI-anchored MT-MMPs and possess a GPI anchor instead of a transmembrane and cytoplasmic tail domain (Table 1.2.1, Table 1.2.3, Fig 1.2.1) (Egeblad, et al., 2002; Handsley, et al., 2005; Kojima, et al., 2000; Nagase, et al., 2006; Pei, 1999; Stamenkovic, 2000).

MT1-MMP (MMP-14) degrades various substrates including type I collagen, fibronectin, laminin, fibrin and gelatin (Table 1.2.1, Table 1.2.3). MT1-MMP is important in angiogenesis as it allows endothelial cells to retain the surrounding matrix for structural support by restricting their proteolytic activity to the pericellular milieu (Hiraoka, et al., 1998; Nguyen, et al., 2000). MT2-MMP (MMP-15) preferentially degrades fibronectin, laminin and tenascin (Table 1.2.2). Both MT1- and MT2-MMP can activate pro-MMP-13 (Stamenkovic, 2000). MT3-MMP (MMP-16) commonly degrades type III collagen, gelatin and fibronectin (Table 1.2.2) (Egeblad, et al., 2002; Stamenkovic, 2000). MT4-(MMP-17), MT5- (MMP-24) and MT6-MMP (MMP-25) are the most recently discovered MT-MMPs. In contrast to other MT-MMPs, MT5-MMP can act as both a cell bound and soluble proteinase for ECM degradation (Pei, 1999).

MT1- and MT3-MMP expression has been observed in fibroblasts, macrophages and osteoclast-like cells at bone resorption sites in rheumatoid arthritis, suggested they might be responsible to the matrix degradation during rheumatoid arthritis development (Pap, et al., 2000). Northern blot analysis has demonstrated MT5-MMP predominantly expressed in the brain, kidney, pancreas and lung (Llano, et al., 1999). In particular, MT5-MMP has been found to be expressed in the cerebellum and may be involved in neuronal development as well as in regulating axonal growth (Hayashita-Kinoh, et al., 2001; Jaworski, 2000; Pei, 1999; Sekine-Aizawa, et al., 2001). MT5-MMP is also detected at high levels in brain tumours such as astrocytomas, compared to normal brain tissue (Llano, et al., 1999). MT6-MMP is predominantly expressed in leukocytes, lung and spleen, and is detected at high levels in colon carcinoma and some astrocytomas and glioblastomas; MT6-MMP is not detected in normal colon or brain tissue (Pei, 1999; Velasco, et al., 2000). All MT-MMPs (except MT4-MMP) can activate pro-MMP-2, which may also facilitate tumour progression (Llano, et al., 1999; Pei, 1999; Nagase, et al., 2006; Stamenkovic, 2000; Velasco, et al., 2000).

TIMPs are physiological MMP inhibitors, and to date four different structurally related members (TIMP-1 to -4) have been identified (Table 1.2.2) (Lambert, et al., 2004; Nagase, et al., 2006). Structurally TIMPs consist of N- and C- terminal domains, each containing six conserved cysteine residues forming three disulfide bonds and the N-terminal folds as an independent unit during the inhibitory activity (Nagase, et al., 2006; Williamson, et al., 1990). The N-terminal domain provides sufficient MMP inhibition, while the C-terminal domain is important for protein-protein interactions and regulates MMP activation by binding to pro-MMPs (Lambert, et al., 2004).

TIMP-1 is expressed in numerous cultured cell types including fibroblasts, smooth muscle cells, osteoblasts, chondrocytes, epithelial and endothelial cells (Lambert, et al., 2004). In pathology, TIMP-1 associated with poor prognosis in various human cancers including metastatic breast cancer, colorectal cancer, lung carcinoma and lymphoma (Chirco, et al., 2006).

TIMP-2 inhibits MMP-2 and MT1-MMP but at low concentration it forms a tri-molecular complex with MT1-MMP and proMMP-2, mediating activation of proMMP-2 (Goldberg, et al., 1992; Gomez, et al., 1997; Ward, et al., 1991).

TIMP-3 is a unique member of the TIMP family in that it is water insoluble and bound tightly in the ECM, mainly by heparan sulphate proteoglycans (Yu, et al., 2000). TIMP-3 was first identified in chicken embryo fibroblasts and referred to as ChIMP-3, however sequence analysis revealed that this protein was similar to other TIMPs and it was subsequently renamed TIMP-3 (Pavloff, et al., 1992). TIMP-3 is the only TIMP that inhibits ADAMs (a disintegrin and metalloproteinase) family members such as tumour necrosis factor α-converting enzyme, which may account for its ability to induce tumour cell apoptosis (Ahonen, et al., 1998; Smith, et al., 1997). Furthermore TIMP-3 is also the only TIMP to inhibit shedding of interleukin-6 receptors and L-selectin (Borland, et al., 1999; Hargreaves, et al., 1998).

TIMP-4 is structurally similar to TIMP-2, and also inhibits MMP-2 and MT1-MMP, but does not directly promote MMP-2 activation (Hernandez-Barrantes, et al., 2001). TIMP-4 inhibits capillary endothelial cell migration but it does not inhibit proliferation and angiogenesis *in vivo* (Fernandez, et al., 2006).

Besides inhibiting MMPs, TIMPs are also involved in other biological processes including promotion and inhibition of cell growth and angiogenesis, apoptosis and embryogenic implantation (Lambert, et al., 2004). TIMP-1 and -2 induce cell growth in a wide range of cells including keratinocytes, fibroblasts and osteosarcoma cells, while TIMP-3 has been reported to induce cell growth in non-transformed chicken embryonic fibroblasts (Lambert, et al., 2004). Interestingly, TIMP-2 and -3 have also been reported to inhibit cell growth in cultured endothelial cells, several human carcinoma cell lines and in a neuroblastoma mouse model (Bian, et al., 1996; Miyake, et al., 1999; Murphy, et al., 1993; Spurbeck, et al., 2003). As mentioned above, TIMP-2 can activate pro-MMP-2 with MT1-MMP and promote angiogenesis; in contrast, overexpression of TIMP-1 in pancreatic cancer cell lines resulted in angiogenesis inhibition and TIMP-3 was also reported to inhibit angiogenesis in neuroblastoma mouse model (Bloomston, et al., 2002; Goldberg, et al., 1992; Gomez, et al., 1997; Spurbeck, et al., 2003; Ward, et al., 1991). TIMP-1 and -2 were associated with anti-apoptotic activity in several cell lines whereas TIMP-3 promoted apoptosis in smooth muscle cells (Lambert, et al., 2004). Furthermore TIMP-1 and -3 were up-regulated during mouse embryo implantation (Alexander, et al., 1996).

MMP and TIMPs in Uveal Melanoma Growth & Invasion

As discussed above MMPs and TIMPs are involved in many human cancers and several studies have investigated their role in uveal melanomas. MMP-2 has been proposed as a prognostic marker of uveal melanoma (Vaisanen, et al., 1999). Immunoreactivity for MMP-2 has also been observed in RPE, corneal epithelium, fibroblasts in the ciliary body and choroid of melanoma eyes (Vaisanen, et al., 1999). MMP-9 has also been found to be expressed in uveal melanomas, predominantly in epithelioid melanomas or the epithelioid portion of mixed-cell melanomas (El-Shabrawi, et al., 2001; Sahin, et al., 2007). Both MMP-2 and -9 have been associated with a high incidence of metastatic disease in uveal melanoma; tumours expressing the MMP inhibitors, TIMP-1 & -2, were however correlated with a better patient survival rate (El-Shabrawi, et al., 2001; Elshaw, et al., 2001; Vaisanen, et al., 1999). A preliminary study has shown that uveal melanomas with mixed morphology expressed MMP-2, -9, -13 and MT1-MMP (Laver, 2002). Prinomastat, a selective inhibitor of MMP-2, -9, -13 and -14, has been shown to induce apoptosis and necrosis in a rabbit model of uveal melanoma

rabbit, further suggesting a role for MMPs in tumour growth (Ozerdem, et al., 2002). An *in-vitro* study of 15 primary uveal melanoma cell lines found that all secreted pro-MMP-2, with nine secreting pro-MMP-9 (Cottam, et al., 1992). TIMP-3 has been recently suggested to be involved in the development of uveal melanoma with a 5-fold decrease in expression in a metastatic uveal melanoma cell line (van der Velden, et al., 2003). As mentioned previously, angiogenesis and vasculogenic mimicry are critical in the development and metastases of uveal melanomas (Folberg, et al., 2000). MMPs and TIMPs have complex regulatory activities in angiogenesis, including degradation of basement membrane, capillary tube formation, endothelial cell proliferation and migration (Kumar, et al., 1998). Active MMP-2 and MT1-MMP have been reported to cleave Laminin 5γ2 chain to produce γ2' and γ2X fragments, which are necessary for vasculogenic mimicry in aggressive uveal melanoma (Seftor, et al., 2001).

1.3 Adhesion Molecules in Uveal Melanoma Growth and Invasion

Adhesion molecules play an important role in the growth and invasiveness of tumour, and may also contribute to hematogenous tumour dissemination. Tumour cell adhesion molecules can promote cell binding to vascular endothelium, which associated with increased MMP secretion, may be important for allowing tumour cells to enter blood vessels and spread throughput the body.

Uveal melanomas express a variety of adhesion molecules including members of the immunoglobulin (Ig) superfamily and integrins (Anastassiou, et al., 2000a, 2000b; Beliveau, et al., 2000; Elshaw, et al., 2001; Pardo, et al., 2005; Seftor, et al., 1999). In uveal melanoma, for example, intercellular cell adhesion molecule-1 (ICAM-1) has been reported to be strongly expressed in uveal melanomas and correlated with large tumour size (>2000mm^3) (Lawry, et al., 1999). Other immunohistochemical studies have also found that uveal melanoma strongly expresses ICAM-1 80% of tumours – (Anastassiou, et al., 2000b). This study reported decreased ICAM-1 expression associated with an increased risk of metastasis within the first 5 years after diagnosis (Anastassiou, et al., 2000b). Further support for involvement of ICAM-1 in uveal melanoma spread comes from a recent study, that showed that an anti-human ICAM-1 antibody could inhibit the spread of human uveal melanoma cells injected into the anterior chamber or subcutaneously, in a SCID mice mouse model (Wang, et al., 2006).

Sections of primary uveal melanomas with vascular networks have been observed to strongly express integrin VLA-2, whereas loss of VLA-3 and α_v was associated with scleral infiltration and extraocular growth of the tumour (Anastassiou, et al., 2000a). Another study found that compared to a non-invasive cell line, an invasive uveal melanoma cell line expressed $\alpha 1$ and $\alpha 4$ integrin, with higher levels of $\alpha 1$-3, $\alpha 5$ and 6 integrin subunits (Woodward, et al., 2005). *In vitro* studies also showed that membrane-bound integrin, $\alpha 5\beta 1$, was not detectable in epithelioid cell lines, while low levels of $\alpha 5\beta 1$ were found in primary cultured melanocytes, spindle and mixed uveal melanoma cell lines, suggesting that loss of $\alpha 5\beta 1$ might be related to growth of epithelioid uveal melanomas (Beliveau, et al., 2000). Higher levels of $\alpha 5\beta 3$ expression were detected in spindle compared with epithelioid cell lines, suggesting that changes in this integrin may lead to metastases (Seftor, et al., 1999). Spindle cell melanomas and melanocytes were also reported to lack the laminin-binding integrin, $\alpha 6\beta 1$, hence it may be a possible prognostic marker of uveal melanoma (Elshaw, et al., 2001).

The Role of CD146 (Melanoma Cell Adhesion Molecule) in Tumour Development and Metastases

Another member of the Ig superfamily, CD146, was originally identified as a cutaneous melanoma specific protein, and has recently been discovered to be associated with the invasiveness of several uveal melanoma cell lines (Pardo, et al., 2005). CD146 is a cell surface adhesion molecule, previously designated by different names, including MUC18 (Mucin isotype 18), A32 antigen, MCAM, Mel-CAM (melanoma cell adhesion molecule) and S-endo-1, due to its identification in different tissues by several independent research groups (Shih, 1999). The name Mel-CAM or MCAM originally reflected the functional aspect of CD146, since it was shown to be a cell adhesion molecule in cutaneous melanoma cells (Shih, 1999).

Molecular Structure of CD146

CD146 is a highly glycosylated, 113 kDa single chain molecule (Shih, et al., 1994). CD146 contains a V-V-C2-C2-C2 immunoglobulin-like unit in the extracellular domain, an amino acid stretch (LKEEKN) and a relatively short cytoplasmic tail with several

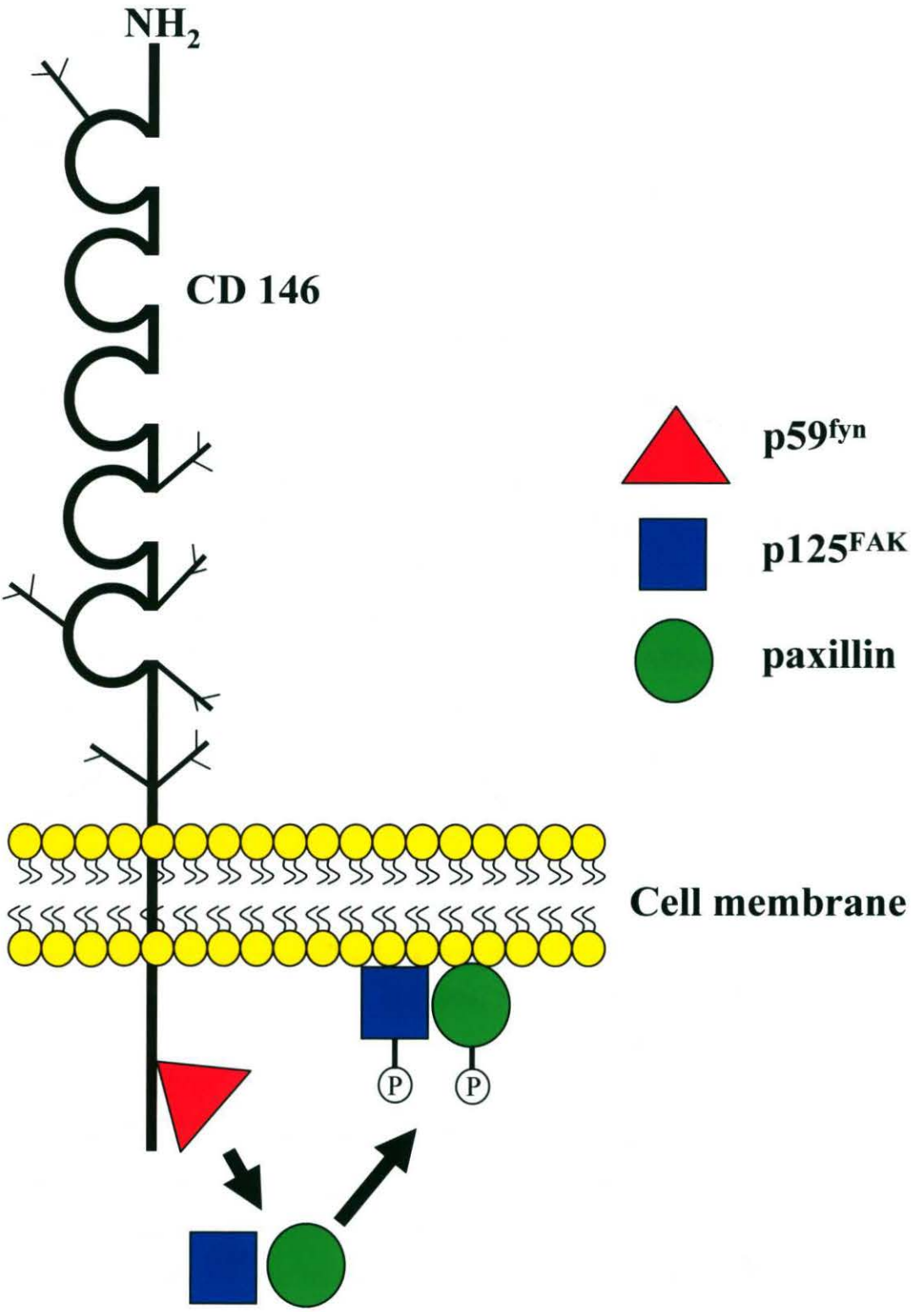

Figure 1.3

Molecular structure of CD146

***Adapted from Shih (1999). J Pathol, 189: 4-11.**

phosphorylation sites (Seftalioglu, et al., 2000; Shih, 1999) (Fig. 1.3). Activation in the cytoplasmic domain of CD146 associates with $p59^{fyn}$, a Src family kinase known to phosphorylate $p125^{FAK}$ and leads to its association with paxillin, a cytoskeletal protein essential in focal adhesion assembly (Anfosso, et al., 1998) (Fig. 1.3).

Functions of CD146

CD146 is involved in numerous biological processes including cell adhesion and migration, vascular development and embryo implantation (Liu, et al., 2004; Shih, et al., 1997). CD146 is expressed in vascular endothelium, activated T-lymphocytes, myofibroblasts, smooth muscle, Schwann cells and retinal ganglion cells (Bardin, et al., 1996; Shih, et al., 1998). It has also been proposed as a marker of angiogenic vascular endothelium (St Croix, et al., 2000; Yan, et al., 2003). Confocal and electron microscopic analysis of confluent human umbilical vein endothelial cells suggested that CD146 is a structural component of the endothelial junctions (Bardin, et al., 2001). Although CD146 has been suggested as a mediator of cell-cell interactions, its heterophilic ligand and mechanism of binding are still unidentified (Bardin, et al., 2001; Shih, et al., 1997).

CD146 in Tumour Development

CD146 is involved in the growth of various tumours including cutaneous melanoma, breast and prostate cancer (Sers, et al., 1994; Shih, et al., 1997; Wu, et al., 2001). CD146 expression is strongly up-regulated in malignant cutaneous melanoma cells compared to benign nevi, particularly in metastatic lesions (Johnson, 1994; Lehmann, et al., 1987, 1989; Wu, et al., 2001). In tissue microarrays of cutaneous melanomas, CD146 immunostaining is reported to be a highly significant independent prognostic marker inversely correlated with survival of melanoma patients (Pacifico, et al., 2005). CD146 expression in cutaneous melanoma cells increased tumour growth and metastases, while decreased expression reduced cell tumourigenicity, further supporting its role in promoting cutaneous melanoma progression (Satyamoorthy, et al., 2001; Xie, et al., 1997). Furthermore both *in vitro* and *in vivo* studies in cutaneous melanoma indicate that CD146 antibody can target both CD146-positive melanoma cells and tumor vascular endothelium, with possible inhibitory therapeutic effects on cutaneous melanoma growth and metastases (Leslie, et al., 2007; McGary, et al., 2003; Melnikova, et al., 2006). CD146

protein has been recently discovered to be associated with invasiveness of some uveal melanoma cell lines (Pardo, et al., 2005). The distribution and expression of CD146 in primary uveal melanoma remains to be been established. The expression of CD146 in primary uveal melanoma and its association with tumour growth is further explored in Chapter 4.

1.4 Risk Factors in Uveal Melanoma: Involvement of Ultraviolet (UV) Radiation

Epidemiological studies indicate that risk factors associated with increased incidence of uveal melanoma include age, occupation (in particular welding), race, iris colour, exposure to sunlamp radiation and cumulative exposure to ultraviolet (UV) radiation, particularly up to the second decade of life (Holly, et al., 1990; Hu, et al., 2005; Li, et al., 2000; Tucker, et al., 1985; Vajdic, et al., 2001, 2002, 2004). The relationship between cutaneous melanoma and UV exposure in particular, suggests that there may be a role for UV in uveal melanoma.

UV Exposure to the Human Eye

Solar radiation that passes through the earth's atmosphere consists of the visible spectrum (400-700 nm) and UV radiation (200-400 nm). UV can be divided into three groups, namely *UV-A* (315-400 nm), *UV-B* (290-315 nm) and *UV-C* (200-290 nm).

When the human eye is exposed to sunlight its anterior portion absorbs most of the UV, leaving approximately 1% UV reaching the retina (Sliney, 2002) (Fig 1.4.1). The cornea absorbs most of the *UV-A* and *UV-B*, and this absorption increases with age (Lerman, 1980). In early childhood the lens absorbs approximately 25% UV, and this increases up to 80% by the age of 80 years (Lerman, 1980). Finally, about 30% of the remaining UV will be further absorbed by the retinal pigmented epithelium (RPE) before it reaches the choroid (Peyman, et al., 1984). Although the choroid and ciliary body are well protected from UV in adults, substantial transmission of *UV-A* and *UV-B* is received in early childhood, and decreases slowly with age (Holly, et al., 1990; Seddon, et al., 1990).

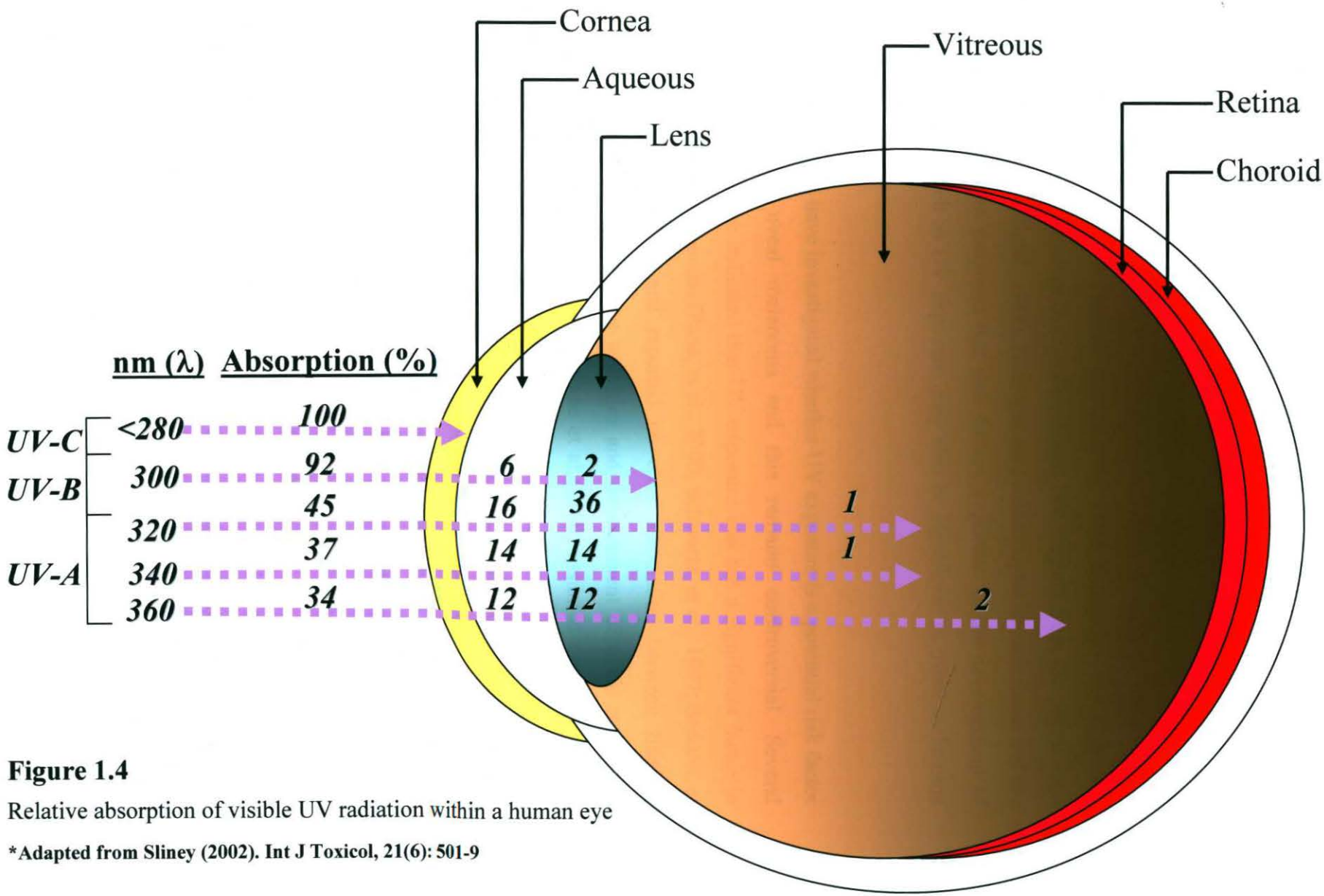

Figure 1.4

Relative absorption of visible UV radiation within a human eye

***Adapted from Sliney (2002). Int J Toxicol, 21(6): 501-9**

UV Exposure: a Risk Factor in Uveal Melanoma?

The Australian environment is known to receive high levels of UV related to its geographical location, and the Australian population is reported to have the highest incidence of cutaneous melanoma in the world (Gies, 2003). Cutaneous melanoma is believed to be derived from cutaneous melanocytes. Both cutaneous and choroidal melanocytes are known to originate from melanoblasts that migrate from the neural crest during embryogenesis (Nordlund, 1989). Differentiated melanocytes in each tissue bed are identical hence it has been proposed that risk factors important in the development of cutaneous melanoma, such as UV exposure, may also be significant in uveal melanoma (Hurst, et al., 2003).

Numerous studies have investigated whether UV exposure is a potential risk factor in the development of uveal melanoma and this remains controversial. Several epidemiological studies have indicated that UV exposure was not a significant factor in the development of uveal melanoma (Pane, et al., 2000; Schwartz, et al., 1997; Seddon, et al., 1990; Shah, et al., 2005) and reported no clear association between lifetime accumulative *UV-B* exposure, outdoor activities and development of uveal melanoma (Pane, et al., 2000; Seddon, et al., 1990). Pane et al (2000) assumed that *UV-B* might contribute to conjunctival melanoma rather than uveal melanoma due to the anterior portion of the eye receiving more UV than the choroid (Pane, et al., 2000). Schwartz *et al* (1997) have also pointed out that if UV is responsible for the development of uveal melanoma then its incidence should be influenced by geographical location similar to cutaneous melanoma, but no such relationship has been found (Schwartz, et al., 1997).

However, other epidemiological studies support a role for UV exposure as a potential risk factor in the development of uveal melanoma. (Holly, et al., 1990; Tucker, et al., 1985; Vajdic, et al., 2002). In particular, an Australian study indicated that sun exposure during the first 20 years of age, as well as outdoor occupations or activities in men before 30 years of age, were the most important risk factors associated with uveal melanoma (Vajdic, et al., 2002). This observation is consistent with the fact that a substantial amount of choroidal exposure to UV occurs during childhood to adolescence when the lens is still transparent (see above) (Holly, et al., 1990; Seddon, et al., 1990).

1.5 Aims

As discussed in this Chapter, growth and development of uveal melanoma involves both cellular and environmental factors. To further investigate these factors, this thesis aimed to:

1. Describe the expression and distribution of MMP-9 and TIMP-3 in primary uveal melanoma tumours and normal human eyes (Chapter 3).

2. Examine the *in vitro* expression of melanoma cell adhesion molecule (CD146) in a series of uveal and metastasis-derived cell lines and primary uveal melanocytes. The expression and distribution of CD146 protein in primary uveal melanoma tumours and normal human eyes, including the relationship of CD146 expression to tumour type was also studied (Chapter 4).

3. Investigate the *in vitro* effects of *UV-B* exposure on growth, viability and MMP production in uveal melanoma cell lines and primary uveal melanocytes (Chapter 5).

Chapter 2

General Materials and Methods

The studies in this thesis were performed according to the Declaration of Helsinki and with approval from the University of Sydney Human Ethics Committee.

2.1 Primary Specimens

Eyes enucleated for uveal melanoma (n=23 age range: 41 to 90 years) were routinely fixed in 10% neutral buffered formalin (NBF) and paraffin embedded (Anatomical Pathology, Prince of Wales Hospital) (Table 2.1). Postmortem eyes from donors (n=3; aged 39, 50 and 78 years old) obtained with consent from the Lions NSW Eye Bank, were fixed in 2% paraformaldehyde and NBF within 5-15 hrs after death and paraffin embedded. These were used as controls in these studies. For all specimens, paraffin sections were cut at 8μm and collected on Super-Frost Plus (Menzel-Glaser) slides.

Histopathology-Paraffin Sections

The histopathology of uveal melanomas was assessed by Hematoxylin & Eosin (H&E) and Periodic Acid Schiff (PAS) staining as follows.

H&E Staining

Sections were dewaxed in xylenes and rehydrated through alcohols to water and stained with Mayer's haematoxylin (DAKO Australia Pty Ltd) for 2 mins, followed by 1% eosin for one min. Stained sections were subsequently dehydrated through alcohols and xylenes, then coverslipped in DePeX (BDH Pty Ltd).

PAS Staining

Sections were dewaxed and rehydrated prior to incubation in 0.5% periodic acid solution for 10 mins. Sections were then stained with Schiff's reagent at room temperature (RT) for 15-30 mins, rinsed in 3 changes of freshly prepared 0.4% sodium metabisulphite for 4 mins each until the pink reaction product reached the desired density. After a further rinse in water to remove excess stain, sections were dehydrated, mounted in DePeX and coverslipped.

Table 2.1: Uveal Melanoma Characteristics

Specimen	Sex	Age (years)	Cell type	*Treatment	Time from detection to enucleation
1	M	41	Spindle B	No	Unknown
2	M	43	Spindle B	No	72 months
3	M	52	Spindle B	No	Unknown
4	M	49	Mixed	No	10 months
5	F	60	Mixed	No	1 month
6	M	64	Mixed	No	1 month
7	M	71	Mixed	No	5 months
8	F	74	Mixed	No	1 year
9	F	82	Mixed	No	2 years 3 months
10	M	90	Mixed	No	0.5 month
11	M	66	Mixed-spindle predominant	No	5.5 months
12	F	43	Mixed-spindle B predominant	No	1.5 months
13	M	53	Mixed-spindle B predominant	No	1 month
14	M	58	Mixed-spindle B predominant	No	1 year
15	F	55	Mixed-spindle A&B predominant	No	4 months#
16	F	63	Mixed-epithelioid predominant	No	6 months
17	F	85	Mixed-epithelioid predominant	No	7 months
18	M	61	Mixed + balloon cells	Plaque	3 years 10 months
19	M	62	Spindle	Plaque	5 years 1 month
20	F	68	Spindle	Plaque	12 years
21	M	77	Mixed	Plaque	1 year 2 months
22	F	81	Epithelioid	Plaque	1 year 11 months
23	F	85	Mixed	Plaque	11 years 9 months

*** I^{125} plaque therapy**

Immunohistochemistry

Sections were stained with various antibodies (Table 2.2). A summary of the method used for single immunolabeling is shown in Figure 2.1. Paraffin sections were dewaxed, rehydrated and rinsed in 0.1 M phosphate buffer with 0.9% sodium chloride (PBS, pH 7.4). Antigen retrieval was used to expose masked antigens; sections were incubated in 0.01 M citrate buffer (pH 6) at 80°C for 15 mins, and then allowed to cool to 40°C, before rinsing in PBS for 10 mins. This was followed by immersion in 5% H_2O_2 for 5 mins to block endogenous peroxidase activity. The sections were rinsed in PBS for 10 mins then circled with Dako pen (DAKO Australia Pty Ltd), incubated in 10% serum (normal sheep serum [NSS], normal donkey serum [NDS] or normal goat serum [NGS] depending on the species in which the secondary antibody was raised in) at room temperature (RT) for 20 mins (Fig 2.1). The sections were then incubated in primary antibodies for 48 to 72 hrs at 4°C (Fig 2.1). Following a 20 min rinse in PBS on a shaking table, sections were then incubated in the appropriate secondary antibody for 1 hr at RT (Table 2.3, Fig 2.1); rinsed in PBS for 20 mins on shaking table, then incubated in ExtrAvidin peroxidase (Sigma) for 1 hr (Table 2.4). Sections were further rinsed in PBS prior to visualization of antibody binding using Vector NovaRED substrate (Vector Labs Pty Ltd) (Table 2.4). The sections were counterstained in hematoxylin for 10-15 seconds, dehydrated through alcohols and xylenes, mounted in DePeX and coverslipped.

2.2 *In-Vitro* Studies

Cell Lines

Ten cell lines were kindly provided as follows: OCM-1, -3 & -8 (Dr J. Kan-Mitchell, Karmanos Cancer Institute, Department of Pathology and Immunology, Wayne State University, Detroit); OMM-1 (Dr G.P. Luyten, Erasmus University, Rotterdam), 92-1 (Dr M.J. Jager, Leiden University Medical Center, Leiden); Mel202 (Dr B. Ksander, Schepens Eye Research Institute, Boston) & OCM-1A, C918, MUM2B & MUM2C (Dr M.J. Hendrix, Children's Memorial Research Center, Northwestern University, Chicago)

Uveal (OCM-1, -3, -8, 92.1, Mel202, C918, OCM-1A) and metastasis-derived (OMM-1, MUM2B, MUM2C) cell lines were maintained in either RPMI-1640 medium (OCM-3 and -8, Mel202, 92-1, C918, MUM2C, MUM2B) or Dulbecco's Modified Eagle's Medium (DMEM) (OCM-1A, OCM-1 and OMM-1) supplemented with 10% heat

Table 2.2 Primary antibodies

Antibody	Species	Manufacturer	Dilution
Melanoma Ab-3 (HMB45/HMB50)	Mouse	NeoMarkers	1:50
Vimentin monoclonal	Rabbit	NeoMarkers	1:500
Vimentin monoclonal	Mouse	Dako	1:50
Anti-human fibroblast	Mouse	Dako	1:25
α-smooth muscle actin	Mouse	Dako	1:40
Glial fibrillary acidic protein (GFAP)	Mouse	NeoMarkers	1:100
MMP-9 polyclonal (latent/active)	Rabbit	NeoMarkers	4μg/ml
TIMP-3 Ab-1 monoclonal	Mouse	Calbiochem	2μg/ml
CD146	Goat	R&D Systems	2μg/ml
CD146	Goat	Santa Cruz	1:500
GAPDH	Mouse	Ambion	0.5μg/ml
Mouse immunoglobulins	Mouse	Dako	1:100
Rabbit immunoglobulins	Rabbit	Zymed	2μg/ml
Goat immunoglobulins	Goat	Zymed	2μg/ml

Table 2.3 Secondary antibodies

Antibody	Species	Manufacturer	Dilution
Alexa-488 conjugated anti-mouse	Goat	Molecular Probes	1:1000
Alexa-488 conjugated anti-rabbit	Goat	Molecular Probes	1:1000
Alexa-488 conjugated anti-goat	Rabbit	Molecular Probes	1:1000
Biotinylated anti-mouse Ig	Sheep	Amersham Pharmacia Biotech	1:100
Biotinylated anti-rabbit Ig	Donkey	Amersham Pharmacia Biotech	1:100
Biotinylated anti-goat Ig	Rabbit	Zymed	1:200
HRP-conjugated anti-goat IgG	Rabbit	Bethyl Laboratories	1:12,500
HRP-conjugated anti-mouse IgG	Goat	Upstate	1:20,000

Table 2.4 Others

Name	Manufacturer	Dilution
ExtrAvidin-peroxidase	Sigma	1:250
Vector NovaRED substrate kit	Vector Labs	N/A
Hoechst Bis-benzimide 33258	Molecular Probes	300nM

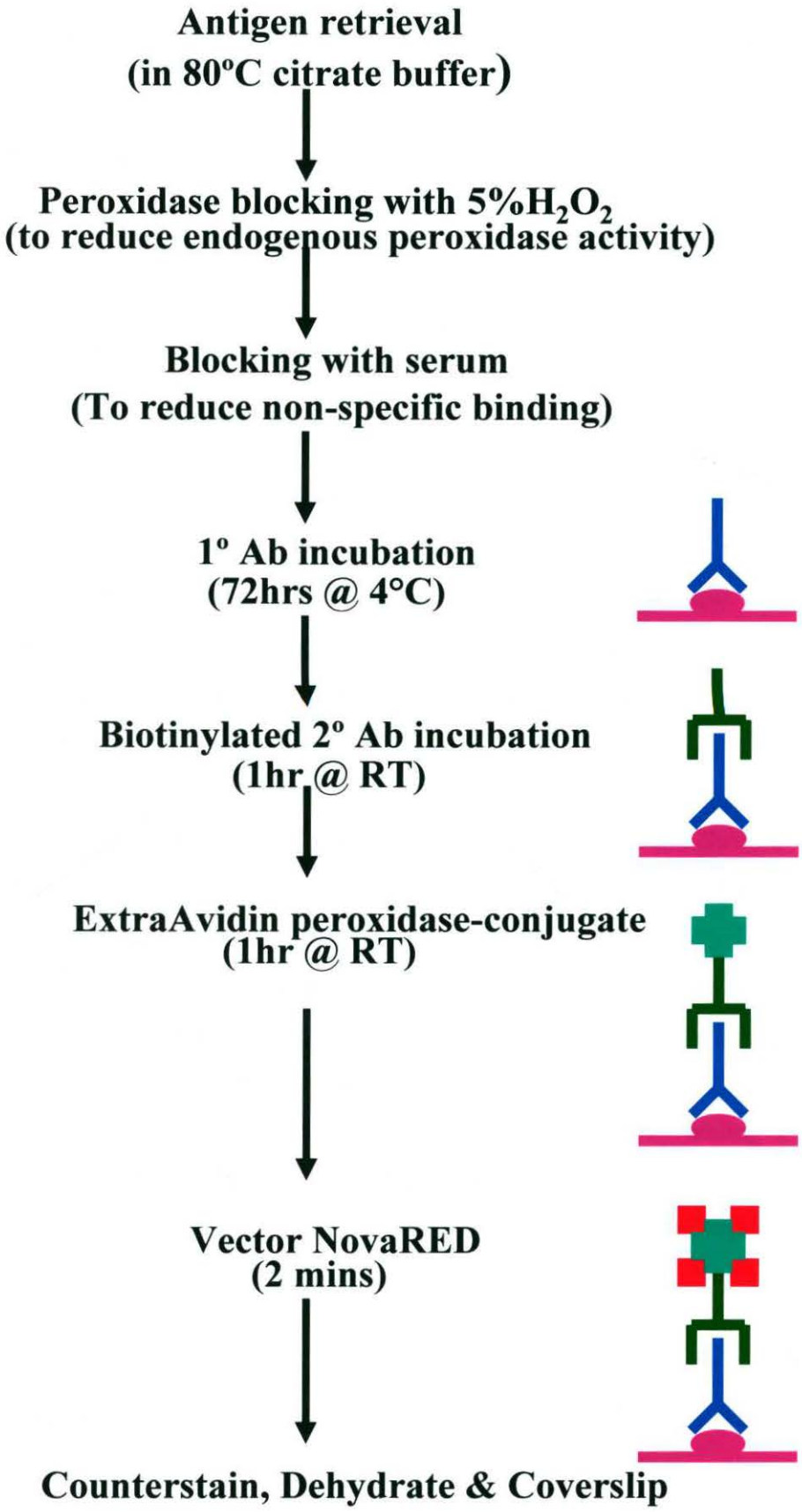

Figure 2.1
Immunohistochemistry protocol for single labelling using biotinylated secondary antibody and Vector NovaRED

inactivated foetal bovine serum (FBS), 2 mM glutamine, 50 IU/ml penicillin and 50 µg/ml streptomycin.

All cell lines were grown in 75cm^2 cell-culture flasks (NUNCLON Surface, NUNC), in a humidified incubator with 5% CO_2. For experiments, cells were detached using 0.25% trypsin/0.1% EDTA for 2 mins, deactivated with culture medium with 10% FBS, centrifuged for 5 mins at 290 *g* and 20°C. The pellet was resuspended in 4-5 ml culture medium, cell number and viability was assessed using 0.4% Trypan Blue and a hemocytometer counting chamber.

Human Uveal Melanocytes

Human uveal melanocytes were isolated from eyes (n=5; average *postmortem* delay approximately 16 hrs), obtained with consent from the Lions NSW Eye Bank (Sydney, Australia). The method for isolation, purification, and cultivation of human uveal melanocytes was based on the methods of Hu *et al* (1993), with minor modifications. Briefly, a circumferential incision was made in the anterior portion of the eye and cornea, anterior sclera, lens, iris, ciliary body, vitreous, retina as well as *ora serrata* were removed leaving the retinal pigmented epithelium (RPE) and choroid within the eyecup. The eyecup was filled with 0.25% trypsin/0.1% EDTA and incubated at 37°C incubator for 45 mins. The trypsin solution in the eyecup was gently pipetted to release the RPE. The trypsin/cell solution was removed and the eyecup rinsed with PBS twice. The choroid was then separated from the sclera, cut into 4 or 5 pieces and immersed in 0.25% trypsin/0.1% EDTA solution and incubated with shaking at 4°C for 18 hrs, then incubated for a further hr at 37°C. Trypsin activity was deactivated by adding 1 ml of Ham's F12 medium with 10% heat-inactivated FBS. The supernatant/released cells were collected and centrifuged for 5 mins at 290 *g* and 20°C. The pellet was resuspended in 1 ml melanocyte growth medium (MGM) [Ham's F12 supplemented with 10% FBS, 2 mM L-glutamine, 50 IU/ml penicillin/50 µg/ml streptomycin and 10 ng/ml cholera toxin (Sigma Chemical Co., USA), 100nM PMA (phorbol 12-myristate 13-acetate) and, 0.1mM isobutylmethylxanthine (IBMX) (Sigma)] and seeded into a 6-well plate (NUNCLON Surface, NUNC). This procedure was repeated a further 2 times, incubating the pieces of choroid in 1.2 U/ml dispase II (neutral protease) (165859, Roche) and 0.5 mg/ml collagenase (Type-1A; made from clostridium histolyticum, Sigma-Aldrich) at 37°C for 1 hr.

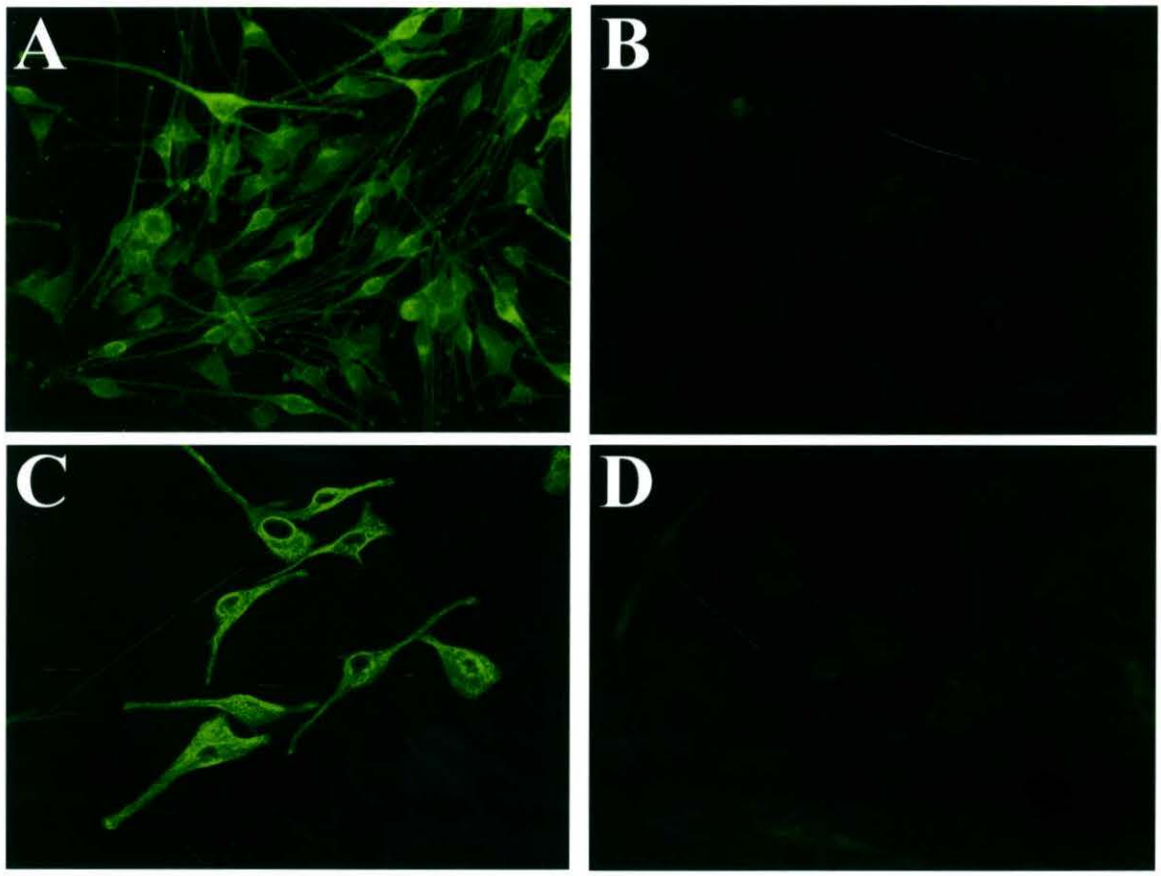

Figure 2.2
Uveal melanocytes immunolabelled with Melanoma Ab-3 (A), non-specific IgG1(B) antibody, vimentin (C) and human prolyl 4-hydroxylase (fibroblasts) antibody (D).

Figure 2.3
Inverted microscopy of uveal (A-G) and metastatic (H-J) cell lines.

A.OCM-1	F.OCM-1A
B.OCM-3	G.C918
C.OCM-8	H.OMM-1
D.92-1	I.MUM2B
E.Mel202	J.MUM2C

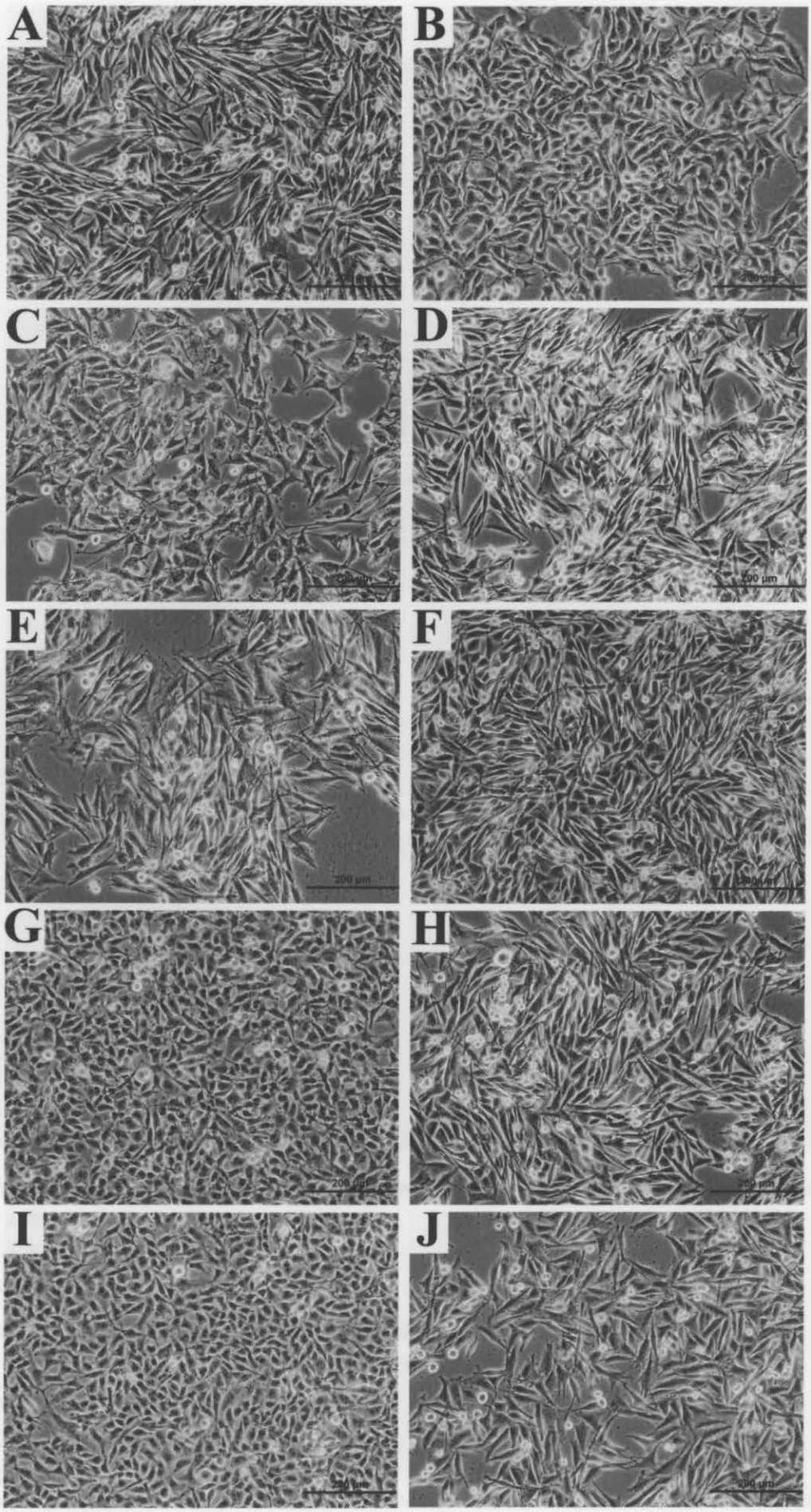
A
B
C
D
E
F
G
H
I
J

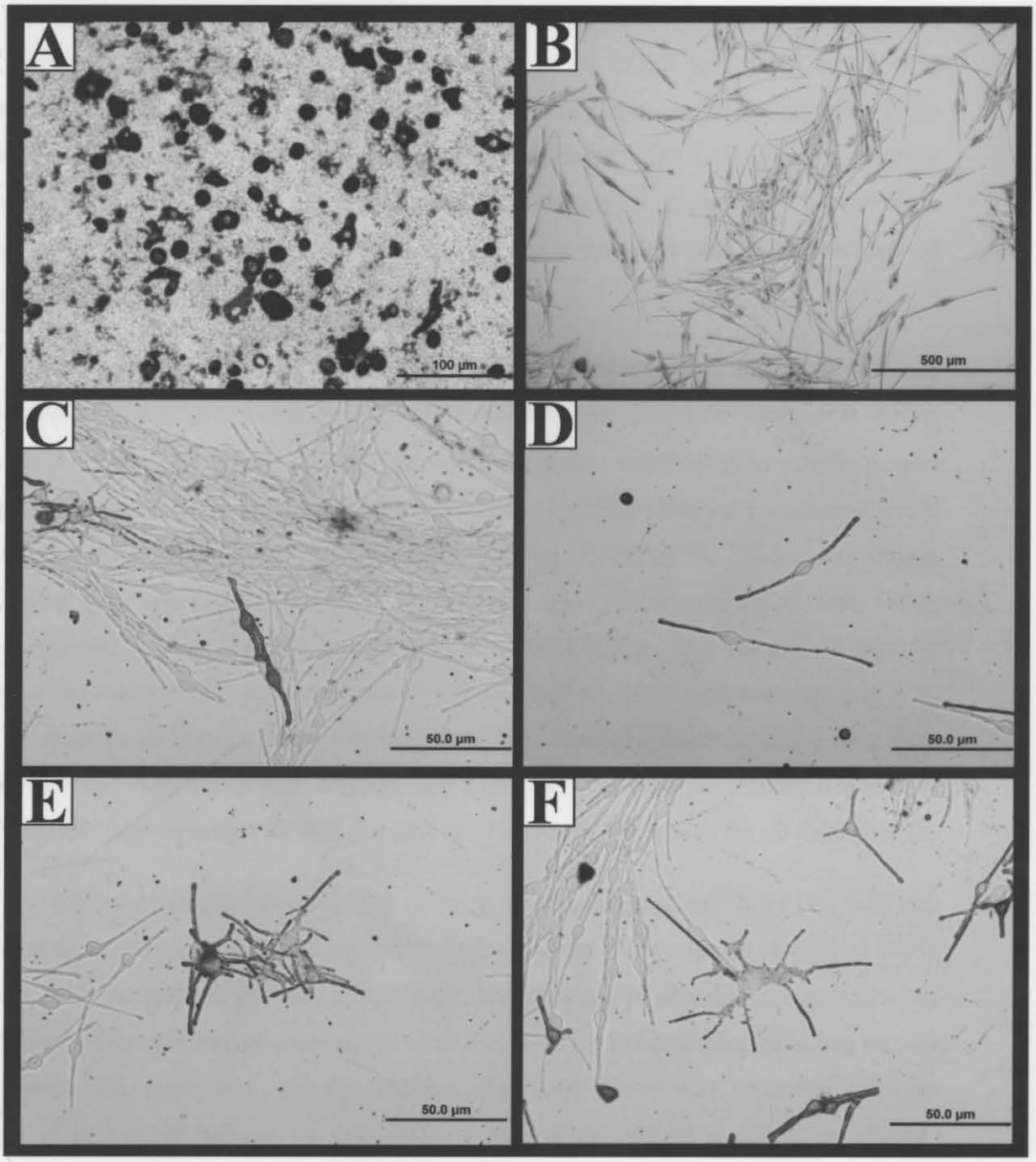

Figure 2.4
Cultured human uveal melanocytes
A. Freshly extracted melanocytes (P0).
B. Melanocytes (P2) after a PBS wash, and grown for a few weeks.
C. Mix of pigmented and depigmented melanocytes in a colony.
D. Melanocytes with bipolar processes.
E. Melanocytes with multiple processes.
F. Melanocyte with dendritic processes.

After 48 hrs, cultures were washed gently with warm PBS to remove debris and red blood cells. A further 1.5 ml of MGM was added. Cultures were allowed to grow for 2-4 weeks. Cells were detached using 0.25% trypsin/0.1% EDTA for 2 mins, deactivated with Ham's F12 medium with 10% FBS, centrifuged for 5 mins at 290 *g* and 20°C. Cells were resuspended in 1ml MGM and placed in 25cm^2 flask (NUNCLON Surface, NUNC) with 6 ml MGM. In general, primary uveal melanocytes grew more slowly than transformed cell lines, required medium renewal twice per week and were passaged on average 7-10 days.

To assess the purity of the melanocytes, ~10^4 cells/well were seeded onto sterile glass coverslips and immunolabelled. The following primary antibodies were used: mouse anti-human fibroblast (prolyl 4-hydroxylase) (1:25; Dako, Denmark), α-smooth muscle actin (1:40; pericytes, Dako), and Melanoma Ab-3 (1:100; antibodies to melanoma and melanocyte-specific antigens HMB-45 and HMB-50, NeoMarkers, USA); and mouse anti-swine vimentin (1:100; Dako). A non-specific IgG1 isotype control (1:100; Dako, Denmark) was used to confirm specificity of immunolabelling. The primary melanocyte cultures used were >95% pure, confirmed by Melanoma Ab-3 immunoreactivity (Fig 2.2), and an absence of human prolyl 4-hydroxylase (fibroblasts) immunolabelling (Fig 2.2). Cultures with >95% purity were subsequently passaged when they became semi-confluent and used for experiments or frozen. Passage (P) 1 to 3 cells were used for all experiments.

Photomicrographs were taken of cultured uveal melanoma cell lines (Fig 2.3) and uveal melanocytes (Fig 2.4) with an inverted phase-contrast microscope (Olympus IX70, Japan), to document cell growth, morphology, and presence or absence of contaminating cells. Several morphological phenotypes were observed for melanocytes including bipolar, multiprocessed, pigmented and dendritiform (Fig 2.4). These may represent different stages of growth in culture, or even suggest subpopulations of melanocytes perhaps including progenitor cells (Xu, et al., 2007).

Immunocytochemistry

Uveal melanocytes and uveal melanoma cells were stained with various antibodies (Table 2.2), and summary of the method used for immunocytochemical staining is shown in Figure 2.5. Sterile glass coverslips were seeded with 2.5-5x10^4 cells and incubated at 37°C for 3 to 5 days. Coverslips were fixed in 2% paraformaldehyde in PBS (pH 7.4) for 10 mins, rinsed in PBS, and incubated for 20 mins at RT with 10% serum (dependent on

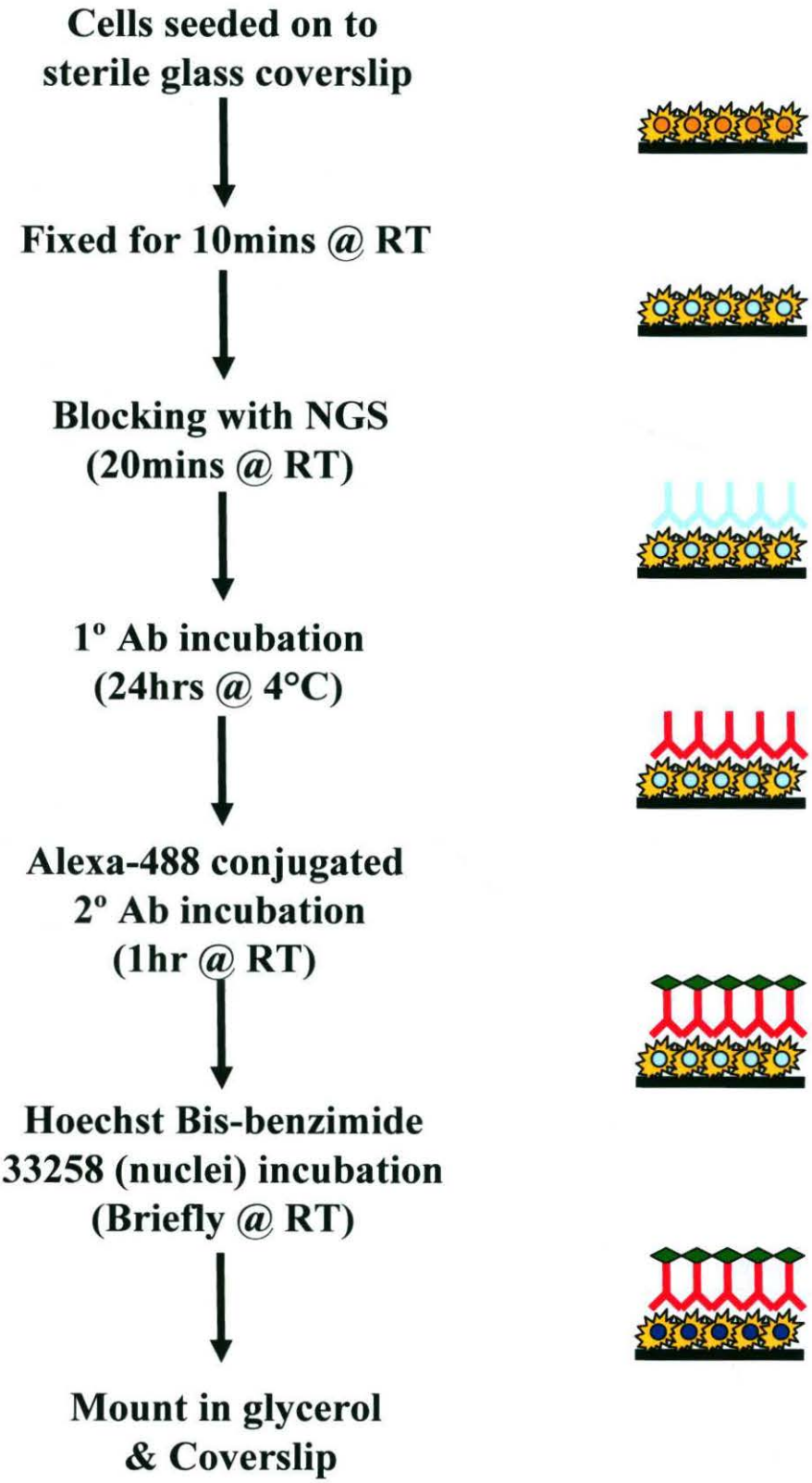

Figure 2.5
Immunocytochemistry protocol for single labelling, visualised using Alexa-488 conjugated secondary antibody

the species of the secondary antibodies) to reduce nonspecific binding (Fig 2.5). Cells were incubated in primary antibodies overnight at 4°C, and labelled for immunofluorescence using the appropriate Alexa-488 conjugated secondary antibody (1:1000, Molecular Probes, USA) for 1 hr at RT. Nuclei were stained with Hoechst Bis-benzimide 33342 (Molecular Probes, USA) (Fig 2.5). Coverslips were rinsed with PBS, mounted in glycerol, and viewed using either inverted fluorescence microscopy (Olympus IX70, Japan) or a LSM 5 PASCAL laser scanning confocal microscope (Carl Zeiss, Germany). For inverted microscopy, images were collected using OLYMPUS DP Controller software and exported to Photoshop for analysis. For confocal microscopy, images were collected either as single scans or as multiple Z-stacks, using LSM 5 PASCAL Version 3.2 SP2 software and exported to Photoshop for analysis.

Chapter 3

Expression and Distribution of MMP-9 & TIMP-3 in Uveal Melanoma

Results from this study are included in the publication: K Lai, RM Conway, R Crouch, MJ Jager and MC Madigan: Expression and Distribution of MMPs and TIMPs in Human Uveal Melanoma. *Exp Eye Res*. PMID: 18423620, Mar 16 2008.

3.1 Introduction

As discussed in Chapter 1.3, MMPs and TIMPs are implicated in the development and growth of uveal melanoma. This topic was originally studied during Honours and demonstrated specific distributions of MMP-1, -2, -19, MT1-MMP and TIMP-2 in a series of uveal melanomas, supporting their role in tumour growth and invasion (Lai, 2002). This included documenting expression in tumour cells, vasculature and stromal cells, as well as topographical variations throughout uveal melanomas.

The current study expands these original observations to include MMP-9 and TIMP-3. Several studies suggest that latent MMP-9 (along with latent MMP-2) is associated with a higher incidence of metastatic disease in uveal melanoma (El-Shabrawi, et al., 2001; Rao, et al., 2004). Epithelioid melanomas or the epithelioid portion of mixed-cell melanomas have been found to predominantly express latent MMP-9 and patients with tumours expressing TIMP-1 and TIMP-2, the main physiological inhibitors of MMP-2 and MMP-9 respectively, have a better survival rate (El-Shabrawi, et al., 2001). A small series of mixed morphology uveal melanomas were also found to express MMP-2, -9, -13 and MT1-MMP (Laver, 2002).

Downregulation of TIMP-3 has recently been shown to be associated with the invasiveness of uveal melanomas (van der Velden, et al., 2003) (see Chapter 1.2). A 5-fold decrease in TIMP-3 gene expression is reported in metastatic uveal melanoma cells when compared to primary uveal melanoma cells, regulated by DNA methylation (van der Velden, et al., 2003). Furthermore, a relationship between TIMP-3 protein expression and chromosome 3 status in uveal melanoma has yet to be established (Nareyeck, et al., 2005).

Aim

The expression of MMP-9 and TIMP-3, including regional differences in immunolabelling of tumour cells, stroma and the vasculature, has not been fully described in uveal melanoma. To better understand the dynamics of the tumour microenvironment, the distribution of MMP-9 and TIMP-3 pattern in different regions of uveal melanomas and adjacent choroid was investigated.

3.2 Materials and Methods

Paraffin Sections

Paraffin sections were cut from eyes enucleated for uveal melanoma, and normal eyes as described in Chapter 2.1. Uveal melanoma specimens included 18 untreated melanomas and 5 I^{125}-treated melanomas (Table 2.1), and the majority of tumours were located in the choroid posterior to the equator. Normal human eyes (n=3; aged 39, 50 and 78 years), provided by the Lions NSW Eye Bank with consent and ethical approval, were fixed in 10% neutral buffered formalin, paraffin-embedded, and used as controls (see Chapter 2.1).

Immunohistochemistry

As described in Chapter 2.1, sections were immunolabelled with antibodies to MMP-9 and TIMP-3 (Table 2.2) and visualized with peroxidase and Vector NovaRed (Vector Laboratories).

Immunostaining of melanomas was graded in masked fashion by 2 independent observers (KL, MM) using a semi-quantitative scale where 0 = none, 1 = weak (low intensity staining of tumour cells regardless of %, and medium intensity staining of ≤20% cells); 2 = moderate (medium intensity staining of >20% tumour cells, high intensity staining of ≤20% tumour cells), and 3 = strong (high intensity staining of >20% tumour cells). Differences in grading were resolved by joint review and if necessary, consultation with a third independent observer. The grading of the 2 observers was significantly correlated ($p<0.001$; Kendall's rank correlation). Non-parametric linear regression analysis was used to test for an association between cell type (1 = spindle; 2 = mixed or 3 = epithelioid), MMP-9 and TIMP-3 immunolabelling (grades 0 to 3), and maximum tumour height (in mm).

The distribution and intensity of MMP-9 and TIMP-3 immunostaining in retina overlying tumours and in regions of choroid and retina without melanoma, as well as in normal choroid and retina, was also assessed.

Additionally, control and melanoma-associated attached retina, as well as detached retina were double immunolabelled with antibodies to MMP-9 (raised in rabbit) and glial fibrillary acidic protein (GFAP) (NeoMarkers; raised in mouse, 4µg/ml). Briefly

paraffin sections were dewaxed, dehydrated and antigen retrieval performed as for single immunolabeling. Blocking of endogenous peroxidase activity was not required. The sections were then circled with Dako pen, incubated with 10% NGS at room temperature for 20 mins. The sections were incubated in a mixture of MMP-9 and GFAP antibodies for 72 hrs at 4°C. After rinsing in PBS on a shaking table for 20 mins, sections were incubated in a mixture of anti-rabbit Alexa-488 and anti-mouse Alexa-594 (Molecular Probes, USA) for an hr at room temperature and protected from light exposure. After rinsing with PBS, sections were mounted in glycerol, coverslipped and viewed with a Zeiss LSM 5 Pascal laser scanning confocal microcope and LSM 5 Pascal Image software. Multichannel excitation bleedthrough was minimized by using fluorochromes with a large difference in peak excitation (488nm and 594nm respectively). Emission bleedthrough was minimized by Multitracking, where signal crosstalk between neighbouring channels was corrected by performing a sequential image capture routine. This process combined images acquired with a single excitation beam/single detection channel acquisition process. This methodology was employed to correct for the effects of emission crosstalk.

3.3 Results

Tumour Histopathology

The histopathology of uveal melanomas was assessed from H&E and PAS stained sections as described in Chapter 2.1. Uveal melanomas displayed spindle cell (n=5/23), or mixed and epithelioid cell (n=17/23) morphology (Fig. 1.1.3A & B). Tumours ranged from 5 to 24mm maximum diameter and 2 to 14mm maximum height (Chapter 2.1, Table 2.1a). Rupture of Bruch's membrane and dome-shaped tumours were observed in 7/23 (30%) of specimens. Melanomas had low mitotic rates (n=13; $\leq$ 5 mitoses/high-power field). Small and large blood vessels were observed throughout all tumours (Fig. 1.1.4A). I^{125}-treated melanomas displayed areas of scarring with remnants of tumour cells, necrosis and increased numbers of leukocytes. For untreated specimens, extracellular matrix (ECM) patterns in PAS-stained sections were classified as described previously (Folberg, et al., 1992, 1993), with the following patterns observed: vessel lumens only (Fig. 1.1.4A), straight channels (Fig. 1.1.4B), incomplete loops (Fig. 1.1.4C) and complete loops and networks (Fig. 1.1.4D). Incomplete loops, complete loops and networks were seen in 1/3 spindle cell tumours and 8/15 mixed and epithelioid tumours. ECM patterns were not assessed in I^{125}-treated melanomas due to the presence of radiation-associated pathology.

Immunohistochemistry

Distinct patterns of immunolabelling for MMP-9 and TIMP-3 were seen in uveal melanomas (see below; Fig. 3.1 & 3.2). Overall no significant association was found between tumour cell type and expression of MMP-9 and TIMP-3 ($P>0.05$; non-parametric regression, Table 3.1). The majority of specimens displayed much reduced immunoreactivity for MMP-9 and TIMP-3 at the tumour-scleral interface (TSI), with a band of increased immunolabelling immediately adjacent to this region (Fig. 3.1). Sections incubated in either rabbit Ig or non-specific mouse anti-IgG1 as controls showed no immunolabelling (Fig. 3.1F & 3.2D respectively).

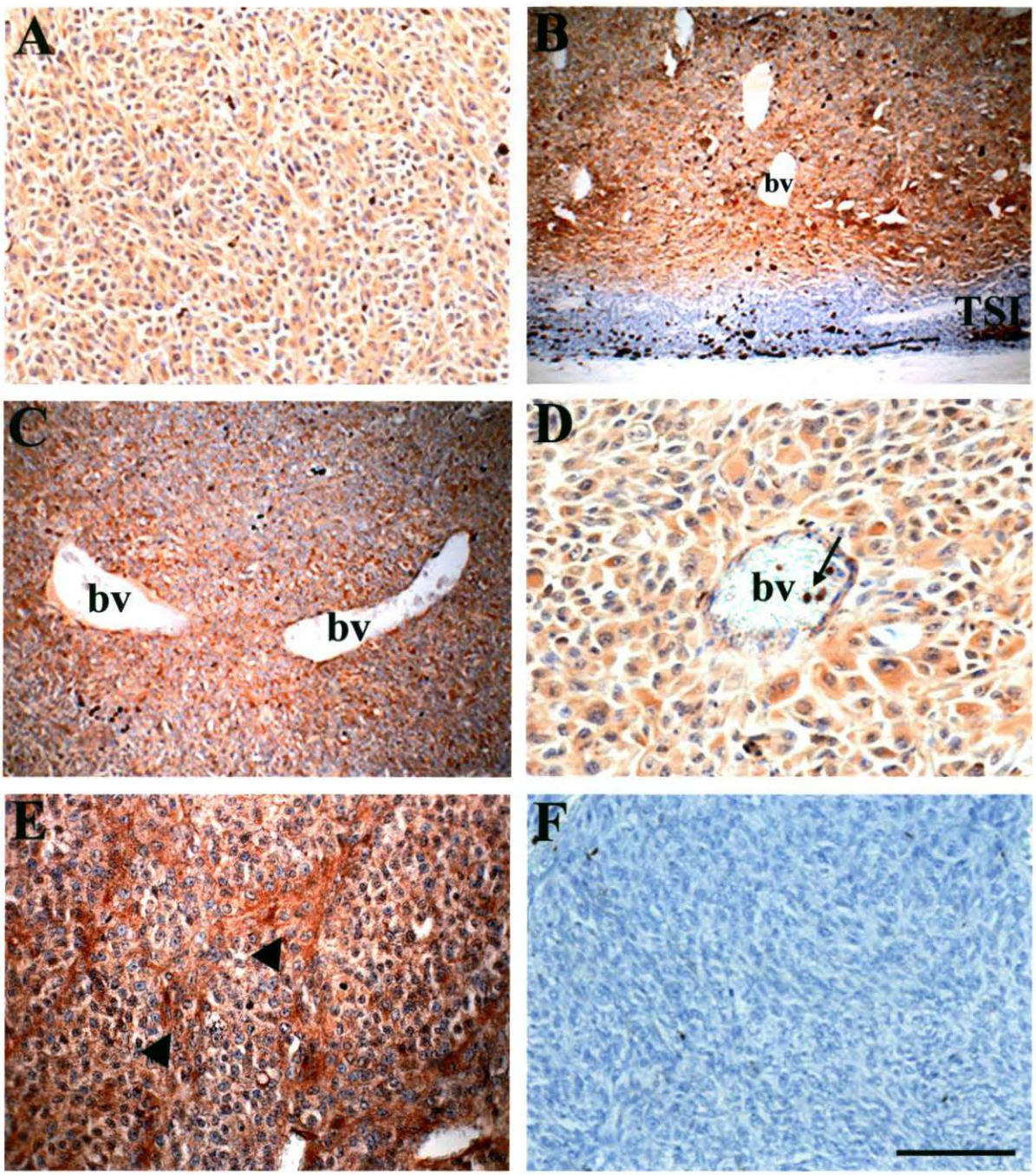

Figure 3.1
Uveal melanoma immunolabelled for MMP-9 and Ig control. A. General MMP-9 immunolabelling of tumour cells. B. The tumour scleral interface shows no MMP-9 immunolabelling. C&D. Tumour cells and vasculature display MMP-9 expression. Intravascular leucocytes are also MMP-9-positive (D; arrow). E. Extravascular matrix patterns immunolabelled for MMP-9 (arrowheads; *cf* PAS staining, Fig 1.1.4). F. Sections incubated with rabbit Ig control. (TSI – tumour scleral interface, bv - blood vessel. Scale bar = 50μm)

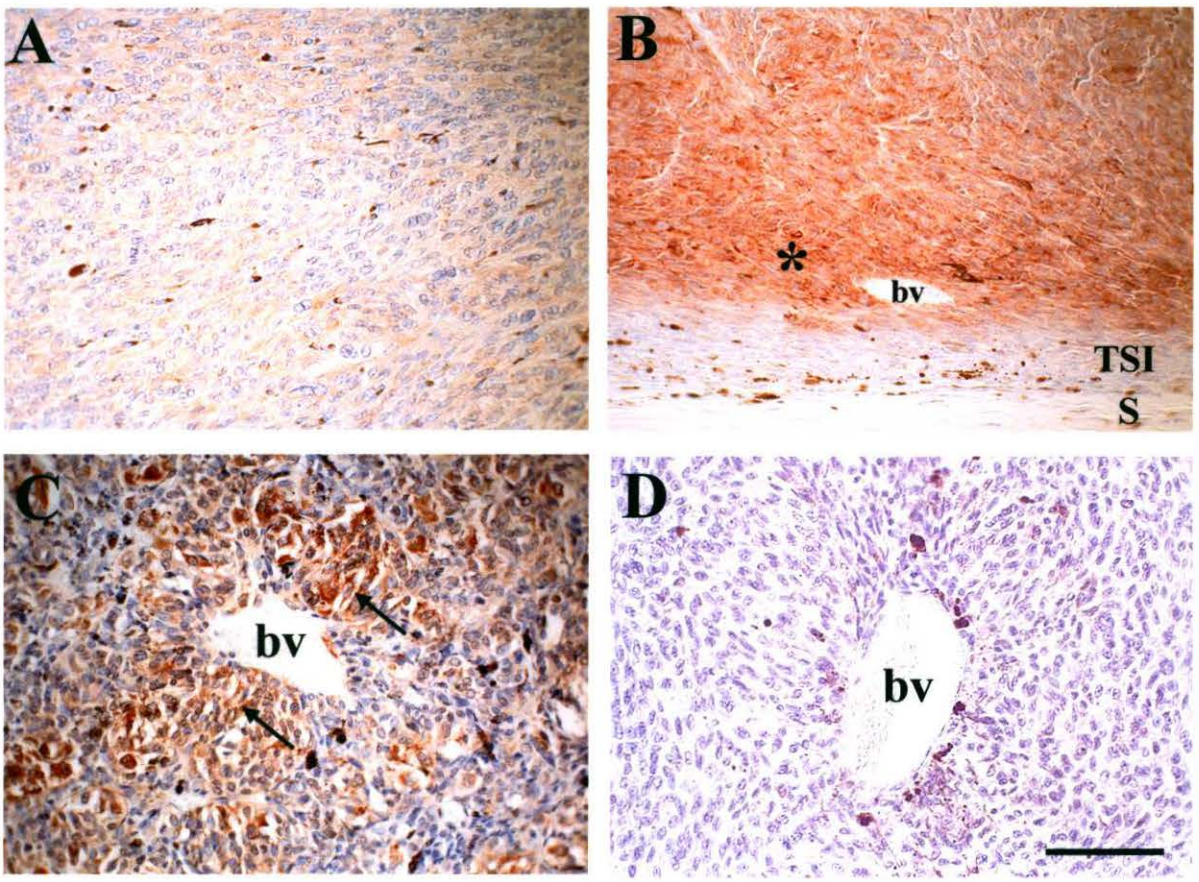

Figure 3.2
Uveal melanoma immunolabelled for TIMP-3 and Ig control. A. General TIMP-3 immunolabelling of tumour cells. B. Localised TIMP-3 immunolabelling in peripheral tumour (*). C. TIMP-3 immunostaining of melanoma cells (mostly epithelioid) surrounding vasculature (arrows). D. mouse IgG1 isotype control showed no reactivity. (bv – blood vessel. TSI – tumour scleral interface. S – sclera. Scale bar = 50μm)

Distribution of MMP-9 in Primary Uveal Melanoma

The majority of tumours showed moderate to strong cytoplasmic MMP-9 immunolabelling (74% ≥Grade 2, Table 3.1; Fig. 3.1). There was less difference in levels of immunostaining of central tumour and regions adjacent to the TSI for MMP-9 than for other MMPs, as observed previously (Lai, 2002; Lai, et al., 2007). Heterogeneous MMP-9 immunolabelling of tumour vessels was observed (Fig. 3.1C&D), and intravascular leukocytes expressed MMP-9 (Fig. 3.1D). Patterns of MMP-9 expression similar to the PAS-positive extravascular matrix patterns described above (Fig. 3.1E *cf* Fig. 1.1.4C & D) were seen in 4/23 mixed/epithelioid tumours. For the I^{125} treated specimens, MMP-9 immunolabelling was observed in the leukocytes and localised near the areas of necrosis and scarring.

Table 3.1 MMP-9 & TIMP-3 Immunostaining of Uveal Melanomas

	n	< Grade 2[a]	≥ Grade 2[a]
MMP-9	23	6/23 (26%)	17/23 (74%)
TIMP-3	23	11/23 (48%)	12/23 (52%)

[a]Average semi-quantitative grade: 0=none, 1= weak (low intensity staining of tumour cells regardless of %, and medium intensity staining of ≤20% cells); 2=moderate (medium intensity staining of >20% tumour cells, high intensity staining of ≤20% tumour cells), and 3= strong (high intensity staining of >20% tumour cells).

Distribution of TIMP-3 in Primary Uveal Melanoma

Cytoplasmic TIMP-3 immunostaining was expressed at moderate to high levels (≥ grade 2) in ~50% of tumours (Table 3.1, Fig 3.2). Peripheral tumour regions (excluding the TSI) showed localized strong TIMP-3 immunolabelling in ~25% of cases (Fig 3.2B). In 5/23 tumours, local areas of tumour cells surrounding blood vessels had intense TIMP-3 immunostaining, although the vasculature did not express TIMP-3 (Fig 3.2C). For the I^{125} treated specimens, TIMP-3 also appeared to be localised in tumour cells near areas of necrosis and scarring, but with lower intensity than MMP-9.

Distribution of MMP-9 and TIMP-3 in Control & Uveal Melanoma Associated Retina

In control and melanoma eyes, weak to moderate MMP-9 immunolabelling was observed throughout the retina including the ganglion cell layer, retinal blood vessels, inner and outer plexiform layers, some Müller cells processes, retinal pigmented epilthelium (RPE), choriocapillaris and large choroidal blood vessels (Fig 3.3 A & B). However, in some regions of detached retina associated with uveal melanoma, increased expression of MMP-9 was seen localised in the macroglia (i.e Müller cells and astrocytes) and plexiform layers (Fig 3.4 A & B). Additionally this localisation was also observed in some regions of retina overlying the tumour (Fig 3.4 C & D). Control and melanoma eyes displayed moderate to strong TIMP-3 expression in Bruch's membrane and drusen (Fig 3.3 D & E). Little or no TIMP-3 immunolabelling was observed in the retina (Fig 3.3D & E).

To further explore the MMP-9 expression in the macroglia associated with retinal detachment, control (n=3) and melanoma-associated retinae (n=7) were double-immunolabelled with MMP-9 and GFAP antibodies. GFAP is known to be up-regulated in activated Müller cells in retinal pathologies including detachment (Erickson, et al., 1987). The detached retina was generally disorganised, with loss of the outer plexiform layer, much reduced inner plexiform layer and possible loss of neurons (Fig 3.4B). In both control and melanoma-associated attached retinae, MMP-9 immunolabelling was similar to that seen in immunoperoxidase labelled sections while GFAP was observed in the macroglia (Fig. 3.5A). In some regions of the detached retinae, MMP-9 and GFAP were co-localised within the macroglia (Fig 3.5 B & C).

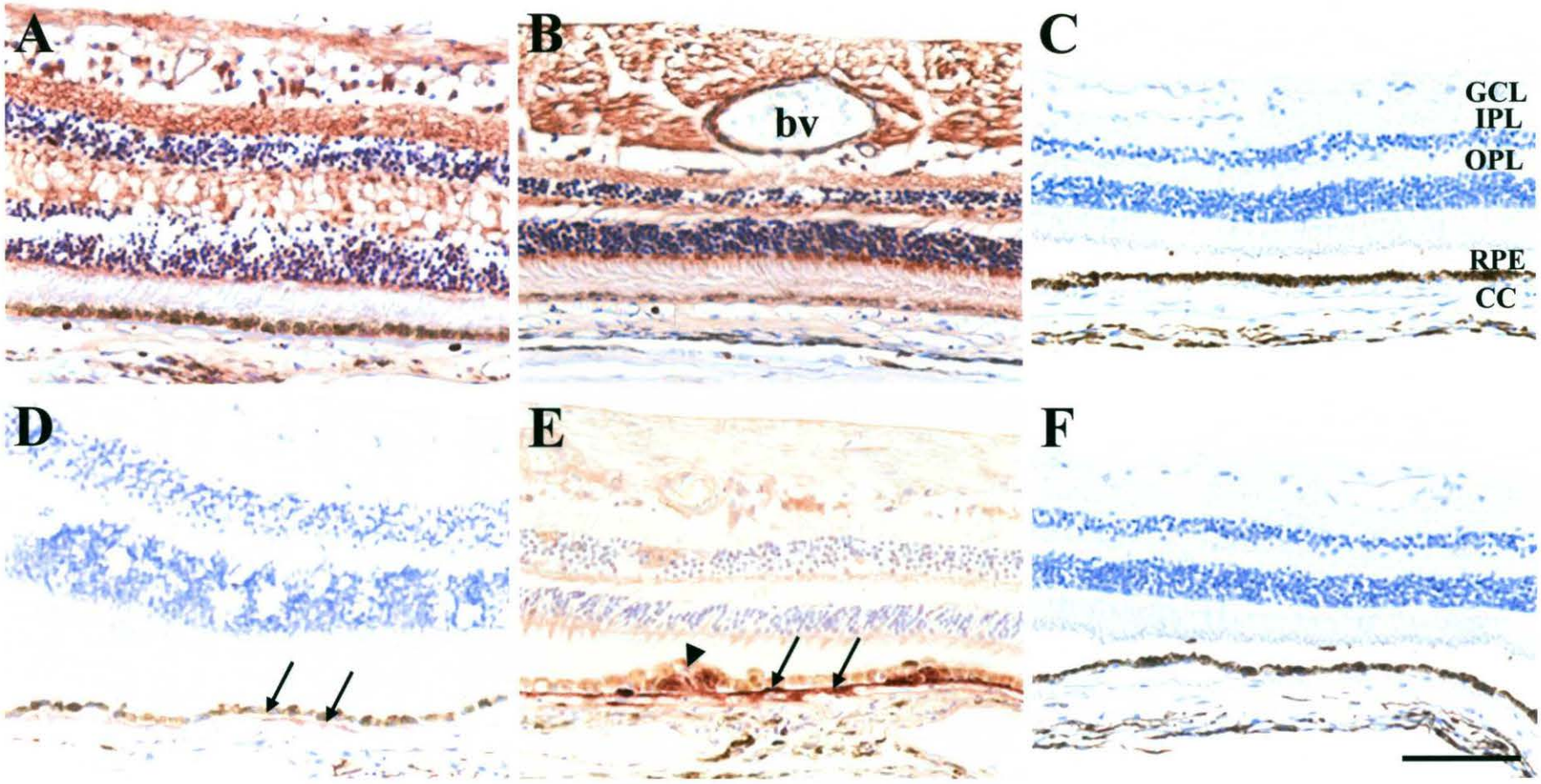

Figure 3.3
Control and uveal melanoma retina immunolabelled for MMP-9, TIMP-3 and Ig control. A&B. MMP-9 immunolabelling of blood vessels, ganglion cell layer, inner and outer plexiform layers, choriocapillaris and RPE in (A) control and (B) melanoma eyes. D&E. TIMP-3 immunolabelling of Bruch's membrane (arrows) in (D) control and (E) melanoma eyes. TIMP-3 immunolabelling of drusen is also observed in a melanoma eye (arrowhead). C&F. Mouse IgG1 isoptype control (C) and rabbit Ig control (F) showed no reactivity. (bv - blood vessel, GCL - ganglion cell layer, IPL - inner plexiform layer, OPL - outer plexiform layer, RPE - retinal pigmented epithelium, CC - choriocapillaris. Scale bar = 100μm)

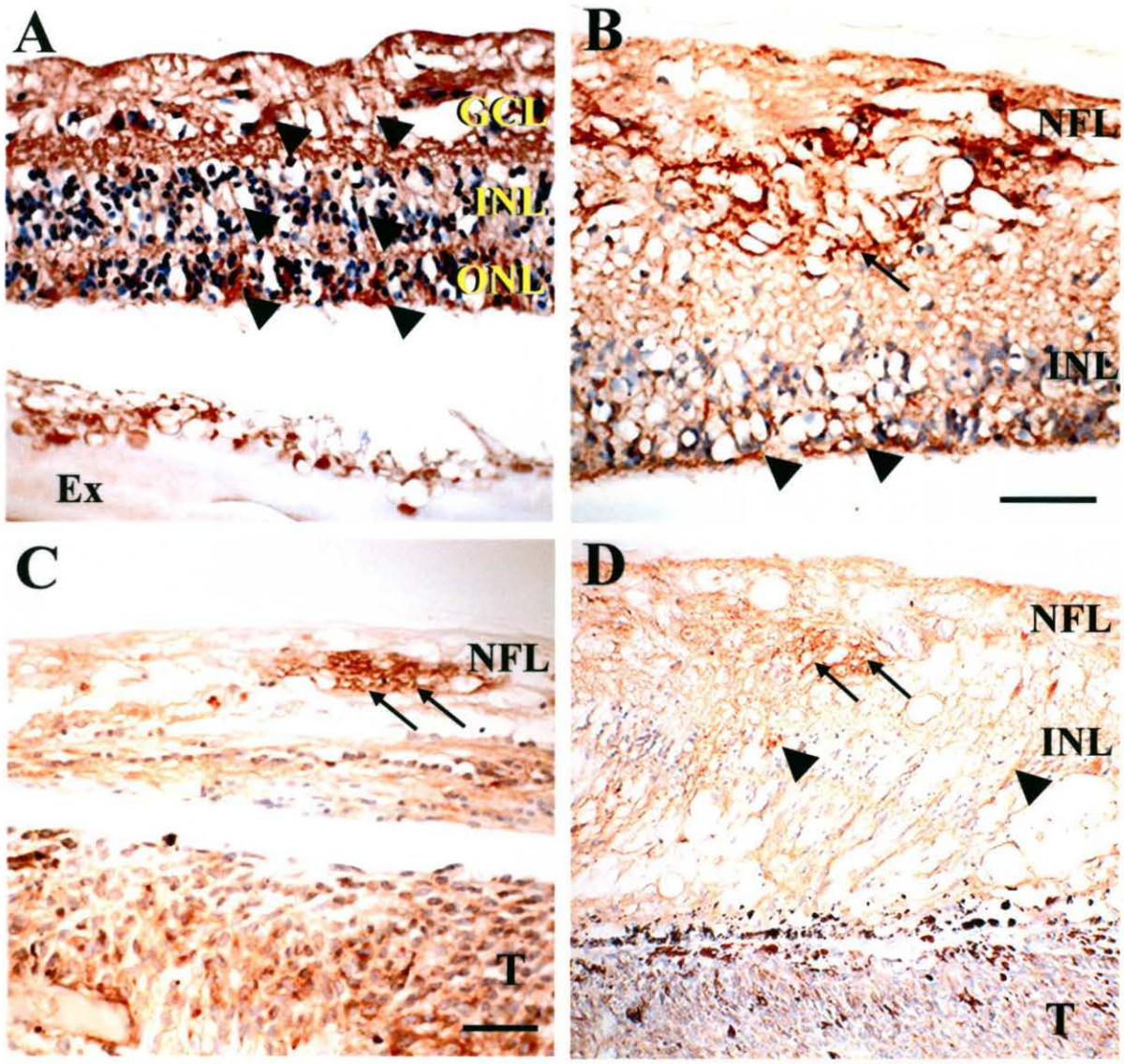

Figure 3.4
MMP-9 immunolabelling in detached retina associated with melanoma. A. MMP-9 is seen in presumptive Müller cell processes extending from the inner retina to the outer nuclear layer (arrowheads). B. Localised MMP-9 in the astrocytes and Müller cells. C. MMP-9 localised in the astrocyte (arrows) in the retina overlying the tumour. D. In another retina overlying the tumour, increased MMP-9 immunolabelling is seen in both astrocytes (arrows) and end processes of Müller cells (arrowheads). (NFL – nerve fibre layer, GCL – ganglion cell layer, INL – inner nuclear layer, ONL – outer nuclear layer, Ex – exudate, T – tumour. Scale bar = 50μm)

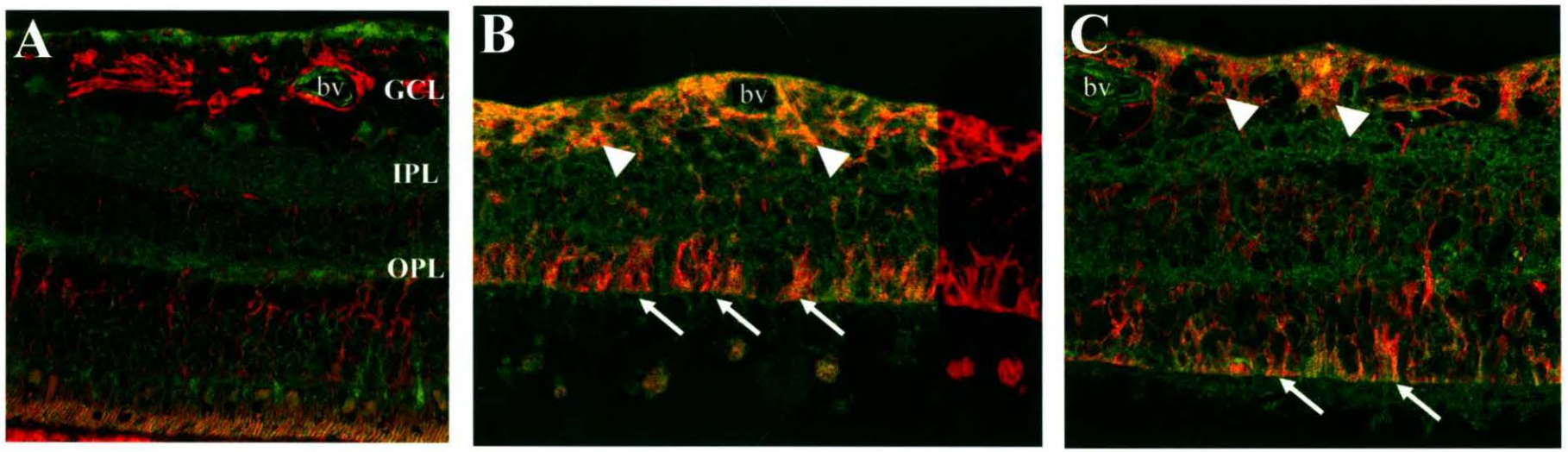

Figure 3.5
MMP-9 (green) and GFAP (red) double-immunolabelling in retina. A. Attached retina associated with melanoma displayed similar MMP-9 expression to immunoperoxidase stained sections (Fig 3.3). GFAP is observed in the macroglia (predominantly astrocytes & some Müller cell processes). B & C. Regions of detached retina displayed co-localisation of MMP-9 & GFAP in astrocytes (arrow heads) and Müller cell processes (arrows) extending from inner to outer retina. In B, the distribution of GFAP in the detached retina is seen with the red channel only. (bv – blood vessel, GCL – ganglion cell layer, IPL – inner plexiform layer, OPL – outer plexiform layer)

3.4 Discussion

Distinct patterns of immunostaining for MMP-9 and TIMP-3 were observed in uveal melanomas, although a statistically significant association between tumour type and expression of MMP-9 and TIMP-3 was not found, most probably related to the small number of specimens. Survival analysis for these patients was not possible as tumours were collected recently and this information was not available.

Distribution of MMP-9 in Uveal Melanoma

In the present study, heterogeneous MMP-9 expression was observed in both melanoma cells and tumour blood vessels. Moderate to high levels of MMP-9 expression were observed in the majority of all uveal melanoma specimens, consistent with previous studies (El-Shabrawi, et al., 2001; Laver, 2002; Rao, et al., 2004). As mentioned in Chapter 1.1.4B angiogenesis, plays an important role in the development of uveal melanoma (Folberg, et al., 1993; reviewed Jager, et al., 2004). Uveal melanomas also display an additional microcirculation - extravascular matrix channels (vasculogenic mimicry) - produced by tumour cells themselves (see Chapter 1.1.4B) (Folberg, et al., 2004; Maniotis, et al., 1999). Angiogenic factors including vascular endothelial growth factor (VEGF) and bFGF have been reported to be expressed in uveal melanoma cells, tumour vasculature and cell lines (Abdel-Rahman, et al., 2005; Boyd, et al., 2002; Missotten, et al., 2006; Notting, et al., 2006).

MMPs have been implicated in both angiogenesis and vasculogenic mimicry related to their ability to degrade vascular basement membranes as well as to activate growth factors including VEGF, bFGF and TGF-β (Iida, et al., 2007; Seftor, et al., 2001; Raffetto, et al., 2008). A recent study also showed that VEGF-A and MMP-9 were associated with metastatic uveal melanoma (Sahin, et al., 2007). MMP-2, -9 and MT1-MMP have been reported to facilitate tumour angiogenesis, cell migration and invasion (Egeblad, et al., 2002; Hofmann, et al., 2000; Sato, et al., 1994; Stamenkovic, 2000). Human endothelial cells have been found to constitutively secrete pro-MMP-2, further supporting a role of MMP-2 in regulating angiogenesis (Lafleur, et al., 2001; Nguyen, et al., 2001). Consistent with these observations, (latent and active) MMP-2 and MT1-MMP expression were previously observed in tumour vasculature (Lai, et al., 2007), as well as heterogeneous MMP-9 expression in the present study.

Gene microarray analyses of aggressive uveal melanoma cell lines have also found highly increased levels of MMP-1, -2, -9 and MT1-MMP, and laminin 5γ2 compared with poorly aggressive cell lines (Seftor, et al., 2001). The matrix networks formed by these aggressive melanoma cells, when grown in collagen I gels were immunolabelled for these MMPs (Seftor, et al., 2001). MMP-2 and MT1-MMP also cleave laminin 5γ2 to produce pro-migratory fragments critical for the formation of laminin-rich PAS-positive extravascular matrix networks (vasculogenic mimcry), characteristic of aggressive uveal melanomas (Folberg, et al., 1992; Hendrix, et al., 2003; Seftor, et al., 2001). Although evidence of MMP-9 expression similar to PAS-positive patterns was observed in several tumours in the present study, no such patterns were found for MMP-2 and MT1-MMP in the previous study (Lai, et al., 2007).

Distribution of TIMP-3 in Uveal Melanoma

TIMP-3 can regulate various MMPs and tumour invasion, as well as inhibiting angiogenesis and inducing apoptosis (Ahonen, et al., 1998; Qi, et al., 2003; Smith, et al., 1997). As such, loss of TIMP-3 may contribute to tumour growth, and TIMP-3 downregulation associated with changes in methylation has been found in several cancers including uveal melanoma (Mino, et al., 2007; Mylona, et al., 2006; van der Velden, et al., 2003). Furthermore, gene microarray studies have indicated a significant inverse relationship between TIMP-3 mRNA and chromosome 3 status, where no expression of TIMP-3 was found in 6/10 tumours with monosomy 3 (associated with metastases and poor prognosis) (Nareyeck, et al., 2005).

Considerable variation has been reported in levels and extent of TIMP-3 immunostaining in primary uveal melanomas (Nareyeck, et al., 2005; van der Velden, et al., 2003). In one study, an association between TIMP-3 and tumour histopathology (number of mitoses, cell type and presence of PAS+ loops and networks) could not be confirmed (van der Velden, et al., 2003). However, a trend between TIMP-3 protein expression and tumour cell type ($p=0.11$) and loops and/or networks ($p=0.06$) has been reported, with TIMP-3 seen in 50% of tumours, of which only 3 had > 5% TIMP-3 positive tumour cells (Nareyeck, et al., 2005). In the present study, heterogeneous TIMP-3 expression was observed in all uveal melanomas, although no association was found between tumour type and level of expression.

Angiogenesis involves generating new blood vessels from the pre-existing vessels and is a critical event during uveal melanoma development (reviewed Jager, et al., 2004). Angiogenesis requires various factors including VEGF and MMPs (Pepper, et al., 1996); (review Jager, et al., 2004). Proteinase and collagenase activities are tightly regulated during angiogenesis, otherwise they can lead to vascular regression and haemorrhage (reviewed Oh, et al., 2001; Saunders, et al., 2006)). An *in vivo* and *in vitro* study demonstrated that pericyte-derived TIMP-3 stablises vascular tube formation during angiogenesis (Saunders, et al., 2006). TIMP-3 has been suggested to interact with proteoglycans within the vascular basement membrane matrix, maintaining contact between pericytes and endothelial cells; this localisation of TIMP-3 has implications for vascular stabilization (Davis, et al., 2005; Saunders, et al., 2006). Furthermore, TIMP-3 has also been shown to inhibit MMPs and VEGF-related angiogenesis (Egeblad, et al., 2002; Qi, et al., 2003). In some tumours in the present study, tumour cells surrounding vessels displayed TIMP-3 but not in the tumour vasculature (Fig 3.2C). These observations and the previous studies discussed above, may suggest that TIMP-3 produced by vascular-associated tumour cells plays a role in stabilising mature tumour vasculature, similar to pericytes in other systems (Saunders, et al., 2006).

Distribution of MMP-9 and TIMP-3 in Retina and Choroid

Whether latent and active MMP-9 are expressed in the human retina remains controversial. Several studies have reported no latent and active MMP-9 immunoreactivity in normal human retina while others have observed MMP-9 expression in the ganglion cell layer as well as cultured Müller cells and RPE (Ahir, et al., 2002; Limb, et al., 2002; Salzmann, et al., 2000; Sivak, et al., 2002; Webster, et al., 1999). In the present study both latent and active MMP-9 immunolabelling was observed in normal and melanoma eyes. There appeared to be no obvious differences in MMP-9 expression in normal retina and in attached retina associated with melanoma, suggesting that MMP-9 is likely to be involved in normal retinal physiology and angiogenesis. Other studies in CNS, including retina, have suggested a physiological role for MMP-9 in maintaining neuronal integrity (Dzwonek, et al., 2004; Papp, et al., 2007). Furthermore, the MMP-9 antibody used in this study detected both latent and active forms and future studies comparing the distribution of latent and active MMP-9 separately, may further clarify its functional significance in normal retina.

In some regions of detached retina associated with melanoma, MMP-9 appeared to be localised predominantly in Müller cells. Müller cells stabilise the retinal architecture, provide structural support to retinal neurons and blood vessels and are involved in preventing aberrant photoreceptor migration into the subretinal space (Newman, et al., 1996; reviewed Bringmann, et al., 2006). Physiologically, Müller cells maintain the homeostasis of the retinal extracellular environment including ions, water, neurotransmitter molecules and pH, provide nutrients to the retinal neurons and remove metabolic waste (reviewed Bringmann, et al., 2006; reviewed Reichenbach, et al., 2007). Müller cells are well known to become activated in response to retinal injury (reviewed Bringmann, et al., 2006; reviewed Reichenbach, et al., 2007). Furthermore, they can proliferate and also act as progenitor cells following neurotoxic injury to the rat retina (Ooto, et al., 2004). MMP-9 in Müller cells has been suggested to constitute an early response to retinal pathology, including detachment (Limb, et al., 2002). Taken together, these observations suggest that MMP-9 may be involved in Müller cell activation in response to long-term serous retinal detachment associated with melanoma growth.

In the normal human eye, TIMP-3 is expressed in the RPE and Bruch's membrane (Fariss, et al., 1997; Vranka, et al., 1997). Pathologically, TIMP-3 is associated with Sorsby's retinal dystrophy, a hereditary macular disorder which leads to blindness in the third or fourth decade of life (Weber, et al., 1994). In the present study, both normal and melanoma eyes expressed TIMP-3 in Bruch's membrane and RPE. Interestingly, TIMP-3 expression in Bruch's membrane of melanoma eyes appeared to be uneven and punctated. This may be due to the physical rupture of Bruch's membrane by the tumour (see Chapter 1.1.3). Another possibility may be that growth factors bound within the ECM are released from the matrix and activated, associated with melanoma growth and MMP production.

Chapter 4

Distribution and Expression of CD146 in Human Uveal Melanoma

Results from this study are included in the publication: K Lai, V Sharma, MJ Jager, RM Conway, MC Madigan; Expression and Distribution of MUC18 in Human Uveal Melanoma. *Virchows Archiv* 451(5):967-76, 2007.

4.1 Introduction

As discussed in Chapter 1.3, the Ig superfamily protein CD146 is involved in tumour development and expressed in malignancies including cutaneous melanoma. Recent studies using 2-D gel electrophoresis found CD146 expression in several uveal melanoma cell lines (Pardo, et al., 2005, 2006). Moreover, cell lines with increased levels of CD146 protein also displayed an increased potential for *in vitro* invasiveness, suggesting an association between CD146 and uveal melanoma growth (Pardo, et al., 2006). CD146 expression is also reported to be induced (epigenetically) in poorly aggressive uveal melanoma cells (OCM-1A) grown in collagen I matrix pre-conditioned by aggressive metastatic uveal melanoma cells (MUM2B), further supporting a role for CD146 in uveal melanoma invasion (Seftor, et al., 2006). The expression and distribution of CD146 in primary uveal melanomas remains to be established.

Aims

This study extended the *in vitro* observations in previous studies, to a series of uveal and metastasis-derived cell lines and primary uveal melanocytes using diagnostic RT-PCR, Western blotting and immunocytochemistry. Furthermore, the distribution of CD146 protein in primary human uveal melanomas and normal eyes was studied using immunhistochemistry.

4.2 Materials and Methods

In vitro Studies

Diagnostic Reverse Transcription (RT)-PCR

RT-PCR was performed on 7 uveal (OCM-1, -3, -8, 92.1, Mel202, C918, OCM-1A) and 3 metastasis-derived melanoma cell lines (OMM-1, MUM2B, MUM2C) and cultured normal human uveal melanocytes (NHM; n=2). The methods for isolation and culture of primary uveal melanocytes have been described in Chapter 2.2.

RNA Extraction

Melanoma cells and human uveal melanocytes were seeded in 6-well plates at a density of 10^6 and $5x10^5$ cells per well respectively. Melanoma cells were cultured for 24 hrs while the uveal melanocytes required 2-3 days to become semi-confluent, as their growth rates are slower than melanoma cell lines (Chapter 2.2). RNA was extracted by lysing the cells directly in the well with 1 ml of Trizol (Invitrogen Life Technologies Pty Ltd). Cell lysates were collected by sterile glass pipette and transferred into a sterile Eppendorf tube and incubated for 5 mins, after which 200 µl chloroform (per 1ml of Trizol) was added and the tube was shaken vigorously for 15 seconds and left at RT for 3 mins. Following centrifugation at 13,000 *g* at 4°C for 15 mins, the upper aqueous phase (RNA) was collected and transferred into sterile Eppendorf tube. RNA was precipitated by adding approximately 500 µl cold isopropanol (per 1ml of Trizol). Samples were stored at -20°C for 20 mins; centrifuged at 13,000 *g* for 15 mins at 4°C. The supernatants were removed and the RNA pellet washed in 1ml cold 75% ethanol with vortexing and centrifuged at 7,500 *g* at 4°C for 5 mins. The supernatant was removed and the RNA air-dried for approximately 20 mins. An appropriate volume of RNase-free water (10-30 µl) was added to the RNA, followed by incubation at 42°C for 10 mins to re-dissolve the RNA. The RNA was quantified using a spectrophotometer (SmartSpec 3000, BIORAD) at 260 and 280 nm to determine purity and concentration. The $A_{260/280}$ of RNA ideally should be 1.8-2, however for human uveal melanocytes the $A_{260/280}$ was affected by the presence of melanin (Dorrie, et al., 2006), and readings were usually lower; an $A_{260/280}$ above 1.6 was found to be acceptable for melanocytes.

Reverse Transcription (RT)

RNA was reverse transcribed to cDNA (single strand DNA) before polymerase chain reaction (PCR). For each sample, 3 μg RNA was mixed and centrifuged briefly with 1 μl of 10mM DNTP mix and 1 μl Oligo (dT) (0.5 μg/μl) (Invitrogen). Samples were then made up to 10μl with DEPC-treated water, and placed immediately on ice. Samples were heated at 65°C for 5 mins and placed on ice for at least 1 min, then gently mixed with RT master mix (Table 4.1) and centrifuged briefly. For each cDNA sample, an RT minus control was included; the SuperScript III RT enzyme (Invitrogen) was omitted and replaced with DEPC-treated water (Table 4.1).

Table 4.1: Master Mix for cDNA Transcription.

	RT master mix	RT minus master mix
10XRT buffer	2μl	2μl
25mM $MgCl_2$	4μl	4μl
0.1M DTT	2μl	2μl
RNaseOUT (40U/μl)	1μl	1μl
SuperScript III RT	1μl	---
DEPC-treated water	---	1μl

Samples were incubated at 50°C for 50 mins, the reaction terminated at 85°C for 5 mins and then placed on ice. The sample was collected by brief centrifugation. A further 1μl E.coli RNase H (Invitrogen) was added to each sample, and then incubated for 20 mins at 37°C. cDNA was quantified using a spectrophotometer (SmartSpec 3000, BIORAD) at 260 and 280nm to determine concentration. cDNAs were stored at -20°C prior to PCR.

Polymerase Chain Reaction (PCR)

Polymerase Chain Reaction (PCR) amplifies a specific region of DNA between two oligonucleotide primers (Alberts, et al., 1996). Primers are designed in opposite

direction strands of DNA for amplification. The two strands of template DNA are denatured and separated by increasing the reaction temperature up to 94°C. The annealing stage is a key variable in the optimization of PCR, and allows primers to bind the template DNA at a temperature between 40°C and 60°C depending on the GC content and the sequence of the primers. Finally the extension stage at 72°C allows the DNA to extend from the primers (72°C). The newly synthesised DNA can now be used as a template for the next cycle until amplification is completed (Alberts, et al., 1996).

CD146 primers were designed from gene Accession No. M28882.1 using Primer 3 (GenBank, NIH) software and synthesised by Invitrogen Pty Ltd. The primer sequences used were:

Forward: 5'-ACCCTGAATGTCCTCGTGAC-3'

Reverse: 5'-TCTCTGTGGAGGTGCTGTTG-3' (amplicon 209bp)

The accuracy of the primers was virtually tested using Amplify 1.2 software and the NCBI nucleotide-nucleotide BLAST search.

For RT-PCR, 60 ng of each cDNA sample in 14.25 µl Milli-Q water was mixed with 8.75 µl of PCR master mix [1.25 µl 50 mM $MgCl_2$, 2.5 µl 10 mM dNTP mix, 2.5 µl 10xNH4 reaction buffer (BIOLINE), 0.5 µl BIOTAQ Red DNA polymerase (BIOLINE) and 1 µl each of each specific primer pair]. Samples were incubated at 94°C for 3 mins (initial denaturation), then amplified through 35 cycles of PCR [denaturation at 94°C for 35 seconds, annealing for 35 seconds (temperature dependent on the primer sequences), extension at 72°C for 35 seconds and a further extension at 72°C for 5 mins]. Products were maintained at 4°C when RT-PCR was completed. An RT minus cDNA sample was included used as a control. Amplification products were separated by electrophoresis on 1.5% agarose gels with 1 µl ethidium bromide, TrackIt 100bp DNA ladder (Invitrogen) was also loaded to verify the product size. PCR results were visualised with a BioRad GelDoc system and WinFast software. Products were subsequently extracted and purified from agarose gels (JETQUICK Gel Extraction Spin, Genomed, Germany), and verified by dye-determination DNA sequencing of both strands (Australian Genome Research Facility, Queenland).

Western Blotting

Western blotting was used to detect the CD146 protein in 7 uveal and 3 metastasis-derived melanoma cell lines and primary uveal melanocytes. Cells were seeded in a 6-well plate ($5x10^5$ cells/well) and grown until ~ 70-80% confluent. Medium was removed from the well and cells were rinsed with PBS prior to protein extraction. Whole cell lysates were extracted by adding 350µl/well CellLytic-M Mammalian Cell Lysis/Extraction Reagent (Sigma-Aldrich Pty Ltd, Australia) supplemented with protease inhibitor cocktail (Complete Mini Tablets, Roche Products Pty Ltd, Australia) for 20 mins on a shaking table on ice. Cell lysates were collected and centrifuged for 15 mins at 12,000 *g* to pellet the cell nuclei and membranes. The protein lysates were aliquoted and stored at -80°C until used.

The protein concentration of each sample was measured using the DC protein assay reagent kit (BioRad Laboratories, Sydney Australia). Equal amounts of protein (15µg) were used for each sample. Protein samples were mixed with 5x loading buffer contain 2% 2ME (2-β-Mercaptoethanol) (BioRad Laboratories, Sydney Australia) as a reducing agent, and heated at 95°C for 10 mins to denature the protein. Samples were loaded on 10% polyacrylamide gels in the presence of sodium dodecyl sulphate (SDS) (Life Technologies Inc., USA). A broad range molecular weight standard (BioRad Laboratories, Sydney Australia) was also loaded in adjacent lanes to estimate the molecular weight of the bands. Proteins were separated by electrophoresis carried at 4°C with a constant voltage of 120V for 3 hrs. After electrophoresis, gels were placed face-to-face with 0.45µm Invitrolon PVDF membrane (Invitrogen), sandwiched between filter paper and pads, and placed in the gel cassette. Cassettes were placed into the electrophoresis chamber filled with cold TGS buffer (Tris/Glycine/SDS, pH 8.3). Transfer was carried out at 4°C and 250mA (constant current) for 3 hrs.

After transfer, the membrane was removed from the gel and washed in Milli-Q water, then blocked in 5% skim milk in Tween-TBS (0.05% Tween-20 in TBS ie. 50µl/100ml TBS) at 4°C overnight. After rinsing in Tween-TBS, membranes were incubated in goat anti-human polyclonal CD146 antibody (Santa Cruz, diluted 1:500 in 1% BSA and Tween-TBS) (Table 2.2a) at 4°C overnight. Membranes were then rinsed with Tween-TBS and incubated in perioxidase-linked secondary antibody (1:12,500 with 1% BSA in Tween-TBS) (Table 2.2b). The membrane was rinsed in 6 changes of Tween-

TBS each for 5 mins and incubated in ECL reagent (SuperSignal West Dura Extended Duration Substrate, Pierce Biotechnology, IL, USA) for 5 mins. To visualise the immunolabelling, the membrane was exposed to photographic film (X-0MAT BT film, Kodak) and developed.

To confirm that equal amounts of protein were loaded in the gel, the membranes were incubated in Restore Western Blot Stripping Buffer (Pierce) at 37°C for an hr. The membrane was rinsed in two changes of Tween-TBS for 5 mins each, and incubated in GAPDH antibody (0.5μg/ml with 1% BSA in Tween-TBS) (Table 2.2a) at 4°C overnight. After rinsing, membranes were incubated in a peroxidase-conjugated anti-mouse secondary antibody (1:20,000 with 1% BSA in Tween-TBS) (Table 2.2b), and viewed as above. Immunoblotting was repeated on 3 separate occasions.

Immunoblots (n=3) were analysed using a Syngene G:Box, Chemi XT 16 Camera and GeneSnap (Syngene) software. The average sum of intensities of CD146 bands and GAPDH bands for each cell line were analysed using GeneTools (Syngene) (Ver. 3.07(g)) software and the ratios of the average intensities of CD146:GAPDH were calculated.

Immunocytochemistry

Uveal (n=7) and metastasis-derived (n=3) melanoma cell lines and uveal melanocytes (n=2) were grown on coverslips and fixed for immunocytochemistry as described in Chapter 2.2. A polyclonal goat anti-human antibody to the extracellular domain of CD146 (MCAM, R&D Systems Inc, MN, USA; 2μg/ml) was used, with goat immunoglobulins (Ig) (2μg/ml) as a non-specific control (Table 2.2a). Immunolabelling was visualised using rabbit anti-goat Alexa-488 conjugated fluorochrome and laser scanning confocal microscopy (see Chapter 2.2).

Paraffin Sections

Paraffin sections were cut from eyes enucleated for uveal melanoma, and normal eyes as described in Chapter 2.1. As mentioned previously, the specimens included 18 untreated melanomas and 5 I^{125}-treated melanomas, and the majority of tumours were located in the choroid posterior to the equator. Normal human eyes (n=3; aged 39, 50 and 78 years), provided by the Lions NSW Eye Bank with consent and ethical approval, were fixed in 10% neutral buffered formalin, paraffin-embedded, and used as controls (see Chapter 2.1).

Immunohistochemistry

Sections were stained with polyclonal goat anti-human antibody to the extracellular domain of CD146 (R&D Systems) at 2μg/ml in 2%NRS/PBS and visualized with peroxidase and Vector Red using procedures described in Chapter 2.1.

Immunostaining of melanomas was graded in masked fashion by 2 independent observers using a semi-quantitative scale where 0 = none, 1 = weak (low intensity staining of tumour cells regardless of %, and medium intensity staining of ≤20% cells); 2 = moderate (medium intensity staining of >20% tumour cells, high intensity staining of ≤20% tumour cells), and 3 = strong (high intensity staining of >20% tumour cells). The grading of the 2 observers was significantly correlated ($p<0.001$; Kendall's rank correlation). Non-parametric linear regression analysis was used to test for an association between tumour histopathology and CD146 immunolabelling, and between maximum tumour height (in mm) and CD146 immunolabelling.

Additionally the distribution and intensity of CD146 immunostaining in retina overlying tumours, in regions of choroid and retina without melanoma as well as in normal choroid and retina assessed.

4.3 Results

CD146 in Uveal and Metastasis-Derived Cell Lines and Melanocytes

RT-PCR showed CD146 mRNA expression in all melanoma cell lines and 2 NHM (Fig 4.1). The sequence of CD146 was confirmed by Australian Genome Research Facility, Queenland

Immunoblotting showed a positive band at ~130kDa for all cell lines and NHM, with variable levels of CD146 protein expression between samples (Fig 4.2A). Membranes re-probed with GAPDH antibody showed a consistent band at ~35kDa in all lanes, confirming that equal amounts of protein were loaded (Fig 4.2A). The mean ratio of CD146 and GAPDH (from 3 separate immunoblots) showed high levels of CD146 proteins in OCM-3, OCM-8, 92-1, Mel202, OCM-1A, NHM01 and NHM02, relatively less CD146 protein in OCM-1, OMM-1 and MUM2C cell lines and much reduced CD146 protein in C918 and MUM2B cell lines (Fig 4.2B). All cell lines and NHM showed punctate cell membrane CD146 immunolabelling, with no immunostaining for the goat Ig control (Fig 4.3).

CD146 in Primary Uveal Melanomas

Overall ≥ grade 2 immunostaining was observed in 60% (3/5) of I^{125}-treated and 78% (14/18) of untreated melanomas. For untreated melanomas, a significant relationship was found between tumour cell type and average CD146 immunostaining grade (P=0.031, nonparametric regression; Fig 4.4), with more CD146 immunostaining in mixed and epithelioid tumours compared to spindle cell tumours. No relationship between maximum tumour height (mm) and CD146 immunostaining was found for untreated tumours (P>0.05). As tumour specimens were collected over a recent period, the relationship between CD146 expression and survival could not be analysed.

In approximately 50% (9/18) of untreated melanomas, cells at the tumour edges showed moderate to strong cell membrane and cytoplasmic CD146 immunostaining (Fig 4.5A; insert). Within tumours, heterogeneous regions of CD146 membrane and cytoplasmic immunolabelling of tumour cells were observed (Fig 4.5B-E). Blood vessels within all tumours showed intense CD146 immunostaining of vascular endothelium, and often lumen contents (including erythrocytes) (Fig 4.5A, E; Fig 4.6A). Distinct patterns of CD146 immunolabelling (Fig 4.6B), similar in appearance to PAS+ loops and networks,

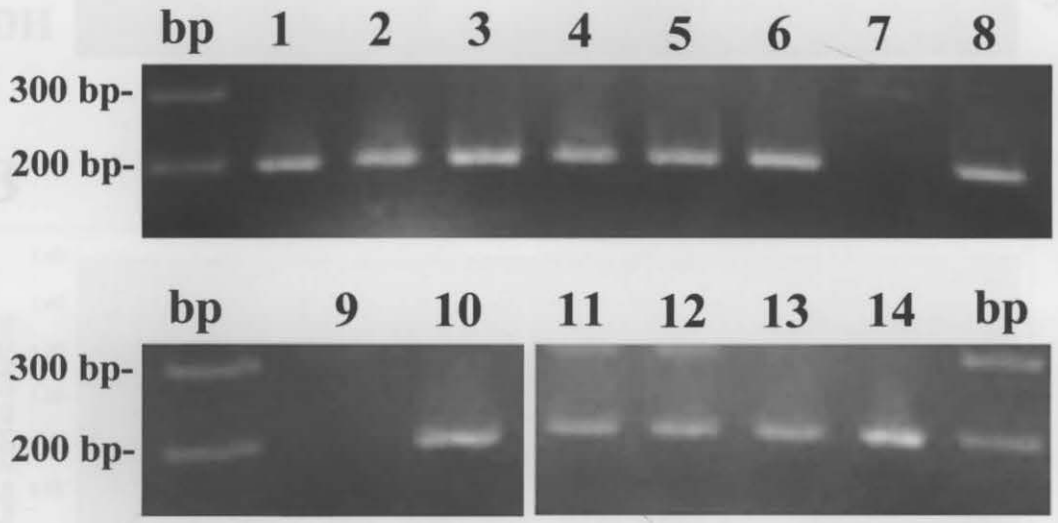

Figure 4.1
Diagnostic RT-PCR showing CD146 mRNA expression in uveal and metastasis-derived cell lines and normal human melanocytes (NHM) (Amplicon 209bp) [Lane 1=OCM-1A, 2=OCM-3, 3=OCM-8, 4=92-1, 5=C918, 6=MUM2C, 7=RT-, 8=NHM01, 9=RT-, 10=NHM02, 11=Mel202, 12=OMM-1, 13=OCM-1 and 14=MUM2B].

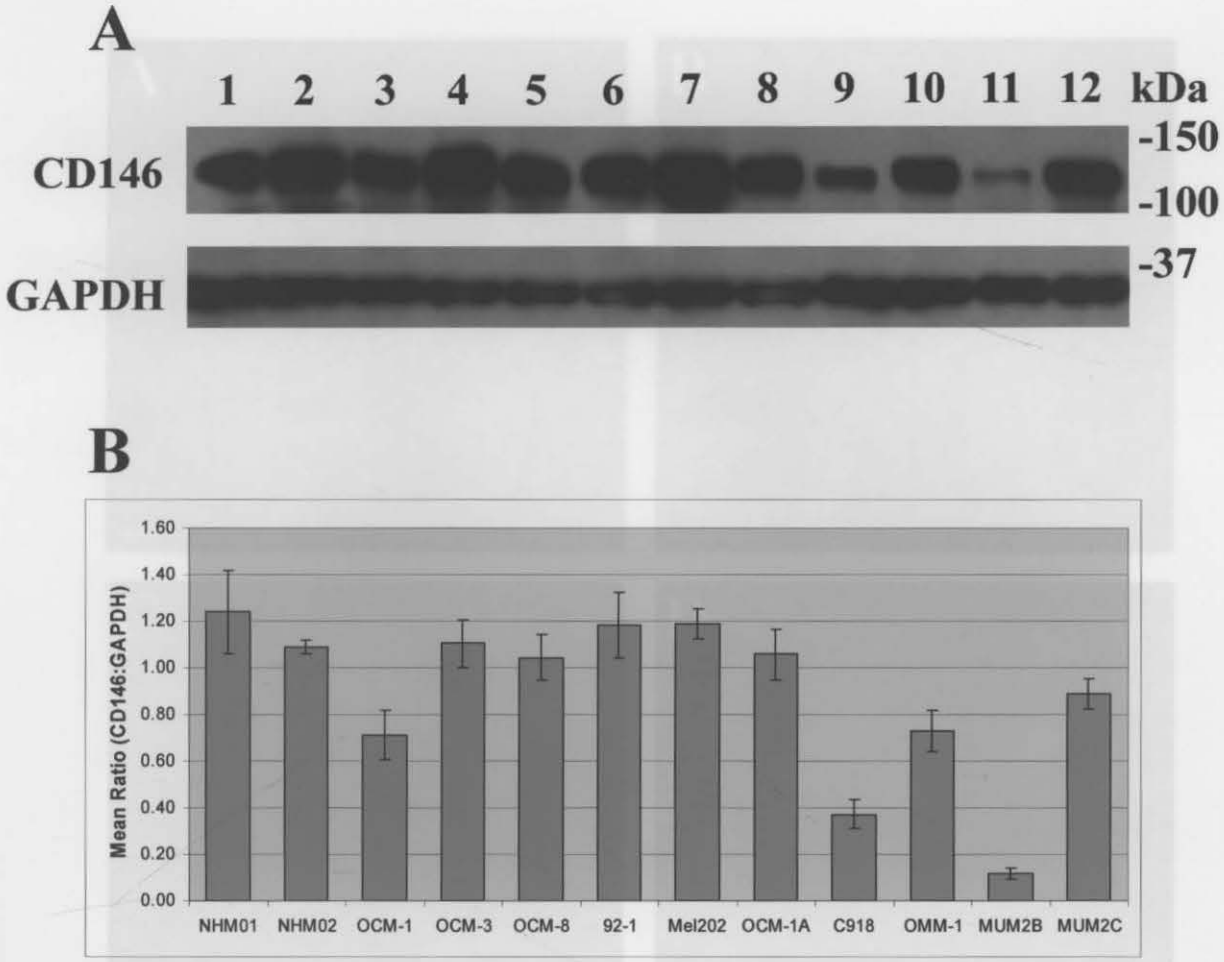

Figure 4.2

(A) Representative immunoblot showing a band at ~130kDa consistent with CD146 protein expression in normal human melanocytes (NHM) (Lanes 1-2), uveal (Lanes 3-9) and metastasis-derived (Lanes 10-12) cell lines. Reprobing of the membrane with GAPDH antibody showed a consistent band at ~35kDa for all cell lines. Molecular mass markers (kDa) are shown on the right. [Lane 1=NHM01, 2=NHM02, 3=OCM-1, 4=OCM-3, 5=OCM-8, 6=92-1, 7=Mel202, 8=OCM-1A, 9=C918, 10=OMM-1, 11=MUM2B and 12=MUM2C]

(B) Histogram of the ratio of the average intensities of CD146 and GAPDH bands calculated from 3 separate immunoblots.

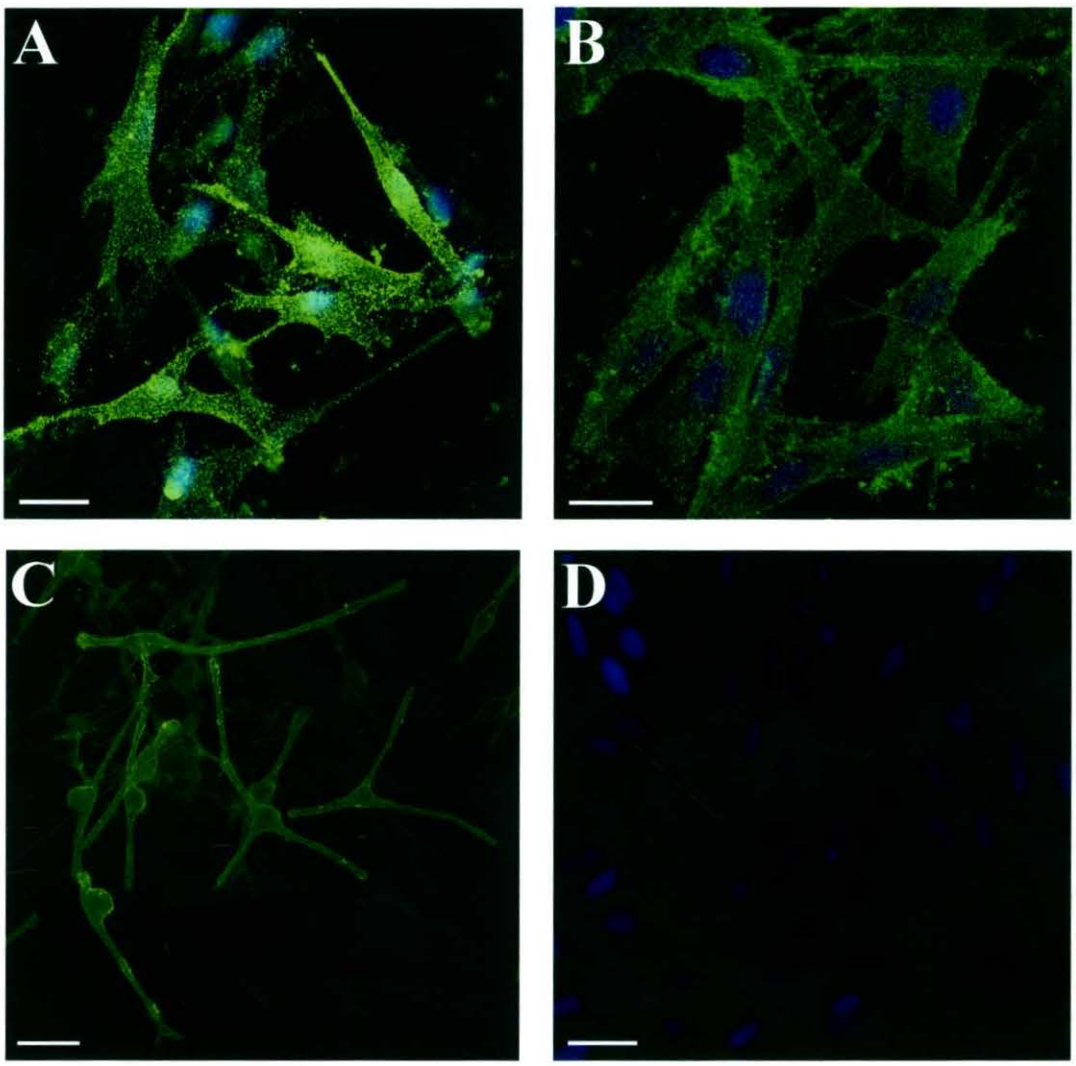

Figure 4.3
Examples of CD146 punctate cell membrane immunolabelling of (A) OCM-1, (B) 92-1 cells and (C) NHM. (D) OCM-1 cells incubated with control goat Ig showed no immunolabelling. Cell nuclei are stained with Hoechst 33342 (blue). (Bar=15μm)

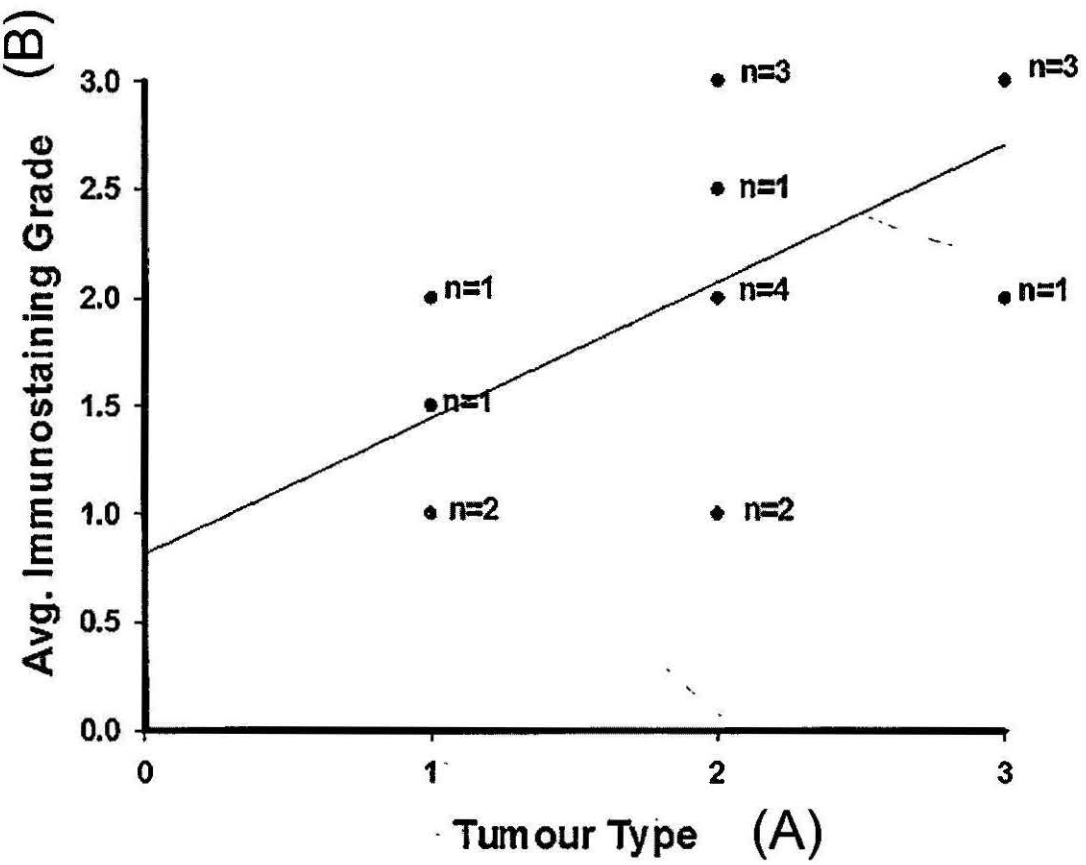

Figure 4.4

Tumour type *vs* average CD146 immunostaining grade for untreated melanomas (n=18; nonparametric linear regression, P=0.031).

(A) Tumour type: (1) spindle; (2) mixed and (3) epithelioid

(B) Average immunostaining: 0=none, 1=weak (low intensity staining of tumour cells regardless of %, and medium intensity staining of 20% cells): 2=moderate (medium intensity staining of >20% tumour cells, high intensity staining of 20% tumour cells), and 3=strong (high intensity staining of >20% tumour cells) (2 independent observers).

Figure 4.5
CD146 immunostaining in uveal melanoma.
(A) Low power micrograph showing CD146 expression at the tumour edge, where cells display membrane and cytoplasmic CD146 immunoreactivity (see insert). The more central regions of the melanoma (*) show lower levels of CD146 compared to the tumour edge. Blood vessels (bv) in the tumour and adjacent choroid display strong CD146 immunostaining. (Bar = 100μm; Inset Bar = 30μm) (B) Grade 1 (low) CD146. Blood vessels show intense CD146 immunolabelling (arrows). (Bar = 35μm) (C-E) Areas of moderate to intense (≥grade 2) cell membrane CD146. A large blood vessel (bv) immunostained with CD146 is seen in (E). (C: Bar = 35μm; D&E: Bar = 30μm)

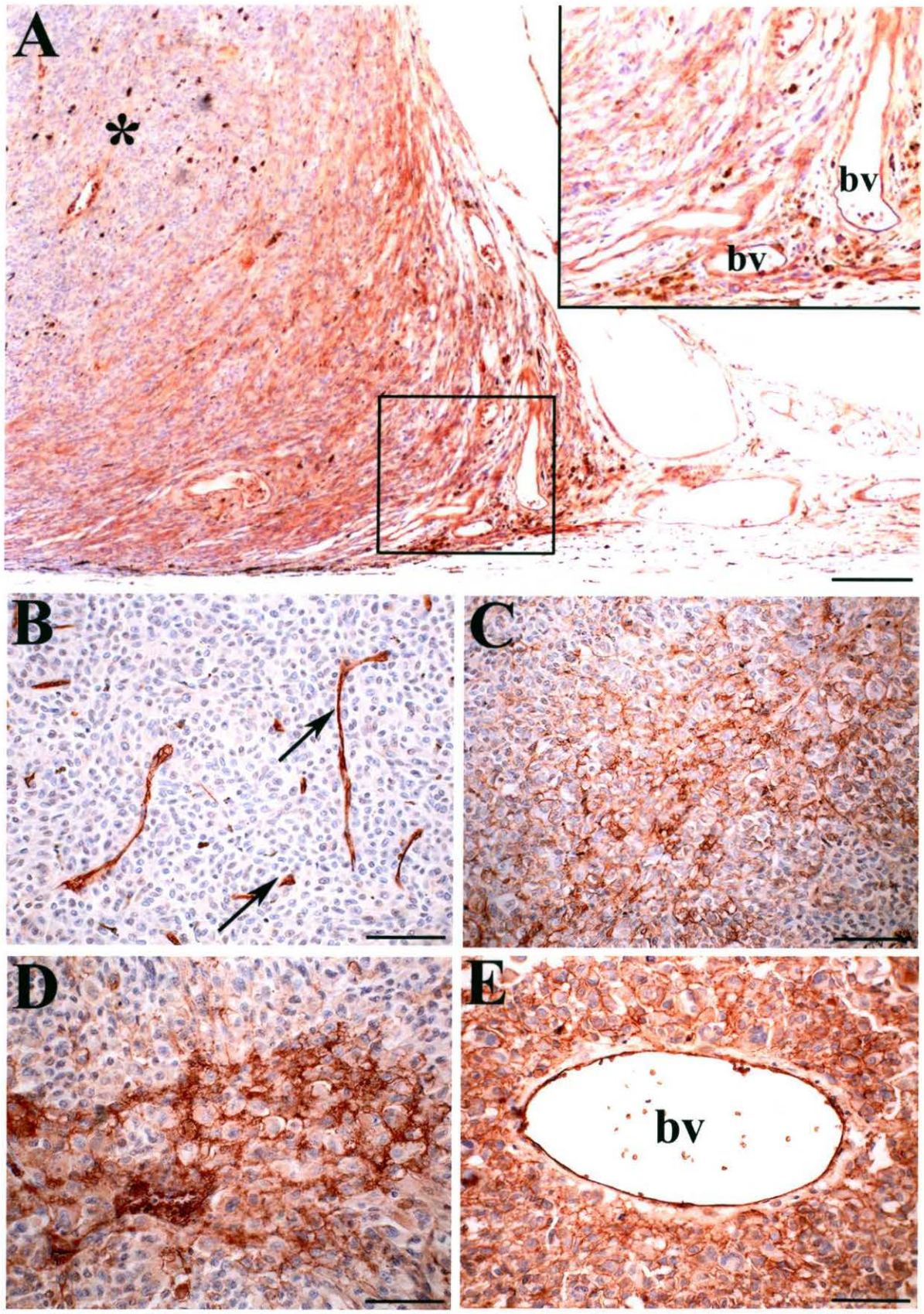
A
*
bv
bv
B
C
D
E
bv

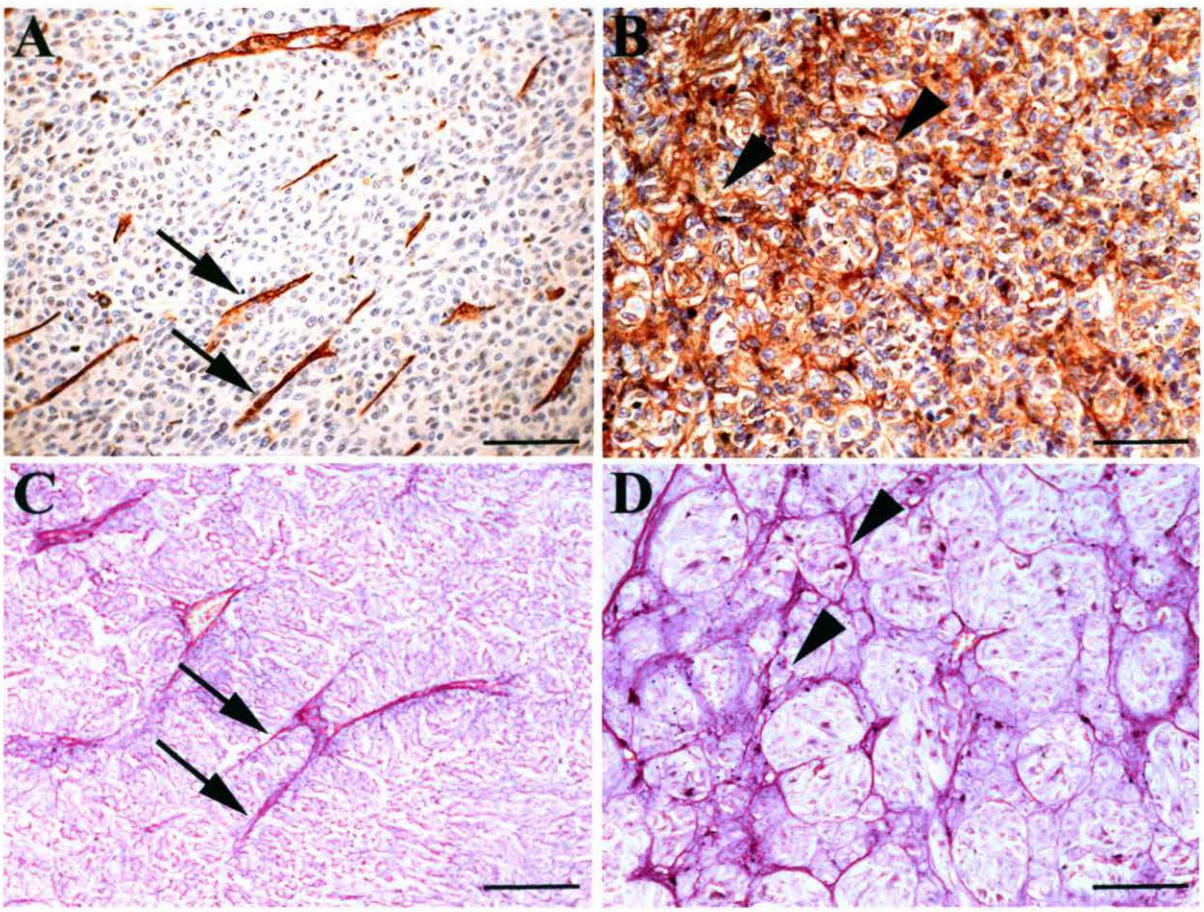

Figure 4.6
(A) CD146 immunostaining (arrows) and (C) PAS staining (arrows) of tumour blood vessels, with no apparent immunostaining of tumour cells. (A&C: Bar = 35μm)
(B) Areas of CD146+ networks (arrowheads) in an epithelioid melanoma appear similar to (D) PAS+ loops and networks (arrowheads). (B&D: Bar = 25μm)

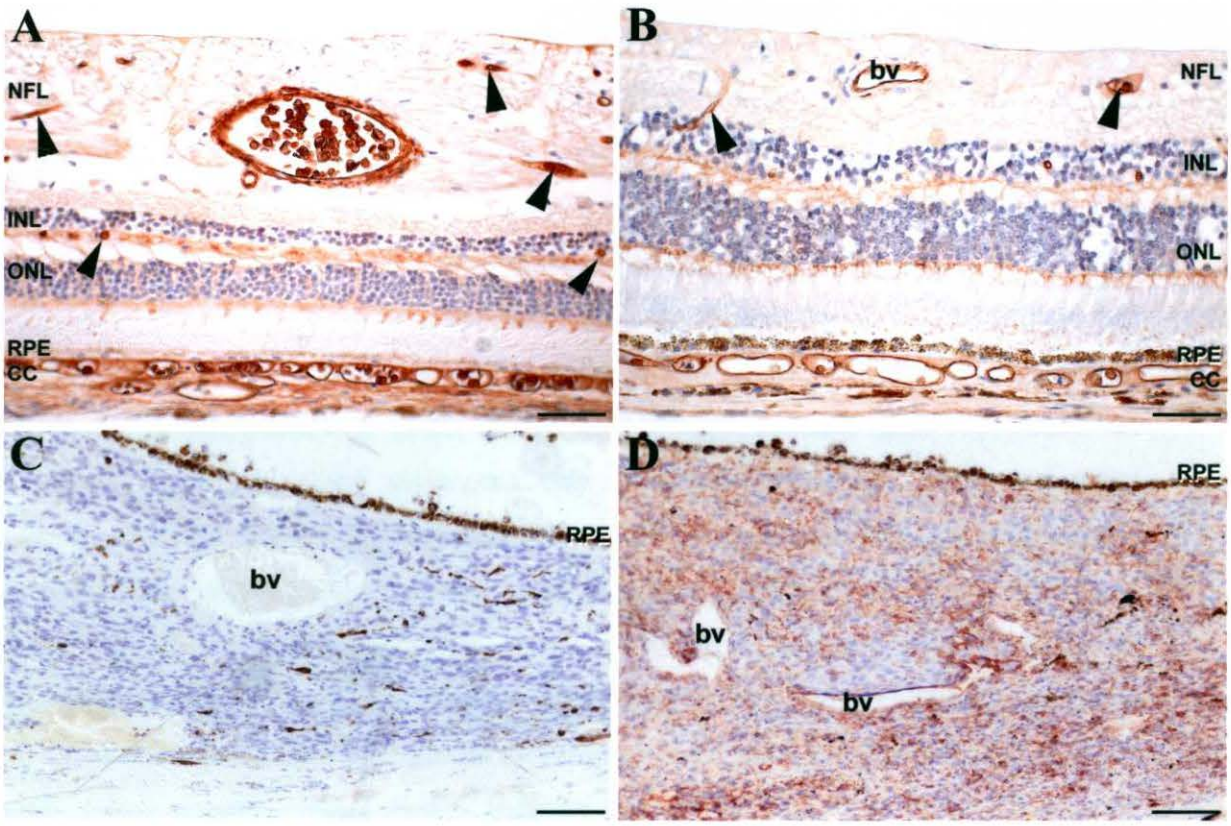

Figure 4.7

(A, B) CD146 immunostaining of retina and choriocapillaris (CC). Blood vessels (arrowheads) display strong CD146 expression, with both the inner and outer retinal vascular plexus clearly seen in melanoma-containing (A) and control (B) eyes. In (A) a large vessel also shows CD146 immunoreactive perivascular cells.

(C) No immunostaining of tumour cells or blood vessels (bv), including lumen contents, is seen with goat IgG control, compared to CD146 immunostaining in the same specimen (D).

(NFL - nerve fibre layer, INL - inner nuclear layer, ONL - outer nuclear layer, RPE - retinal pigmented epithelium) (Bar = 40μm)

4.4 Discussion

CD146 and Uveal Melanoma

In the present study all melanoma cell lines (primary and metastasis-derived) expressed CD146 mRNA and protein (Western blot and immunocytochemistry). However C918 and MUM2B cells showed reduced levels of CD146 protein compared to the other cell lines; C918 uveal melanoma cells and MUM2B metastasis-derived cells are both considered to be highly aggressive (Seftor, et al., 2002). Recent *in vitro* studies also described variable levels of CD146 protein in uveal melanoma cell lines, concluding that CD146 expression was generally associated with an increased potential for *in vitro* invasiveness (Pardo, et al., 2006). Similarly, variable expression of CD146 protein has been reported in ovarian carcinoma cells, although associated with tumour progression, and poor prognosis (Aldovini, et al., 2006). Interestingly, variable gene expression has also been reported in uveal melanoma cell lines and in primary uveal melanoma specimens. *CD146* was upregulated in a primary uveal melanoma cell line compared to two metastasis-derived melanoma cell lines (van der Velden, et al., 2003). However, *CD146* was downregulated in gene arrays of Class 2 primary uveal melanomas (associated with epithelioid morphology, monosomy 3 and poor prognosis) compared with Class 1 uveal melanomas (spindle morphology with good prognosis) (Onken, et al., 2005). Taken together, these studies indicate that while CD146 is involved in uveal melanoma growth and potential invasiveness, more than one signalling pathway may contribute to these processes as suggested by Pardo *et al* (2005, 2006).

In primary uveal melanomas moderate to intense CD146 immunostaining was observed in heterogeneous areas, particularly more so in mixed and epithelioid melanomas. A major role for CD146 in the growth and metastases of cutaneous melanomas has been proposed, with CD146 expression being strongly up-regulated in malignant melanomas of increasing vertical thickness, and particularly in metastatic lesions (Denton, et al., 1992; Johnson, 1994; Kraus, et al., 1997; Lehmann, et al., 1987, 1989). One study has observed a correlation between CD146 expression and tumour thickness, associated with the transition of cutaneous melanoma from the radial to the vertical growth phase (Xie, et al., 1997). However, the present study found no relationship between CD146 expression and maximum tumour height in this series of uveal melanomas.

Over-expression of CD146 in primary cutaneous melanoma cells has been reported to induce increased adhesion between tumour cells themselves, increased tumour cell invasiveness, as well as enhanced interactions between tumour cells and endothelial cells, and decreased tumour cell adhesion to laminin; these effects were reversed by anti-CD146 (MCAM) monoclonal antibody (Xie, et al., 1997). Increased collagenase production was also observed in CD146 transfected cells, contributing to increased tumourigenicity (Xie, et al., 1997). CD146 over-expressing cutaneous melanoma cells induced tumour growth and metastases in nude mice that could be reversed using anti-CD146 (MCAM) monoclonal antibody (Xie, et al., 1997). Further evidence for involvement CD146 in cutaneous melanoma growth comes from recent *in vitro* and *in vivo* studies using antibodies to CD146 to inhibit melanoma cell tumourogenesis and subsequent metastasis; a therapeutic application for CD146 antibodies in controlling cutaneous melanoma growth is currently being investigated (Leslie, et al., 2007; McGary, et al., 2003; Melnikova, et al., 2006). Although these studies indicate a major role for CD146 in cutaneous melanoma growth, other cell adhesion and signalling molecules, for example, N-cadherin, integrins, RAS/ERK and PI3K, are important for tumour growth (Meier, et al., 2005). A recent gene and tissue microarray study reported a significant correlation between progression of cutaneous melanoma and expression of N-cadherin and β3 integrin, but *not* CD146 (Watson-Hurst, et al., 2006). This study did however implicate CD146 (and β3 integrin) in cutaneous melanoma cell migration and invasion (Watson-Hurst, et al., 2006). Over-expression of CD146 has also been associated with tumour progression in prostate and ovarian carcinomas (Wu, et al., 2001), however, this may not be the case for all tumours, as seen for example in breast carcinoma where loss of CD146 occurs with progression (Shih, 1999).

Binding sites for transcription factors including activator protein (AP)-2α, Sp1 and CREB/ATF-1 have been found on the CD146 promoter (Leslie, et al., 2005). Loss of the transcription factor AP-2α has been shown to be involved in progression of several tumours including malignant melanoma (Bar-Eli, 1999), breast and prostate cancers (Bosher, et al., 1995; Ruiz, et al., 2001) and gliomas (Heimberger, et al., 2005). Highly metastatic (AP-2α-negative, CD146-positive) cutaneous melanoma (A375SM) cells transfected with AP-2α displayed greatly reduced levels of CD146 mRNA and protein compared to parental cells (Jean, et al., 1998). These cells also displayed suppressed tumourigenicity and metastatic potential in nude mice that was suggested to be related to AP-2α down-regulation of CD146 gene expression (Jean, et al., 1998). However, other

transcription factors, including Sp1, have been found to be involved in regulating CD146 expression (Karlen, et al., 1999, 2000; Mintz-Weber, et al., 2000). Regulation of other AP-2α-regulated genes important for tumour cell proliferation and apoptosis, invasion and angiogenesis including *c-kit, E-cadherin, MMP-2* and *PAR-1* have also been found to contribute significantly to cutaneous melanoma growth and metastases (Tellez, et al., 2003). The expression of transcription factors including AP-2, Sp1 and CREB/ATF-1, their role in regulating *CD146* and other genes, and their relationship to uveal melanoma phenotype and progression remains to be established.

Soluble forms of CD146 (sCD146) have been reported in supernatants from cultured human umbilical vein endothelial cells (Bardin, et al., 1998). Increased sCD146 has been found in serum from patients with several diseases including rheumatoid arthritis, chronic renal disease and inflammatory bowel disease, reflecting its involvement in endothelial cell dysfunction and vascular permeability (Bardin, et al., 2006). In the present study, high levels of CD146 immunolabelling were observed in endothelial cells and erythrocytes in uveal melanomas; although whether this immunolabelling represents sCD146 remains to be established.

CD146 in Primary Uveal Melanocytes

Normally melanocytes in skin have been reported to display little or no CD146 (Shih, 1999). However, previous studies have shown that cultured cutaneous melanocytes express CD146 protein (Shih, et al., 1994). In sections of normal human eyes in the present study, cells within the choroid did not appear to express CD146 immunoreactivity, although blood vessels were clearly immunolabelled. With immunoblotting and immunocytochemistry, cultured primary uveal melanocytes expressed high levels of CD146 protein. MUC18 expression has been found to be related to the presence of phorbol esters (PMA) or cAMP regulators (IBMX) in glioma and carcinoma cell lines (Rummel, et al., 1996), both included in normal MGM used in the present study. Furthermore, when cutaneous melanocytes were co-cultured with epidermal keratinocytes, CD146 expression was down-regulated associated with E-cadherin expression (Shih, 1999; Shih, et al., 1994). E-cadherin was the most critical adhesion molecule involved in mediating keratinocyte-melanocyte interactions (Shih, 1999; Tang, et al., 1994). In contrast, advanced and metastatic cutaneous melanoma cells do not express E-cadherin, and CD146 expression on these cells was not affected by interactions with keratinocytes (Haass, et al., 2005; Shih, 1999; Shih, et al., 1994). Whether CD146 expression in uveal

melanocytes can be modulated by interactions with stromal cells (fibroblasts) similar to cutaneous melanocytes (discussed above), remains to be investigated both *in situ* and *in vitro*. It is also unclear whether uveal melanocytes and/or choroidal fibroblasts normally express E-cadherin.

CD146 and Tumour Vasculature/Vasculogenic Mimicry

All vascular endothelium, regardless of location or vessel size, constitutively express CD146 (Bardin, et al., 1996, 2001), and consistent with this, strong CD146 immunolabelling was observed in tumour vasculature, and in retinal and choriocapillaris blood vessels in both control and melanoma eyes. CD146 has been reported to be localized at endothelial cell junctions, although outside *adherens* junctions, and associated with actin filaments in the endothelial cytoskeleton (Bardin, et al., 2001). These observations suggest an important role for CD146 in endothelial cell cohesion (Bardin, et al., 2001; Solovey, et al., 2001). Several studies also show that CD146 binding in endothelial cells can regulate intercellular permeability, inducing phosphotyrosine-kinase-dependent outside-in signaling associated with proteins including $p59^{FYN}$, $p125^{FAK}$ and paxillin (Anfosso, et al., 1998, 2001). As mentioned previously, homotypic and heterotypic cell-cell interactions have been observed to be mediated by CD146, although the ligand remains unknown (Bardin, et al., 2001), and CD146-mediated adhesion between melanoma cells and endothelial cells may be important for intravasation and extravasation of cells in tumours (Melnikova, et al., 2006; Shih, et al., 1997; Xie, et al., 1997). Activated peripheral T lymphocytes also express CD146, which may play a role in T-cell extravasation and/or homing (Pickl, et al., 1997; Seftalioglu, et al., 2000). Taken together, these observations suggest that interactions between CD146-positive tumour cells, endothelial cells and perhaps activated T-lymphocytes may play an important role in melanoma (cutaneous and uveal) spread and immunoregulation.

As described in Chapter 1.1.4, PAS+ loops and networks are correlated with more aggressive tumour behaviour and tend to be situated in the periphery of choroidal melanomas (Folberg, et al., 1993, 1996). Similarly in the present study, more peripheral regions of several epithelioid tumours (5/18) displayed patterns of CD146 immunoreactivity that resembled these channels. Although it is tempting to speculate that CD146 might play a role in vasculogenic mimicry in some tumours, comparison of CD146 and PAS-labelled serial sections, and *in vitro* 3D studies including use of CD146 si RNA, would be needed to confirm this theory. The reduced levels of CD146 protein

expression in MUM2B and C918 cell lines also challenges the idea that CD146 may participate in vasculogenic mimicry, since these cells are capable of generating these features in 3D culture (Daniels, et al., 1996; Seftor, et al., 2002). One possible explanation may be that CD146 protein expression is influenced by levels of cell confluency, although when 70-80% confluent cultures were compared to fully confluent cultures, no difference in CD146 protein expression was observed (not shown). The role of other signaling pathways and factors such as AP-2α in these cell lines requires further study.

4.5 Conclusion

Variable levels of expression of CD146 protein were observed in uveal and metastasis-derived melanoma cell lines and uveal melanocytes. In primary mixed and epithelioid tumour specimens, CD146 immunoreactivity was significantly greater than in spindle cell tumours. These observations suggest that while CD146 is important for tumour growth, its expression may not be essential for invasion and metastasis, consistent with findings in other tumours. The role of transcription factors including AP-2 α, and the signaling pathways involved in regulating CD146 expression and activity in uveal melanoma remain to be defined. Finally, interactions between CD146-positive melanoma cells and vasculature, *via* an as yet unidentified ligand, may be important for the hematogenous spread of tumor cells during metastases.

Chapter 5

The Effect of Ultraviolet Radiation on Uveal Melanocytes and Uveal Melanoma Cell Lines: Cell Survival and Matrix Metalloproteinase Production

Results from this study are included in the publication: K Lai, N Di Girolamo, RM Conway, MJ Jager, MC Madigan The Effect of Ultraviolet Radiation on Choroidal Melanocytes and Melanoma Cell Lines: Cell Survival and Matrix Metalloproteinase Production. *Graefes Arch Clin Exp Ophthalmol* 245(5):715-24, 2007.

5.1 Introduction

The role of UV exposure as a potential risk factor in uveal melanoma remains controversial and reviewed in Chapter 1.4. *UV-B* is generally considered to be the major photocarcinogenic component of UV (Mitchell, et al., 1991), causing direct DNA damage, inducing cell death and altering expression of cell-cycle related genes and intracellular proteins including cytokines, growth factors and proteinases, for example, matrix metalloproteinases (MMPs) (Emri, et al., 2000; Kadekaro, et al., 2003; Zhang, et al., 2003). Several studies show that UVR can induce expression of MMPs, particularly in the skin (Brenneisen, et al., 2002; Enk, et al., 2006; Rittie, et al., 2002). *UV-A* and *UV-B* induce MMP-1 in both cultured fibroblasts and cutaneous keratinocytes respectively (Onoue, et al., 2003; Wlaschek, et al., 1994), and *in vitro* studies of cutaneous melanocytes find increased MMP-2 activity in supernatants, and enhanced melanocyte migration following *UV*-B (Wu, et al., 2004). A rapid increase in MMP-1 and MMP-10 mRNA is also reported to be induced in a squamous cell carcinoma cell line following treatment with both *UV-A* and *UV-B* (Ramos, et al., 2004). In terms of ocular disease UVR exposure is strongly associated with cortical cataract (Delcourt, et al., 2000; McCarty, et al., 2000; West, et al., 1998). *UV-B* also induces MMP-1 expression in pterygium and lens epithelial cells (Di Girolamo, et al., 2003; Sachdev, et al., 2004; Wlaschek, et al., 1994); however, the effect of *UV-B* exposure on induction of MMPs in human uveal melanocytes and uveal melanoma cells is not known.

Aims

Given the above observations, this study investigated the *in vitro* effects of *UV-B* exposure on growth, viability and MMP production in primary uveal melanocytes and two uveal melanoma cell lines.

5.2 Materials and Methods

Cells

As described in Chapter 2.2, OCM-1 is a spindle melanoma cell line (Kan-Mitchell, et al., 1989) that is grown in DMEM (ThermoElectron) while OCM-8 is an epithelioid melanoma cell line grown in RPMI 1640 (ThermoElectron) medium. Human uveal melanocytes are isolated and cultured based on the methods of Hu *et al* (1993), as described in detail in Chapter 2.2.

Immunocytochemistry

Immunocytochemical staining was performed on melanocytes and OCM-1 and OCM-8 melanoma cells as described in Chapter 2.2. Briefly cells were seeded on sterile coverslips, fixed and incubated with 10% normal goat serum (NGS). The following primary antibodies were used to assess the purity of melanocyte cultures: mouse anti-human fibroblast (prolyl 4-hydroxylase) (1:25; Dako, Denmark), α-smooth muscle actin (1:40; pericytes, Dako), and Melanoma Ab-3 (1:100; antibodies to melanoma and melanocyte-specific antigens HMB-45 and HMB-50, NeoMarkers, USA). OCM-1 and OCM-8 cells were also incubated with mouse anti-swine vimentin (1:100; Dako) as a positive control. Coverslips were incubated overnight, immunolabelled with the appropriate Alexa-488 conjugated secondary antibody (1:1000, Molecular Probes, USA) and viewed with fluorescence microscopy.

UV-B Irradiation

Initially the morphology and growth of cell cultures, prior to *UV-B* treatment, was examined. To determine the most suitable cell density for these experiments, $2.5X10^4$, $5X10^4$ and 10^5 cells/well for OCM-1 and OCM-8 cell lines were initially seeded in a 6 well plate, and monitored by microscopy over 3 days. On day 3, wells that were seeded with $5X10^4$ cells were approximately 70-80% confluent and displayed good viability; this seeding density was selected for further experiments (Fig 5.1). Melanocytes were seeded between $5X10^4$ and 10^5 cells/well.

To determine the cytotoxic dose response to *UV-B*, uveal melanocytes and melanoma cell lines were initially exposed to *UV-B* from 0, 10, 20 and 30 mJ/cm^2 (Philips *UV-B* bulb TL 20W/12 RS, Sydney, Australia). *UV-B* light intensity was calibrated prior

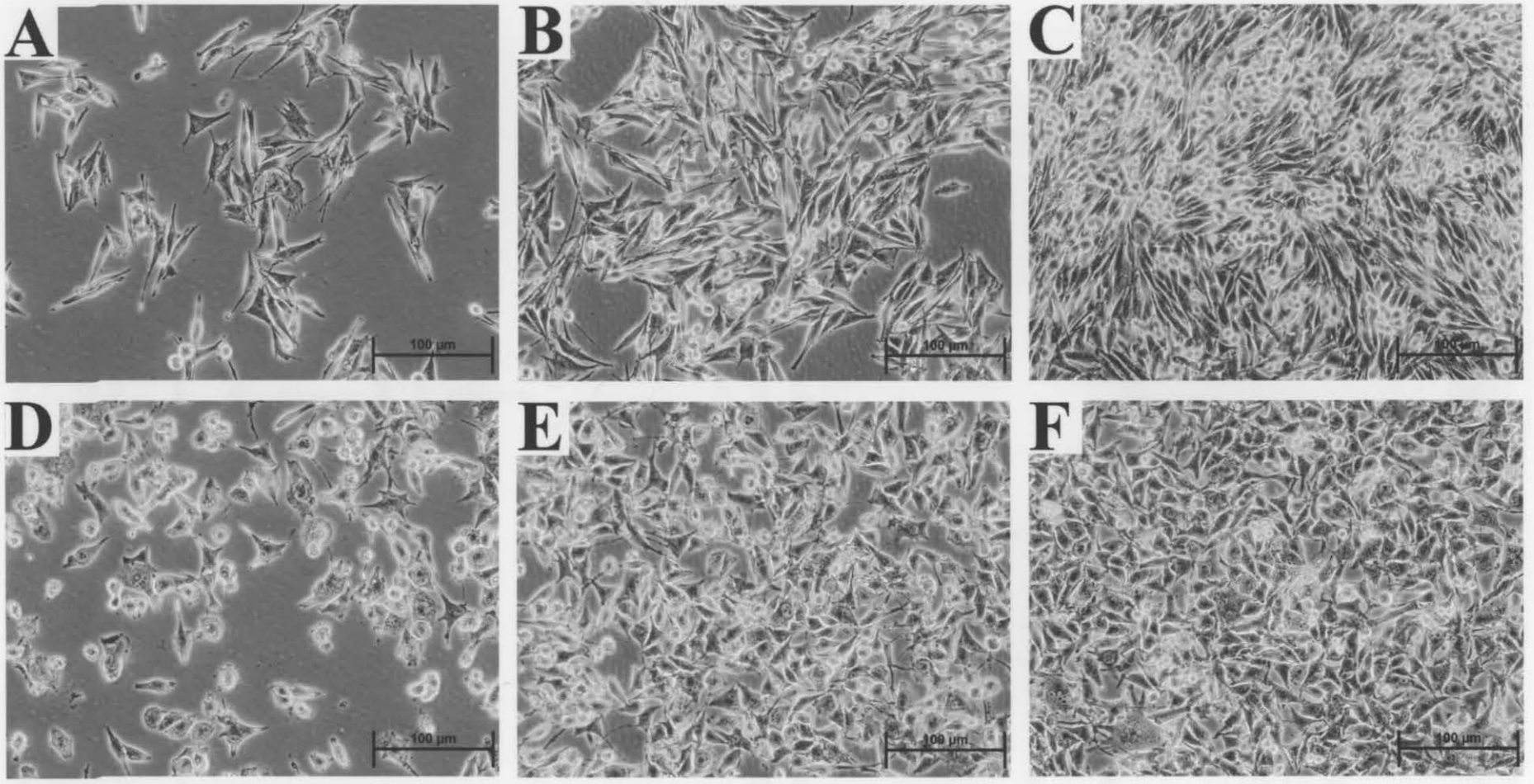

Figure 5.1
OCM-1 (A-C) and OCM-8 (D-F) cell lines were seeded with $2.5X10^4$, $5X10^4$ and 10^5 cells/well respectively, after 3 days in culture.

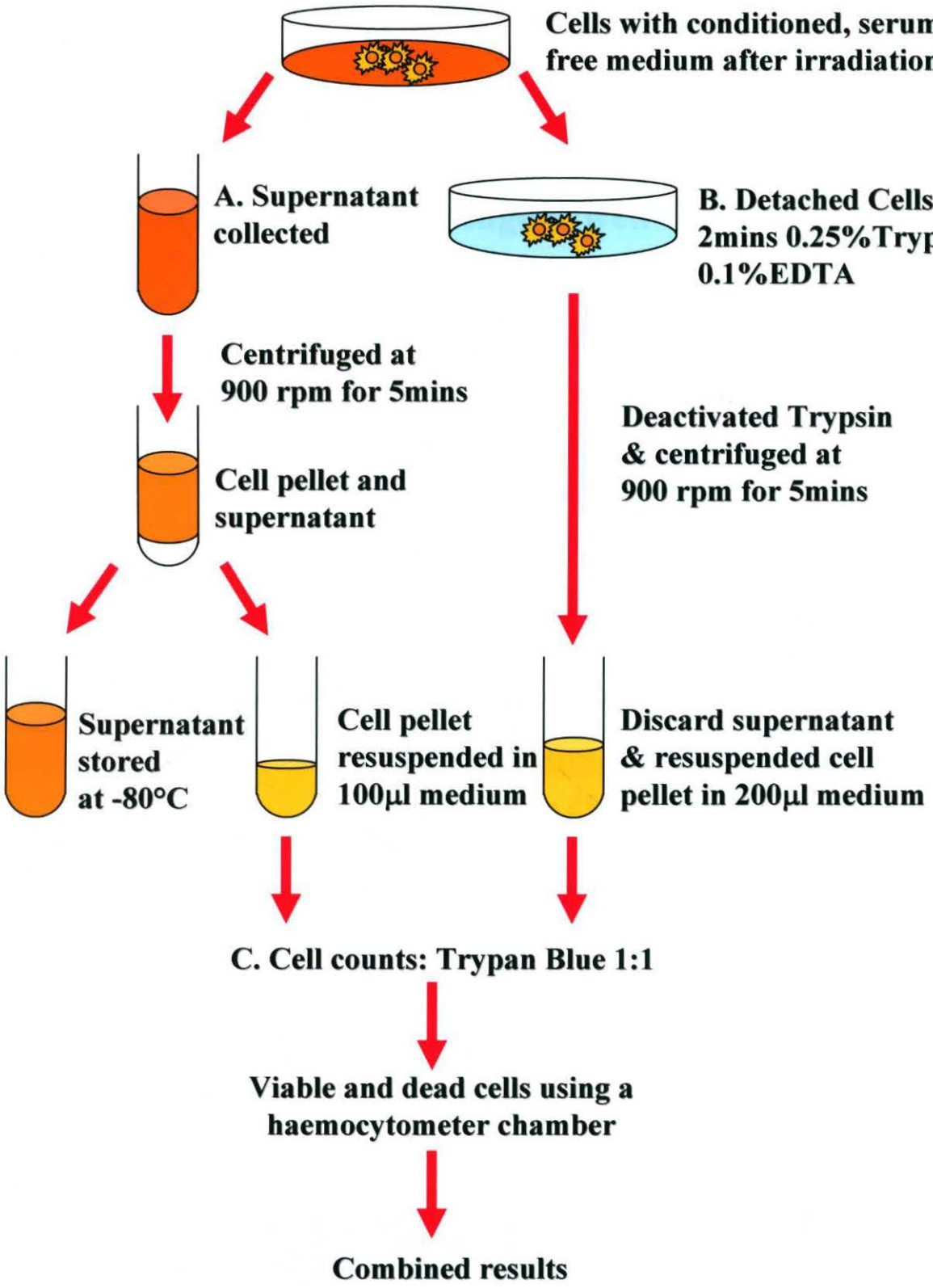

Figure 5.2

A. Floating cells pelleted, and resuspended in 100 µl fresh medium.

B. Adherent cells detached using 0.25% trypsin/0.1% EDTA, centrifuged and resuspended in 200 µl fresh medium.

C. The number and viability of both adherent and floating cell population assessed using Trypan Blue exclusion, and results combined.

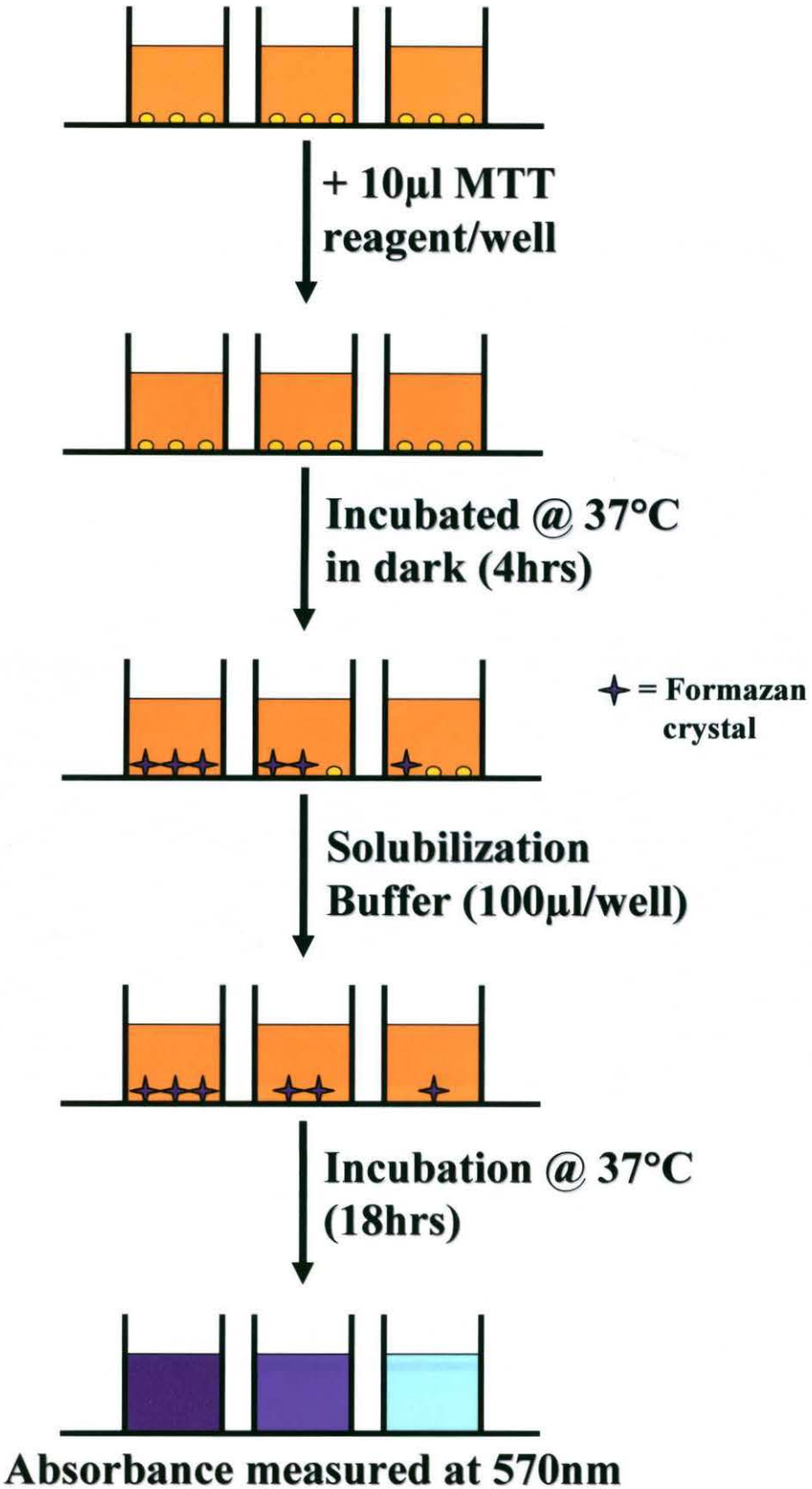

Figure 5.3
MTT assay (Roche cell proliferation kit I 1465007) for cell proliferation and viability measurement.
***Adapted from Apoptosis and Cell Proliferation 2nd edition, Boehringer Mannheim**

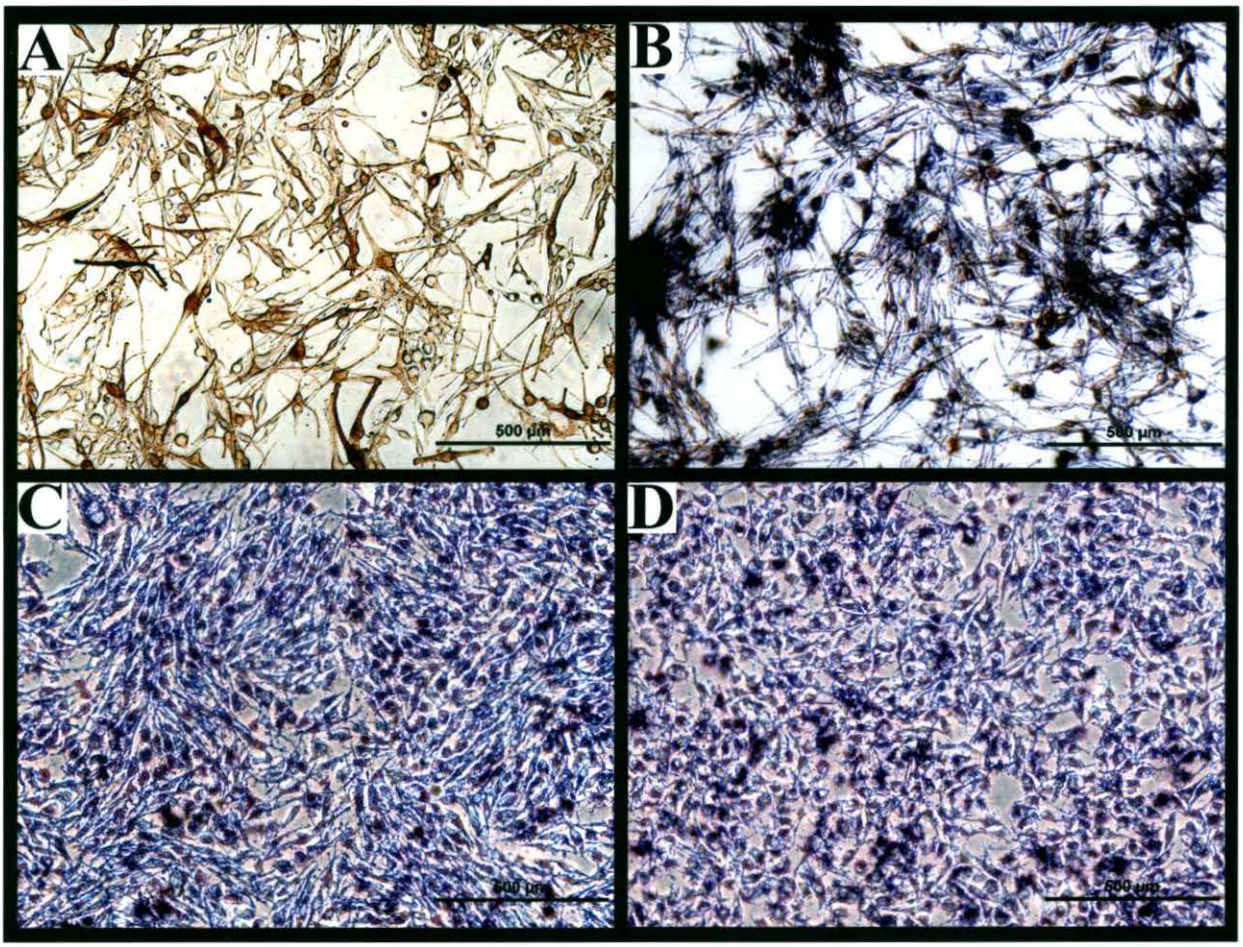

Figure 5.4

A. Cultured primary uveal melanocytes.

B. Primary uveal melanocytes, C. OCM-1 and D. OCM-8 cell lines were incubated with MTT reagent forming water-insoluble formazan salt (purple crystals).

to each experiment using a radiometer IL1400A (International Light, USA). Cell monolayers in PBS were irradiated with the appropriate *UV-B* dose and changed into serum-free medium. Cell viability (%) was determined using trypan blue exclusion and hemacytometer counting. Viability of uveal melanocytes was reduced to 50% (LD50) with 30 mJ/cm^2 *UV-B* (n=2, 48 hrs after treatment). The LD50 for OCM-8 and OCM-1 cells was 5 and 10 mJ/cm^2 *UV-B* respectively (72 hrs after treatment). Subsequent experiments to measure MMP production were performed with ≤10 mJ/ cm^2 *UV-B* for melanocytes and < 5 mJ/cm^2 *UV-B* for melanoma cells.

Viability and Proliferation Post UV-B

After *UV-B* irradiation, conditioned cell medium was collected at 0, 8, 24, 36, 48 and 72 hrs in Eppendorf tubes, centrifuged for 5 mins at 1200 *g* and 4°C and the supernatant collected and stored at -80°C for gelatin zymography (see below). The cell number and viability (%) of floating and adherent cells was assessed using trypan blue exclusion at each time point as follows. Floating cells were pelleted during collection of supernatants, resuspended in 100 µl fresh medium, and the cell number and viability was assessed (Fig 5.2). Adherent cells were detached using 0.25% trypsin/0.1% EDTA for 2 mins at 37°C, centrifuged for 5 mins at 290 *g* and 20°C, and cells resuspended in 200 µl fresh medium (Fig 5.2). The number and viability of the adherent cell population was then determined. For each time point and treatment, the total cell number and viability was calculated as the floating plus adherent cell populations (Fig 5.2).

An MTT assay was used to further assess the sensitivity of uveal melanocytes and melanoma cells to *UV-B*. MTT assays measure the activity of viable cells based on the reduction of the tetrazolium salt 3-(4,5-dimethylthiazol-2-yl)-2,5-diphenyltetrazolium bromide (MTT). This reaction produces a water-insoluble formazan salt, which must be solubilized and then quantified using a multiwell scanning spectrophotometer (plate reader) with a 570 nm filter (Mosmann, 1983). The number of viable cells is directly proportional to the amount of formazan product produced by living cells, and thus the absorbance reading. Uveal melanocytes (n=3, duplicate) and melanoma cells (n=3; triplicate) were seeded at 5x10^4 cells/well in multi-well plates, grown in serum-free medium as for gelatin zymography (see below) and treated with a range of doses of *UV-B* (0 to 30 mJ/cm^2 for melanocytes, and 0, 2.5 and 3.5 mJ/cm^2 for melanoma cells) as described above. Separate plates of cells were prepared for each time point, and cells were incubated for 24 and 48 hrs. At each time point, MTT reagent (Roche Applied Science,

Mannheim, Germany) was added to each well and cells incubated for an additional 4 hrs at 37°C (Fig 5.3), followed by incubation in solubilization solution (10% sodium dodecyl sulfate in 0.01M HCl, Roche Applied Science) for 18 hrs at 37°C (Fig 5.4). Absorbance at 570 nm was detected using a Bio-Rad 550 microplate reader (Bio-Rad Laboratories Inc., USA). Data were analysed using a non-parametric Kruskal-Wallis Conover-Inman test (StatsDirect Software v2.4.5).

Gelatin Zymography

To assess the effect of *UV-B* on the production of MMP-2 and -9, melanocytes (10^5 cells/well) and melanoma cells ($5x10^4$ cells/well) were initially seeded into 6-well plates with growth medium, and incubated at 37°C for 72 hrs. After removing the medium, cells were rinsed with PBS, then incubated in serum-free MGM, DMEM or RPMI plus ITS+3 liquid media supplement (Sigma) respectively for 24 hrs before *UV-B*. After irradiation, conditioned media was collected at 0, 8, 24, 36, 48 and 72 hrs, centrifuged at 4°C for 5 mins at 160 *g* and supernatants aliquoted and stored at -80°C. Each time point had separate wells and the conditioned media was not diluted at any stage.

Enzymatic activity for MMP-2 and -9 in conditioned media samples was evaluated using gelatin zymography. Samples were mixed with 5x loading buffer and run on a 10% polyacrylamide gel containing 1 mg/ml gelatin in the presence of sodium decyl sulphate (SDS) (Life Technologies Inc., USA) under non-reducing conditions. A broad range molecular weight standard (Bio-Rad) was run in adjacent lanes to estimate the molecular weight of each gelatinolytic band. Electrophoresis was carried out at 4°C with a constant voltage of 120 V for 3 hrs. Gels were then washed in 2.5% Triton X-100 (BDH Chemicals, Australia) for 1 hr at RT, and rinsed for 30 mins at RT in developing buffer (50 mM Tris-HCl, 100 mM NaCl, 10 mM $CaCl_2$ and 0.02% (w/v) sodium azide, pH 7.5). Gels were placed in fresh developing buffer, incubated for 18 hrs at 37°C, stained with 0.2% Coomassie Brilliant Blue R250 (Research Organics Inc., USA) for 1 hr at RT and destained in 10% acetic acid/ 30% ethanol for 2 hrs. Gels were incubated in gel drying solution (40% methanol/5% glycerol) for 1 hr and finally preserved between cellophane sheets. Gels were scanned and converted to Adobe Photoshop images.

5.3 Results

Morphology & Immunocytochemistry of Melanoma Cells & Melanocytes

Given the possibility that *UV-B* influences not only cell death but cell morphology, initially the general morphology of untreated cell cultures was considered. OCM-1 cells displayed typical spindle morphology as described previously (Kan-Mitchell, et al., 1989) (Fig 2.3, 5.5A). In comparison, OCM-8 cells had an epithelioid morphology, often with extensive processes (Fig 2.3, 5.5C). Uveal melanocytes initially displayed a bipolar morphology with thin processes and prominent cell bodies. However, with time in culture, many melanocytes extended multiple cell processes (Fig 2.4, 5.5E) and displayed variable melanin content (Fig 2.4, 5.5E). OCM-1, OCM-8 cells and melanocytes were strongly immunoreactive for vimentin antibody, which clearly showed cytoplasmic filaments and general cell morphology (Fig 5.6).

Effects of UV-B on Viability and Cell Growth

Cell death was increased in melanoma cells for *UV-B* up to 20 mJ/cm^2 (Fig 5.5). Some OCM-1 cells exposed to high dose *UV-B* also displayed irregular morphology with increased numbers of processes and flattened appearance (Fig 5.5B). Melanocytes initially exposed to 30 mJ/cm^2 *UV-B* showed obvious cell death when compared to untreated cells (Fig 5.5E&F). Trypan blue exclusion showed that melanocyte viability of did not decrease below 95% up to 10 mJ/cm^2 *UV-B* (Table 5.1) while OCM-1 and OCM-8 viability had decreased to approximately 80% and 70% respectively at 48 hrs (Table 5.1).

To further determine whether melanoma cells were more *UV-B* sensitive than melanocytes, OCM-1 and OCM-8 cells and melanocytes were irradiated and viability measured by MTT assay. Comparison of control and *UV-B* treated melanocytes showed a significant reduction in mean absorbance (viability) at 24 and 48 hrs for 10, 20 and 30 mJ/cm^2 ($p<0.01$; Fig 5.7). By contrast, after 48 hrs OCM-1 and OCM-8 melanoma cells showed significant reductions in mean absorbance (viability) for 2.5 and 3.5 mJ/cm^2 *UV-B* compared to controls ($p<0.02$; Fig 5.7). Control OCM-8 cell viability was also observed to be reduced with exposure to serum free medium over time (Fig 5.7).

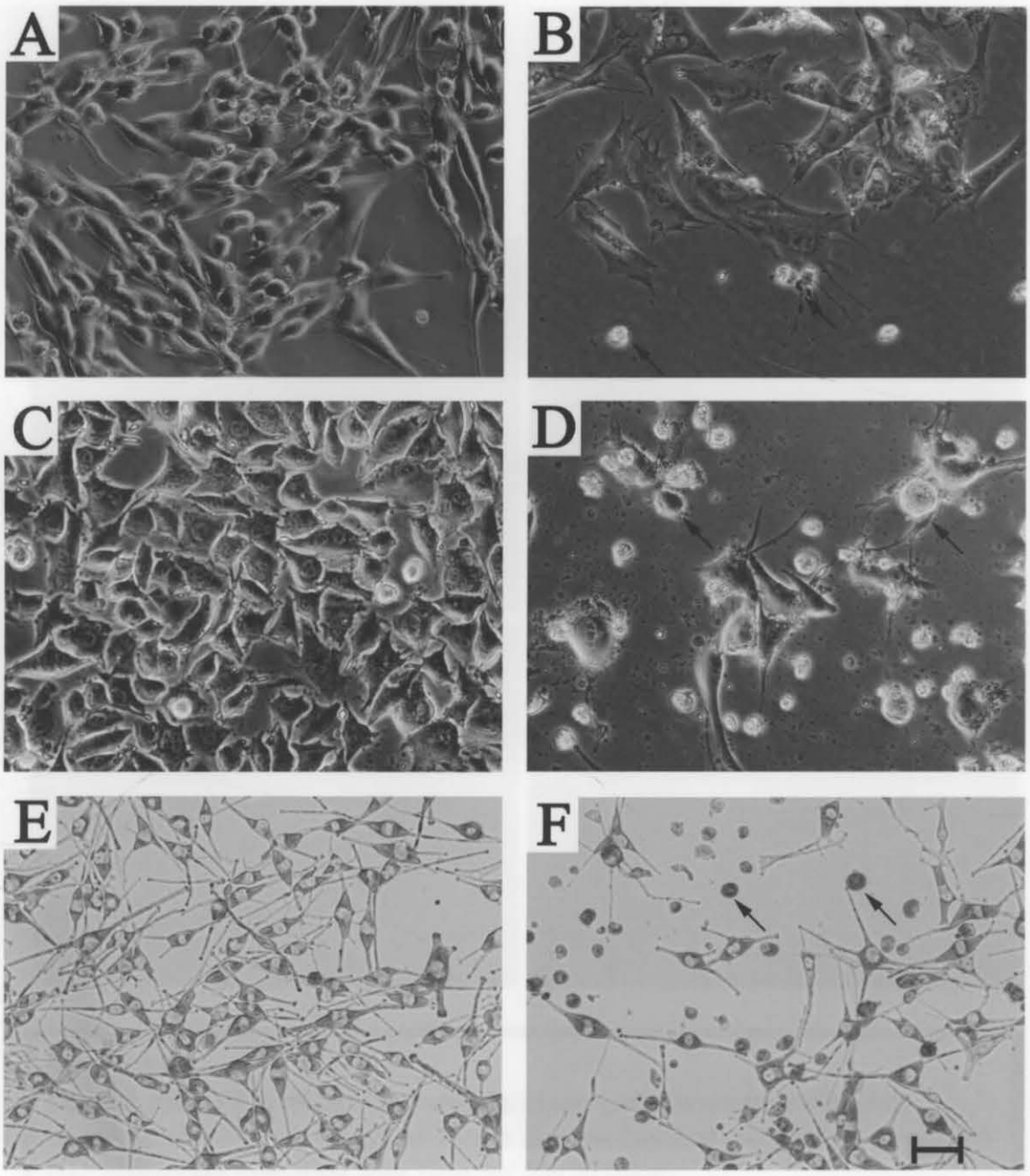

Figure 5.5
Untreated OCM-1 (A), OCM-8 (C) melanoma cells, and primary uveal melanocytes (E). After *UV-B* exposure OCM-1 (B) and OCM-8 (D) melanoma cells show evidence of cell death up to 20 mJ/cm^2 (arrows). Many *UV-B* treated OCM-1 cells also show a flattened morphology and more cell processes (B) compared to untreated cells (A). In cultures of primary uveal melanocytes, dead cells (arrows) are seen after treatment with 30 mJ/cm^2 *UV-B* (F). (Bar=50 μm).

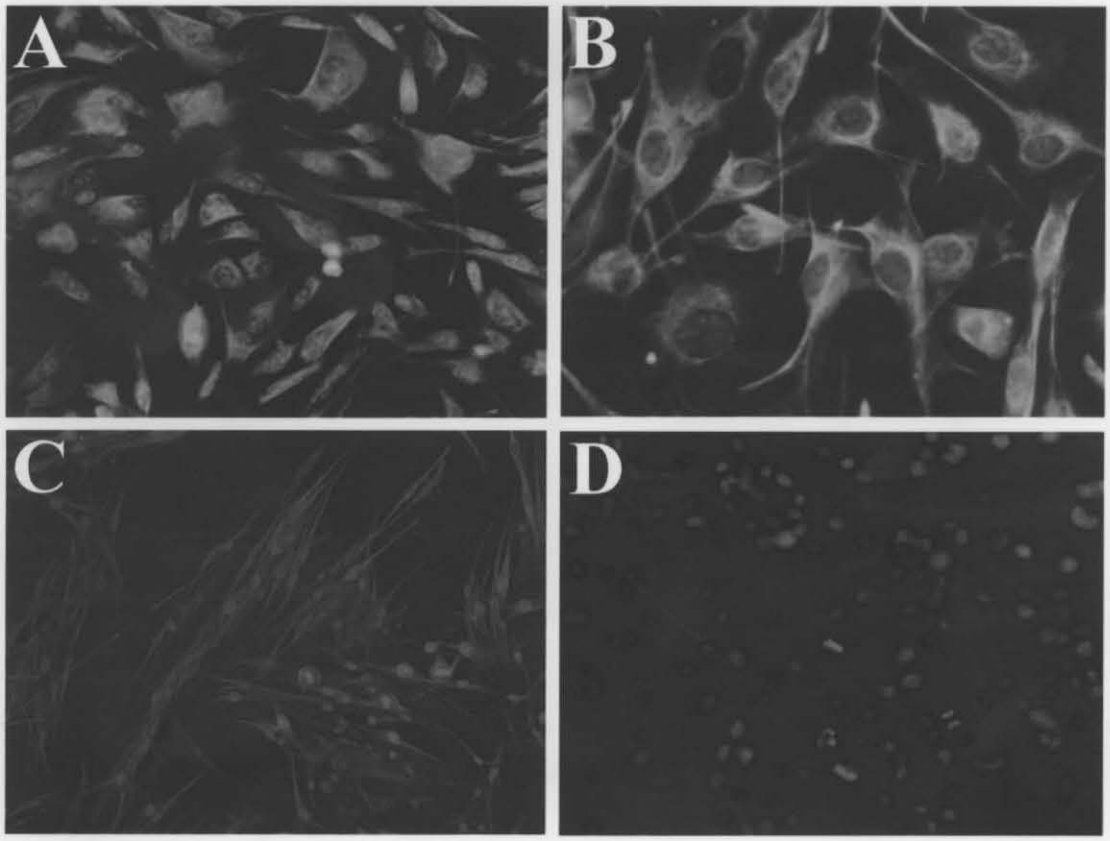

Figure 5.6
OCM-1 cells, OCM-8 cells and uveal melanocytes immunolabelled with vimentin antibody (A-C). OCM-8 cells immunolabelled using rabbit Ig control (D). Nuclei are identified with Hoechst 33426 (blue).

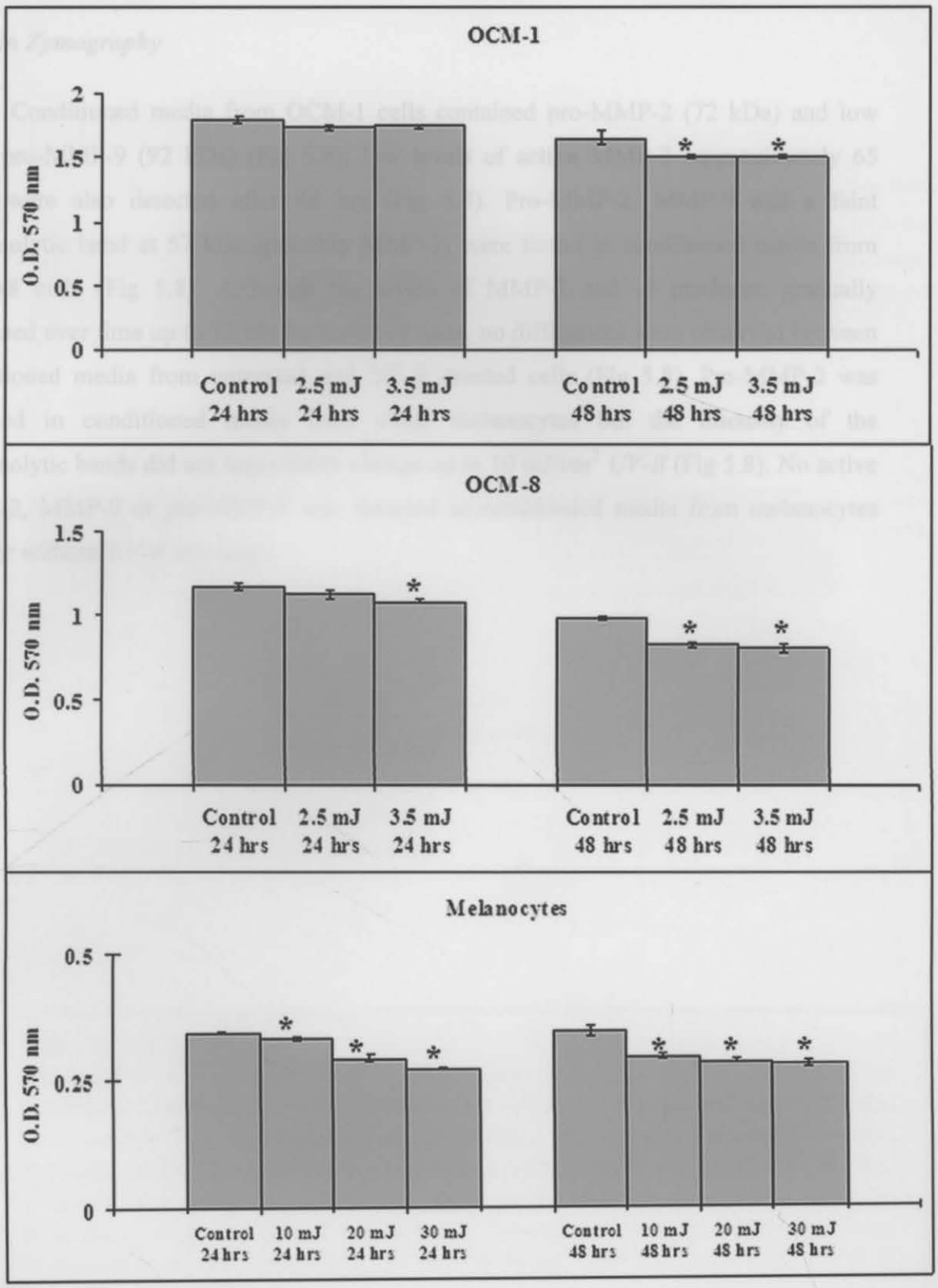

Figure 5.7
Mean absorbance (± SEM) of OCM-1, OCM-8 and melanocytes after different doses of *UV-B* treatment (mJ/cm^2) measured at 24 and 48hrs using an MTT assay.
*$p<0.02$, Kruskal-Wallis Conover-Inman non-parametric test for comparisons of control and *UV-B* treatments.

Gelatin Zymography

Conditioned media from OCM-1 cells contained pro-MMP-2 (72 kDa) and low level pro-MMP-9 (92 kDa) (Fig 5.8); low levels of active MMP-2 (approximately 65 kDa) were also detected after 48 hrs (Fig 5.8). Pro-MMP-2, MMP-9 and a faint gelatinolytic band at 57 kDa (possibly MMP-1) were found in conditioned media from OCM-8 cells (Fig 5.8). Although the levels of MMP-2 and -9 produced gradually increased over time up to 72 hrs for both cell lines, no differences were observed between conditioned media from untreated and *UV-B* -treated cells (Fig 5.8). Pro-MMP-2 was detected in conditioned media from uveal melanocytes but the intensity of the gelatinolytic bands did not appreciably change up to 10 mJ/cm^2 *UV-B* (Fig 5.8). No active MMP-2, MMP-9 or pro-MMP-9 was detected in conditioned media from melanocytes with or without *UV-B* exposure.

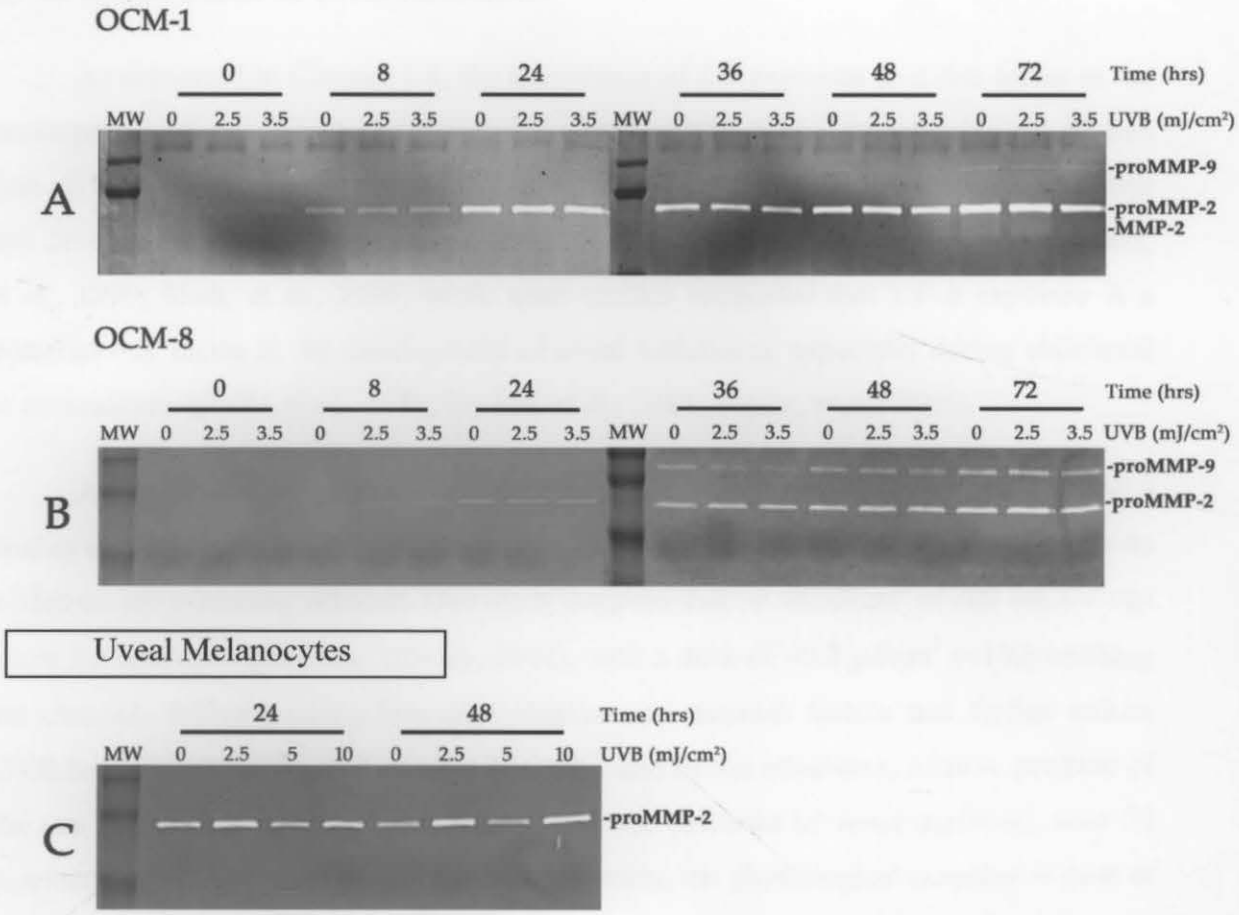

Figure 5.8

Pro-MMP-2 (72 kDa), MMP-2 (65 kDa) and pro-MMP-9 (92 kDa) in conditioned media from cultured melanoma cell lines (A & B) and cultured uveal melanocytes (C) measured by zymography. (A) & (B) are representative examples of OCM-1 and OCM-8 melanoma cells respectively, at time points 0 to 72 hours after treatment, as indicated. Melanoma cell lines were treated with *UV-B* at doses of 0, 2.5 or 3.5 mJ/cm^2. (C) Representative zymograms for uveal melanocytes at two time-points, 24 and 48 hours, after treatment with *UV-B* 0, 2.5, 5 or 10 mJ/cm^2.

5.4 Discussion

UV-B: A Risk Factor in Uveal Melanoma?

As discussed in Chapter 1.4, the importance of *UV* exposure as a risk factor in the development of uveal melanoma remains controversial. Some epidemiological studies find no clear association between lifetime cumulative *UV-B* exposure, outdoor activities and development of uveal melanoma (Pane, et al., 2000; Schwartz, et al., 1997; Seddon, et al., 1990; Shah, et al., 2005) while other studies supported that *UV-B* exposure is a potential risk factor in the development of uveal melanoma, especially during childhood to adolescence (Holly, et al., 1990; Tucker, et al., 1985; Vajdic, et al., 2002).

Although several studies have estimated the amount of *UV-B* received inside a human eye, estimates of the cumulative dose of UVR reaching the retina and choroid over a lifetime are extremely difficult. One study suggests that ~0.08mJ/cm^2 of 300 nm *UV* can reach the lens on a given day (Sliney, 2002), with a dose of <0.8 μJ/cm^2 (<1%) reaching the choroid. Without taking into physiological and external factors that further reduce UVR reaching the retina and choroid like orbit and eyelid structures, relative position of the sun and the surrounding environment (e.g. the presence of water surfaces), over 70 years this approximates to about 20 mJ/cm^2. Clearly, the physiological cumulative dose of *UV-B* will be less than this level. However as a starting point to test the *in vitro* effects of *UV-B* on uveal melanocytes and melanoma cells growth, a single dose model of *UV-B* exposure with levels 0 to 30 mJ/cm^2 was used. Other studies investigating the role of *UV-B* in the pathogenesis of cutaneous melanoma and pterygium *in vitro* have similarly used an initial single dose of radiation (Di Girolamo, et al., 2003; Zhang, 2005).

In the present study *UV-B* induced cell death at lower doses for melanoma cells (non-pigmented) than primary melanocytes. One possible explanation for this difference in sensitivity to *UV-B* is that melanin, which can absorb 400 – 600 nm light (Peyman, et al., 1984), may protect melanocytes against *UV-B*-induced damage (Kadekaro, et al., 2003). However, even at early passages in the present study, not all cultured melanocytes displayed melanin granules. Furthermore, in addition to melanin, cutaneous melanocytes contain pheomelanin that is reported to display photosensitizing properties (Wenczl, et al., 1998). Uveal melanocytes also contain pheomelanin (Hu, et al., 2002) although its role in the response of these cells to UVR exposure remains to be determined. Taken together,

these observations suggest a limited role for melanin in protecting melanocytes from. *UV-B* Alternatively melanocytes may be more resistant to *UV-B* exposure than melanoma cells related to the expression of genes involved in DNA damage response and cell cycle regulation. Consistent with this, the viability of uveal melanocytes did not significantly decrease with exposure to <10 mJ/cm^2 *UV-B* treatment.

UV-B can induce DNA damage and activate several apoptotic pathways *via* the action of p53 (Fisher, 2001), a tumour suppressor gene also reported as a risk factor in uveal melanoma (Coupland, et al., 2000). Cutaneous melanocytes are found to be more resistant to *UV-B* induced apoptosis than keratinocytes, related to the differential expression of several apoptotic regulators including *Bcl-2* family genes (Bivik, et al., 2005; Bowen, et al., 2003). These studies suggest that apoptosis-resistant cutaneous melanocytes may initially survive UVR -induced DNA changes, accumulate further DNA damage over time and eventually form malignant lesions (Bivik, et al., 2005; Bowen, et al., 2003). Whether uveal melanocytes behave similarly following low dose UVR exposure during the early years of life, and then accumulate DNA damage with aging to later progress to melanomas remains to be determined. As discussed above, cumulative exposure to UVR is reported as a risk factor for uveal melanoma (Holly, et al., 1990; Vajdic, et al., 2002), and these tumours usually grow slowly and are diagnosed much later in life, generally between 50 to 75 years of age (Jager, et al., 2004).

UV-B and MMPs

Several studies report latent MMP-1, -2, -3 and -9 expression in normal human choroid (Guo, et al., 1999; Leu, et al., 2002). In the present study, isolated uveal melanocytes grown in serum-free medium expressed only pro-MMP-2 that could not be induced or activated by *UV-B* at doses up to 10 mJ/cm^2. A recent study reported that choroidal and iris melanocytes cultured in serum-containing medium produced pro-MMP-2 and low levels of MMP-9 (Chu, et al., 2004). Although gelatin zymography is a sensitive assay, latent or active MMP-9 could not be detected in conditioned media from primary uveal melanocytes in the present study. A major difference between the present study and that of Chu *et al* (2004) is the absence of serum in the culture medium.

Cutaneous melanocytic naevi cells and lesional keratinocytes express varying levels of MMP-2, TIMP-2 and MT1-MMP that can be modulated by *UV*-B (Krengel, et al., 2002). In contrast overall MMP production in cultured uveal melanoma cells and

melanocytes increased over time independently of *UV-B*. However, a differential expression of MMPs is seen in the conditioned medium from OCM-8 cells compared to the less invasive OCM-1 cells (see Fig 5.7), perhaps reflecting the more invasive nature of epithelioid OCM-8 cells. Uveal melanomas containing epithelioid cells are generally associated with increased metastatic potential and a poor prognosis compared to melanomas with spindle cell morphology (Kanski, 1994). Gene expression studies distinguished two classes of uveal melanoma, Class 1 tumours with a spindle cell/melanocyte morphology and excellent prognosis, and Class 2 tumours associated with epithelioid morphology and metastatic disease (Onken, et al., 2004). Epithelioid choroidal melanomas are reported to display increased immunoreactivity for MMP-2 and particularly MMP-9, compared to spindle-type tumours (El-Shabrawi, et al., 2001; Vaisanen, et al., 1999). A marked downregulation of *TIMP-3* (MMP inhibitor) gene expression is also observed in the progression from melanocytes to metastasis (van der Velden, et al., 2003).

As discussed above *UV-B* exposure is reported to upregulate MMP production by keratinocytes and melanocytic cells (Krengel, et al., 2002) consistent with a role for cellular interactions in melanocytic tumour growth. UVR-responsive cytokines produced by keratinocytes such as IL-1 and TNF-α, are also reported to stimulate active MMP-9 secretion in the advanced stages of cutaneous melanoma (Shellman, et al., 2006). Stromal cell-derived MMPs are important for tumour growth, angiogenesis and metastasis (Jodele, et al., 2006), and tumour cells including cutaneous melanoma cells, are reported to produce factors such as extracellular matrix metalloproteinase inducer protein (EMMPRIN) that can induce MMP production by stromal cells (Kanekura, et al., 2002; Sun, et al., 2001). Taken together with the findings in this study, these observations suggest that although *UV-B* does not induce melanoma cells *in vitro* to produce/activate MMP-2 and -9, UVR of solid tumours such as uveal melanoma, may modulate MMP production by stromal cells *in situ*. To further study these interactions and the effects on MMP production/activation, co-cultures of uveal melanoma cells and fibroblasts irradiated with varying doses of *UV-B* could be investigated.

5.5 Conclusion

This is the first *in vitro* study to investigate the effects of *UV-B* exposure on the growth, survival and MMP production in uveal melanocytes and melanoma cells. Decreased survival of uveal melanoma cells, but not melanocytes, following low doses of

UV-B exposure suggests differences in cellular responses to DNA damage that may be important in subsequent transformation of melanocytes to melanomas. *UV-B* did not induce the production and/or activation of MMP-2 and -9 in melanocytes or melanoma cells. Future studies could investigate the expression of DNA damage response genes such as *p53*, *p21* and *GADD45* that can be regulated following UVR exposure, and may be important for uveal melanoma development, particularly with low dose UVR.

Chapter 6

Conclusions

Growth and development of uveal melanoma involves both cellular and environmental factors. Previous studies have suggested that proteinases and adhesion molecules are involved in tumour growth; additionally, epidemiological studies have also implicated long-term UV exposure as a risk factor for developing uveal melanoma. The role(s) of these factors in uveal melanoma pathogenesis were more comprehensively investigated in this thesis. The group of primary uveal melanoma specimens examined for MMP-9, TIMP-3 and CD146 immunolabelling in Chapter 3 and 4, represent one of the larger series of tumours studied to date.

MMPs & TIMPs in Uveal Melanoma

The results in Chapter 3, together with observations from earlier studies (Lai, 2002), clearly showed distinct distributions of immunostaining for several classes of MMPs (MMP-1, -2, -9, -19, MT1-MMP) and physiological inhibitors of MMPs (TIMP-2 & -3), consistent with regional differences in the tumour microenvironment seen histologically in uveal melanoma. The microenvironment of uveal melanoma is complex, including a heterogeneous population of both spindle and epithelioid cells, stromal cells (including fibroblast), immune cells, vasculature, growth factors, cytokines and matrix, all of which can affect uveal melanoma growth.

Consistent with previous studies, MMP-9 was strongly expressed in most tumours including heterogeneous expression on tumour vasculature. Additionally, MMP-9 was also expressed by intravascular leucocytes; this may be important for leukocyte movement into tumours, and contribute to leukocyte extravasation and tissue invasion. Tumor-infiltrating macrophages in uveal melanoma have been associated with adverse prognosis, epithelioid cell type and high microvascular density (Makitie, et al., 2001). Evidence of patterns of MMP-9 expression similar to PAS-positive networks (vasculogenic mimicry) was seen in some uveal melanomas; however, the involvement of MMP-9 in formation of extravascular channels requires further study, including three-dimensional culture experiments and gene profiling.

As discussed in Chapter 1 and 3, TIMP-3 can regulate various MMPs and tumour invasion, as well as inhibit angiogenesis and induce apoptosis (Ahonen, et al., 1998; Qi, et al., 2003), and loss of TIMP-3 may be involved in tumour growth. *TIMP-3* gene downregulation associated with changes in methylation has been recently found in various cancers including uveal melanoma (Mylona, et al., 2006; van der Velden, et al., 2003). In

Chapter 3, heterogeneous TIMP-3 immunolabelling was observed in all uveal melanomas, with weak expression in ~ 50% of specimens. Considerable variation has been reported in the levels and extent of TIMP-3 immunostaining in the only two studies of primary uveal melanoma to date (Nareyeck, et al., 2005; van der Velden, et al., 2003). Gene microarray studies recently found downregulated *TIMP-3* mRNA expression in Class 2 uveal melanomas with a poor prognosis (Singh, et al., 2007). These studies indicate that hypermethylation silences *TIMP-3*, and the therapeutic potential of agents that modify methylation and chromatin arrangement (such as histone deacetylase inhibitors) remains an area of interest for future studies.

TIMP-3 may also play a role in stabilising the mature tumour vasculature by interacting with proteoglycans within the vascular basement membrane matrix (Chapter 3.4). Future studies could use 3D cultures of human umbilical vein endothelial cells (HUVECs), co-cultures of HUVECs and pericytes and co-cultures of HUVECs and uveal melanoma cells to study the role of melanoma cell-derived TIMP-3 on vascular tube formation and stability.

In conclusion, the distinct immunostaining patterns observed for MMP-9 and TIMP-3 within uveal melanoma are consistent with their involvement in tumour growth and angiogenesis. This includes expression in tumour cells, vasculature and leukocytes, as well as regional variations in expression that have not been described previously. Agents that modulate MMPs and TIMPs may be worth consideration for therapy, given that ~50% of patients with uveal melanoma will develop metastatic disease within 10 years of diagnosis.

CD146 in Uveal Melanoma

The Ig superfamily protein CD146 is involved in tumour development and expressed in malignancies including cutaneous melanoma. Recent studies using 2-D gel electrophoresis found CD146 expression in several uveal melanoma cell lines (Pardo, et al., 2005, 2006). In Chapter 4, the expression and distribution of CD146 in primary uveal melanomas was described for the first time, where CD146 immunoreactivity was found to be significantly stronger in mixed and epithelioid tumours compare to spindle cell tumours. Furthermore, variable levels of CD146 protein were observed in uveal and metastasis-derived melanoma cell lines and uveal melanocytes. These observations suggest that while CD146 is important for tumour growth, its expression may not be

essential for invasion and metastasis, consistent with findings in other tumours. The role of transcription factors including AP-2 α, and the signaling pathways involved in regulating CD146 expression and activity in uveal melanoma remain to be defined. Interactions between CD146-positive melanoma cells and vasculature, *via* an as yet unidentified ligand, may also be important for the hematogenous spread of tumor cells during metastases. The present study further supported CD146 involvement in uveal melanoma including hematogenously spread.

As mentioned in Chapter 4.4, soluble CD146 (sCD146) has been reported in several diseases (Bardin, et al., 2003, 2006; Neidhart, et al., 1999) The present study found high levels of CD146 expression on the luminal surface of vascular endothelial cells and intravascular erythrocytes in uveal melanomas. To further investigate the involvement of sCD146 in uveal melanoma, levels of sCD146 in serum samples from melanoma patients and healthy persons, could be compared using ELISA and western blotting.

CD146 also displayed PAS-like patterns in several tumours, similar to MMP-9. Although it is tempting to speculate whether MMP-9 and CD146 are contributing in vasculogenic mimicry, further studies are required to confirm this theory since uveal melanoma is a heterogenous tumour hence these observations might be circumstantial. Future experiments with *in vitro* 3D cultures and serial primary tumour sections might be able to confirm the current findings.

A Role for UV in Growth of Uveal Melanoma?

As discussed in Chapter 5, the importance of *UV-B* exposure as a risk factor in the development of uveal melanoma remains controversial, with equivocal findings from epidemiological studies. The *in vitro* study in Chapter 5 is the first to investigate the biological effects of *UV-B* exposure on the growth, survival and MMP production in uveal melanocytes and melanoma cells. Decreased survival of uveal melanoma cells, but not melanocytes, following low doses of *UV-B* exposure suggests differences in cellular responses to DNA damage that may be important in subsequent transformation of melanocytes to melanomas. Although *UV-B* did not affect the production and activation of MMP-2 and -9 in both uveal melanoma cells and melanocytes, it may affect other factors which can influence cell proliferation and survival, including cell cycle & DNA damage response genes such as *p53*, *p21* and *GADD45*. Future studies could investigate

the expression of these genes following UV exposure in uveal melanoma.

Uveal melanoma is generally a slow growing tumour, more common in older people, and associated with long term exposure to *UV-B* in earlier life. While the current study used a single dose of *UV-B*, future studies applying cumulative doses of *UV-B* could be used to investigate regulation of both genes and proteins important in uveal melanoma development. These studies would also be important for discovering pathways involved in melanocyte-to-melanoma transformation. It is also important to understand the effects of *UV-B* on the tumour microenvironment as described above (Chapter 6.1). One limitation of the present study was that the *in vitro* experiments were performed on either melanoma cell lines or primary melanocyte cultures alone. The effects of *UV-B* on neighbouring cells in the *in situ* environment such as fibroblasts, endothelial cells, immune cells and RPE would be interesting to consider.

References

Aalto, Y, Eriksson, L, Seregard, S, Larsson, O and Knuutila, S (2001) Concomitant loss of chromosome 3 and whole arm losses and gains of chromosome 1, 6, or 8 in metastasizing primary uveal melanoma. Invest Ophthalmol Vis Sci 42:313-7.

Abdel-Rahman, MH, Craig, EL, Davidorf, FH and Eng, C (2005) Expression of vascular endothelial growth factor in uveal melanoma is independent of 6p21-region copy number. Clin Cancer Res 11:73-8.

Ahir, A, Guo, L, Hussain, AA and Marshall, J (2002) Expression of metalloproteinases from human retinal pigment epithelial cells and their effects on the hydraulic conductivity of Bruch's membrane. Invest Ophthalmol Vis Sci 43:458-65.

Ahonen, M, Baker, AH and Kahari, VM (1998) Adenovirus-mediated gene delivery of tissue inhibitor of metalloproteinases-3 inhibits invasion and induces apoptosis in melanoma cells. Cancer Res 58:2310-5.

Al-Jamal, RT, Makitie, T and Kivela, T (2003) Nucleolar diameter and microvascular factors as independent predictors of mortality from malignant melanoma of the choroid and ciliary body. Invest Ophthalmol Vis Sci 44:2381-9.

Alberts, B, Bray, D, Lewis, J and Raff, M (1996) Molecular Biology of the Cell. Garland Publishing Inc, New York.

Aldovini, D, Demichelis, F, Doglioni, C, Di Vizio, D, Galligioni, E, Brugnara, S, Zeni, B, Griso, C, Pegoraro, C, Zanńoni, M, Gariboldi, M, Balladore, E, Mezzanzanica, D, Canevari, S and Barbareschi, M (2006) M-CAM expression as marker of poor prognosis in epithelial ovarian cancer. Int J Cancer 119:1920-6.

Alexander, CM, Hansell, EJ, Behrendtsen, O, Flannery, ML, Kishnani, NS, Hawkes, SP and Werb, Z (1996) Expression and function of matrix metalloproteinases and their inhibitors at the maternal-embryonic boundary during mouse embryo implantation. Development 122:1723-36.

Anastassiou, G, Schilling, H, Djakovic, S and Bornfeld, N (2000)a Expression of VLA-2, VLA-3, and alpha(v) integrin receptors in uveal melanoma: association with microvascular architecture of the tumour and prognostic value. Br J Ophthalmol 84:899-902.

Anastassiou, G, Schilling, H, Stang, A, Djakovic, S, Heiligenhaus, A and Bornfeld, N (2000)b Expression of the cell adhesion molecules ICAM-1, VCAM-1 and NCAM in uveal melanoma: a clinicopathological study. Oncology 58:83-8.

Anfosso, F, Bardin, N, Frances, V, Vivier, E, Camoin-Jau, L, Sampol, J and Dignat-George, F (1998) Activation of human endothelial cells via S-endo-1 antigen (CD146) stimulates the tyrosine phosphorylation of focal adhesion kinase p125(FAK). J Biol Chem 273:26852-6.

Anfosso, F, Bardin, N, Vivier, E, Sabatier, F, Sampol, J and Dignat-George, F (2001) Outside-in signaling pathway linked to CD146 engagement in human endothelial cells. J Biol Chem 276:1564-9.

Arentsen, JJ and Green, WR (1975) Melanoma of the iris: report of 72 cases treated surgically. Ophthalmic Surg 6:23-37.

Baggetto, LG, Gambrelle, J, Dayan, G, Labialle, S, Barakat, S, Michaud, M, Grange, JD and Gayet, L (2005) Major cytogenetic aberrations and typical multidrug resistance phenotype of uveal melanoma: current views and new therapeutic prospects. Cancer Treat Rev 31:361-79.

Bar-Eli, M (1999) Role of AP-2 in tumor growth and metastasis of human melanoma. Cancer Metastasis Rev 18:377-85.

Bardin, N, Anfosso, F, Masse, JM, Cramer, E, Sabatier, F, Le Bivic, A, Sampol, J and Dignat-George, F (2001) Identification of CD146 as a component of the endothelial junction involved in the control of cell-cell cohesion. Blood 98:3677-84.

Bardin, N, Frances, V, Combes, V, Sampol, J and Dignat-George, F (1998) CD146: biosynthesis and production of a soluble form in human cultured endothelial cells. FEBS Lett 421:12-4.

Bardin, N, Frances, V, Lesaule, G, Horschowski, N, George, F and Sampol, J (1996) Identification of the S-Endo 1 endothelial-associated antigen. Biochem Biophys Res Commun 218:210-6.

Bardin, N, Moal, V, Anfosso, F, Daniel, L, Brunet, P, Sampol, J and Dignat George, F (2003) Soluble CD146, a novel endothelial marker, is increased in physiopathological settings linked to endothelial junctional alteration. Thromb Haemost 90:915-20.

Bardin, N, Reumaux, D, Geboes, K, Colombel, JF, Blot-Chabaud, M, Sampol, J, Duthilleul, P and Dignat-George, F (2006) Increased expression of CD146, a new marker of the endothelial junction in active inflammatory bowel disease. Inflamm Bowel Dis 12:16-21.

Basset, P, Bellocq, JP, Wolf, C, Stoll, I, Hutin, P, Limacher, JM, Podhajcer, OL, Chenard, MP, Rio, MC and Chambon, P (1990) A novel metalloproteinase gene specifically expressed in stromal cells of breast carcinomas. Nature 348:699-704.

Bechrakis, NE, Hocht, S, Martus, P, Kreusel, KM, Heese, J and Foerster, MH (2004) [Endoresection following proton beam irradiation of large uveal melanomas]. Ophthalmologe 101:370-6.

Beliveau, A, Berube, M, Rousseau, A, Pelletier, G and Guerin, SL (2000) Expression of integrin alpha5beta1 and MMPs associated with epithelioid morphology and malignancy of uveal melanoma. Investigative Ophthalmol Vis Sci 41:2363-72.

Bian, J, Wang, Y, Smith, MR, Kim, H, Jacobs, C, Jackman, J, Kung, HF, Colburn, NH and Sun, Y (1996) Suppression of in vivo tumor growth and induction of suspension cell death by tissue inhibitor of metalloproteinases (TIMP)-3. Carcinogenesis 17:1805-11.

Bivik, CA, Andersson, EB and Rosdahl, IK (2005) Wavelength-specific effects on UVB-induced apoptosis in melanocytes. A study of Bcl-2/Bax expression and keratinocyte rescue effects. Melanoma Res 15:7-13.

Blom, DJ, Luyten, GP, Mooy, C, Kerkvliet, S, Zwinderman, AH and Jager, MJ (1997) Human leukocyte antigen class I expression. Marker of poor prognosis in uveal melanoma. Invest Ophthalmol Vis Sci 38:1865-72.

Bloomston, M, Shafii, A, Zervos, EE and Rosemurgy, AS (2002) TIMP-1 overexpression in pancreatic cancer attenuates tumor growth, decreases implantation and metastasis, and inhibits angiogenesis. J Surg Res 102:39-44.

Bode, W (1995) A helping hand for collagenases: the haemopexin-like domain. Structure 3:527-30.

Bode, W, Gomis-Ruth, FX, Huber, R, Zwilling, R and Stocker, W (1992) Structure of astacin and implications for activation of astacins and zinc-ligation of collagenases. Nature 358:164-7.

Boire, A, Covic, L, Agarwal, A, Jacques, S, Sherifi, S and Kuliopulos, A (2005) PAR1 is a matrix metalloprotease-1 receptor that promotes invasion and tumorigenesis of breast cancer cells. Cell 120:303-13.

Borland, G, Murphy, G and Ager, A (1999) Tissue inhibitor of metalloproteinases-3 inhibits shedding of L-selectin from leukocytes. J Biol Chem 274:2810-5.

Bosher, JM, Williams, T and Hurst, HC (1995) The developmentally regulated transcription factor AP-2 is involved in c-erbB-2 overexpression in human mammary carcinoma. Proc Natl Acad Sci U S A 92:744-7.

Bowen, AR, Hanks, AN, Allen, SM, Alexander, A, Diedrich, MJ and Grossman, D (2003) Apoptosis regulators and responses in human melanocytic and keratinocytic cells. J Invest Dermatol 120:48-55.

Boyd, SR, Tan, DS, de Souza, L, Neale, MH, Myatt, NE, Alexander, RA, Robb, M, Hungerford, JL and Cree, IA (2002) Uveal melanomas express vascular endothelial growth factor and basic fibroblast growth factor and support endothelial cell growth. Br J Ophthalmol 86:440-7.

Brenneisen, P, Sies, H and Scharffetter-Kochanek, K (2002) Ultraviolet-B irradiation and matrix metalloproteinases: from induction via signaling to initial events. Ann N Y Acad Sci 973:31-43.

Brinckerhoff, CE, Rutter, JL and Benbow, U (2000) Interstitial collagenases as markers of tumor progression. Clinical Cancer Research 6:4823-30.

Bringmann, A, Pannicke, T, Grosche, J, Francke, M, Wiedemann, P, Skatchkov, SN, Osborne, NN and Reichenbach, A (2006) Muller cells in the healthy and diseased retina. Prog Retin Eye Res 25:397-424.

Browning, DJ and Antoszyk, AN (2003) Retinal tear and detachment after transpupillary thermotherapy for choroidal melanoma. Am J Ophthalmol 135:729-30.

Carmeliet, P and Jain, RK (2000) Angiogenesis in cancer and other diseases. Nature 407:249-57.

Chen, X, Maniotis, AJ, Majumdar, D, Pe'er, J and Folberg, R (2002) Uveal melanoma cell staining for CD34 and assessment of tumor vascularity. Invest Ophthalmol Vis Sci 43:2533-9.

Chirco, R, Liu, XW, Jung, KK and Kim, HR (2006) Novel functions of TIMPs in cell signaling. Cancer Metastasis Rev 25:99-113.

Choti, MA and Bulkley, GB (1999) Management of hepatic metastases. Liver Transpl Surg 5:65-80.

Chu, SC, Hu, DN, Yang, SF, Yang, PY, Hsieh, YS, Huang, SM, Yu, G and McCormick, SA (2004) Uveal melanocytes produce matrix metalloproteinases-2 and -9 in vitro. Pigment Cell Res 17:636-42.

Clarijs, R, van Dijk, M, Ruiter, DJ and de Waal, RM (2005) Functional and morphologic analysis of the fluid-conducting meshwork in xenografted cutaneous and primary uveal melanoma. Invest Ophthalmol Vis Sci 46:3013-20.

Clark, IM and Cawston, TE (1989) Fragments of human fibroblast collagenase. Purification and characterization. Biochem J 263:201-6.

COMS (1998) Histopathologic characteristics of uveal melanomas in eyes enucleated from the Collaborative Ocular Melanoma Study. COMS report no. 6. Am J Ophthalmol 125:745-66.

COMS (2001) Assessment of metastatic disease status at death in 435 patients with large choroidal melanoma in the Collaborative Ocular Melanoma Study (COMS): COMS report no. 15. Arch Ophthalmol 119:670-6.

COMS (2006) The COMS Randomized Trial of Iodine 125 Brachytherapy for Choroidal Melanoma: V. Twelve-Year Mortality Rates and Prognostic Factors: COMS Report No. 28. Arch Ophthalmol 124:1684-93.

Concha, A, Esteban, F, Cabrera, T, Ruiz-Cabello, F and Garrido, F (1991) Tumor aggressiveness and MHC class I and II antigens in laryngeal and breast cancer. Semin Cancer Biol 2:47-54.

Cottam, DW, Rennie, IG, Woods, K, Parsons, MA, Bunning, RA and Rees, RC (1992) Gelatinolytic metalloproteinase secretion patterns in ocular melanoma. Invest Ophthalmol Vis Sci 33:1923-7.

Coupland, SE, Anastassiou, G, Stang, A, Schilling, H, Anagnostopoulos, I, Bornfeld, N and Stein, H (2000) The prognostic value of cyclin D1, p53, and MDM2 protein expression in uveal melanoma. J Pathol 191:120-6.

Courdi, A, Caujolle, JP, Grange, JD, Diallo-Rosier, L, Sahel, J, Bacin, F, Zur, C, Gastaud, P, Iborra-Brassart, N, Herault, J and Chauvel, P (1999) Results of proton therapy of uveal melanomas treated in Nice. Int J Radiat Oncol Biol Phys 45:5-11.

Cruess, AF, Augsburger, JJ, Shields, JA, Donoso, LA and Amsel, J (1984) Visual results following cobalt plaque radiotherapy for posterior uveal melanomas. Ophthalmology 91:131-6.

Cuenod, CA, Fournier, L, Balvay, D and Guinebretiere, JM (2006) Tumor angiogenesis: pathophysiology and implications for contrast-enhanced MRI and CT assessment. Abdom Imaging 31:188-93.

Dahlenfors, R, Tornqvist, G, Wettrell, K and Mark, J (1993) Cytogenetical observations in nine ocular malignant melanomas. Anticancer Res 13:1415-20.

Damato, B (2004) Developments in the management of uveal melanoma. Clin Experiment Ophthalmol 32:639-47.

Daniels, KJ, Boldt, HC, Martin, JA, Gardner, LM, Meyer, M and Folberg, R (1996) Expression of type VI collagen in uveal melanoma: its role in pattern formation and tumor progression. Lab Invest 75:55-66.

Davis, GE and Senger, DR (2005) Endothelial extracellular matrix: biosynthesis, remodeling, and functions during vascular morphogenesis and neovessel stabilization. Circ Res 97:1093-107.

de Coignac, AB, Elson, G, Delneste, Y, Magistrelli, G, Jeannin, P, Aubry, JP, Berthier, O, Schmitt, D, Bonnefoy, JY and Gauchat, JF (2000) Cloning of MMP-26. A novel matrilysin-like proteinase. Eur J Biochem 267:3323-9.

Delcourt, C, Carriere, I, Ponton-Sanchez, A, Lacroux, A, Covacho, MJ and Papoz, L (2000) Light exposure and the risk of cortical, nuclear, and posterior subcapsular cataracts: the Pathologies Oculaires Liees a l'Age (POLA) study. Arch Ophthalmol 118:385-92.

Denton, KJ, Stretch, JR, Gatter, KC and Harris, AL (1992) A study of adhesion molecules as markers of progression in malignant melanoma. J Pathol 167:187-91.

Dhanaraj, V, Ye, QZ, Johnson, LL, Hupe, DJ, Ortwine, DF, Dunbar, JB, Jr., Rubin, JR, Pavlovsky, A, Humblet, C and Blundell, TL (1996) Designing inhibitors of the metalloproteinase superfamily: comparative analysis of representative structures. Drug Design & Discovery 13:3-14.

Di Girolamo, N, Coroneo, MT and Wakefield, D (2003) UVB-elicited induction of MMP-1 expression in human ocular surface epithelial cells is mediated through the ERK1/2 MAPK-dependent pathway. Invest Ophthalmol Vis Sci 44:4705-14.

Diener-West, M, Earle, JD, Fine, SL, Hawkins, BS, Moy, CS, Reynolds, SM, Schachat, AP and Straatsma, BR (2001) The COMS randomized trial of iodine 125 brachytherapy for choroidal melanoma, III: initial mortality findings. COMS Report No. 18. Arch Ophthalmol 119:969-82.

Diener-West, M, Hawkins, BS, Markowitz, JA and Schachat, AP (1992) A review of mortality from choroidal melanoma. II. A meta-analysis of 5-year mortality rates following enucleation, 1966 through 1988. Arch Ophthalmol 110:245-50.

Djonov, V, Hogger, K, Sedlacek, R, Laissue, J and Draeger, A (2001) MMP-19: cellular localization of a novel metalloproteinase within normal breast tissue and mammary gland tumours. J Pathol 195:147-55.

Dorrie, J, Wellner, V, Kampgen, E, Schuler, G and Schaft, N (2006) An improved method for RNA isolation and removal of melanin contamination from melanoma tissue: implications for tumor antigen detection and amplification. J Immunol Methods 313:119-28.

Dzwonek, J, Rylski, M and Kaczmarek, L (2004) Matrix metalloproteinases and their endogenous inhibitors in neuronal physiology of the adult brain. FEBS Lett 567:129-35.

Egeblad, M and Werb, Z (2002) New functions for the matrix metalloproteinases in cancer progression. Nat Rev Cancer 2:161-74.

El-Shabrawi, Y, Ardjomand, N and Radner, H (2001) MMP-9 is predominantly expressed in epithelioid and not spindle cell uveal melanoma. J Pathol 194:201-6.

Elshaw, SR, Sisley, K, Cross, N, Murray, AK, MacNeil, SM, Wagner, M, Nichols, CE and Rennie, IG (2001) A comparison of ocular melanocyte and uveal melanoma cell invasion and the implication of alpha1beta1, alpha4beta1 and alpha6beta1 integrins. Br J Ophthalmol 85:732-8.

Emri, G, Wenczl, E, Van Erp, P, Jans, J, Roza, L, Horkay, I and Schothorst, AA (2000) Low doses of UVB or UVA induce chromosomal aberrations in cultured human skin cells. J Invest Dermatol 115:435-40.

Enk, CD, Jacob-Hirsch, J, Gal, H, Verbovetski, I, Amariglio, N, Mevorach, D, Ingber, A, Givol, D, Rechavi, G and Hochberg, M (2006) The UVB-induced gene expression profile of human epidermis in vivo is different from that of cultured keratinocytes. Oncogene 25:2601-14.

Erickson, PA, Fisher, SK, Guerin, CJ, Anderson, DH and Kaska, DD (1987) Glial fibrillary acidic protein increases in Muller cells after retinal detachment. Exp Eye Res 44:37-48.

Ericsson, C, Seregard, S, Bartolazzi, A, Levitskaya, E, Ferrone, S, Kiessling, R and Larsson, O (2001) Association of HLA class I and class II antigen expression and mortality in uveal melanoma. Invest Ophthalmol Vis Sci 42:2153-6.

Fariss, RN, Apte, SS, Olsen, BR, Iwata, K and Milam, AH (1997) Tissue inhibitor of metalloproteinases-3 is a component of Bruch's membrane of the eye. Am J Pathol 150:323-8.

Feldman, ED, Pingpank, JF and Alexander, HR, Jr. (2004) Regional treatment options for patients with ocular melanoma metastatic to the liver. Ann Surg Oncol 11:290-7.

Dhanaraj, V, Ye, QZ, Johnson, LL, Hupe, DJ, Ortwine, DF, Dunbar, JB, Jr., Rubin, JR, Pavlovsky, A, Humblet, C and Blundell, TL (1996) Designing inhibitors of the metalloproteinase superfamily: comparative analysis of representative structures. Drug Design & Discovery 13:3-14.

Di Girolamo, N, Coroneo, MT and Wakefield, D (2003) UVB-elicited induction of MMP-1 expression in human ocular surface epithelial cells is mediated through the ERK1/2 MAPK-dependent pathway. Invest Ophthalmol Vis Sci 44:4705-14.

Diener-West, M, Earle, JD, Fine, SL, Hawkins, BS, Moy, CS, Reynolds, SM, Schachat, AP and Straatsma, BR (2001) The COMS randomized trial of iodine 125 brachytherapy for choroidal melanoma, III: initial mortality findings. COMS Report No. 18. Arch Ophthalmol 119:969-82.

Diener-West, M, Hawkins, BS, Markowitz, JA and Schachat, AP (1992) A review of mortality from choroidal melanoma. II. A meta-analysis of 5-year mortality rates following enucleation, 1966 through 1988. Arch Ophthalmol 110:245-50.

Djonov, V, Hogger, K, Sedlacek, R, Laissue, J and Draeger, A (2001) MMP-19: cellular localization of a novel metalloproteinase within normal breast tissue and mammary gland tumours. J Pathol 195:147-55.

Dorrie, J, Wellner, V, Kampgen, E, Schuler, G and Schaft, N (2006) An improved method for RNA isolation and removal of melanin contamination from melanoma tissue: implications for tumor antigen detection and amplification. J Immunol Methods 313:119-28.

Dzwonek, J, Rylski, M and Kaczmarek, L (2004) Matrix metalloproteinases and their endogenous inhibitors in neuronal physiology of the adult brain. FEBS Lett 567:129-35.

Egeblad, M and Werb, Z (2002) New functions for the matrix metalloproteinases in cancer progression. Nat Rev Cancer 2:161-74.

El-Shabrawi, Y, Ardjomand, N and Radner, H (2001) MMP-9 is predominantly expressed in epithelioid and not spindle cell uveal melanoma. J Pathol 194:201-6.

Elshaw, SR, Sisley, K, Cross, N, Murray, AK, MacNeil, SM, Wagner, M, Nichols, CE and Rennie, IG (2001) A comparison of ocular melanocyte and uveal melanoma cell invasion and the implication of alpha1beta1, alpha4beta1 and alpha6beta1 integrins. Br J Ophthalmol 85:732-8.

Emri, G, Wenczl, E, Van Erp, P, Jans, J, Roza, L, Horkay, I and Schothorst, AA (2000) Low doses of UVB or UVA induce chromosomal aberrations in cultured human skin cells. J Invest Dermatol 115:435-40.

Enk, CD, Jacob-Hirsch, J, Gal, H, Verbovetski, I, Amariglio, N, Mevorach, D, Ingber, A, Givol, D, Rechavi, G and Hochberg, M (2006) The UVB-induced gene expression profile of human epidermis in vivo is different from that of cultured keratinocytes. Oncogene 25:2601-14.

Erickson, PA, Fisher, SK, Guerin, CJ, Anderson, DH and Kaska, DD (1987) Glial fibrillary acidic protein increases in Muller cells after retinal detachment. Exp Eye Res 44:37-48.

Ericsson, C, Seregard, S, Bartolazzi, A, Levitskaya, E, Ferrone, S, Kiessling, R and Larsson, O (2001) Association of HLA class I and class II antigen expression and mortality in uveal melanoma. Invest Ophthalmol Vis Sci 42:2153-6.

Fariss, RN, Apte, SS, Olsen, BR, Iwata, K and Milam, AH (1997) Tissue inhibitor of metalloproteinases-3 is a component of Bruch's membrane of the eye. Am J Pathol 150:323-8.

Feldman, ED, Pingpank, JF and Alexander, HR, Jr. (2004) Regional treatment options for patients with ocular melanoma metastatic to the liver. Ann Surg Oncol 11:290-7.

Fernandez, CA and Moses, MA (2006) Modulation of angiogenesis by tissue inhibitor of metalloproteinase-4. Biochem Biophys Res Commun 345:523-9.

Fisher, DE (2001) The p53 tumor suppressor: critical regulator of life & death in cancer. Apoptosis 6:7-15.

Folberg, R, Fleck, M, Mehaffey, MG, Meyer, M, Bentler, SE, Woolson, RF and Pe'er, J (1996) Mapping the Location of Prognostically Significant Microcirculatory Patterns in Ciliary Body and Choroidal Melanomas. Pathol Oncol Res 2:229-236.

Folberg, R, Hendrix, MJ and Maniotis, AJ (2000) Vasculogenic mimicry and tumor angiogenesis. Am J Pathol 156:361-81.

Folberg, R, Leach, L, Valyi-Nagy, K, Lin, AY, Apushkin, MA, Ai, Z, Barak, V, Majumdar, D, Pe'er, J and Maniotis, AJ (2007) Modeling the behavior of uveal melanoma in the liver. Invest Ophthalmol Vis Sci 48:2967-74.

Folberg, R and Maniotis, AJ (2004) Vasculogenic mimicry. Apmis 112:508-25.

Folberg, R, Mehaffey, M, Gardner, LM, Meyer, M, Rummelt, V and Pe'er, J (1997) The microcirculation of choroidal and ciliary body melanomas. Eye 11:227-38.

Folberg, R, Pe'er, J, Gruman, LM, Woolson, RF, Jeng, G, Montague, PR, Moninger, TO, Yi, H and Moore, KC (1992) The morphologic characteristics of tumor blood vessels as a marker of tumor progression in primary human uveal melanoma: a matched case-control study. Human Pathol 23:1298-305.

Folberg, R, Rummelt, V, Parys-Van Ginderdeuren, R, Hwang, T, Woolson, RF, Pe'er, J and Gruman, LM (1993) The prognostic value of tumor blood vessel morphology in primary uveal melanoma. Ophthalmology 100:1389-98.

Forte, R, Cennamo, G, Staibano, S and De Rosa, G (2005) Echographic examination with new generation contrast agent of choroidal malignant melanomas. Acta Ophthalmol Scand 83:347-54.

Foss, AJ, Alexander, RA, Hungerford, JL, Harris, AL, Cree, IA and Lightman, S (1997) Reassessment of the PAS patterns in uveal melanoma. Br J Ophthalmol 81:240-6.

Foss, AJ, Alexander, RA, Jefferies, LW, Hungerford, JL, Harris, AL and Lightman, S (1996) Microvessel count predicts survival in uveal melanoma. Cancer Res 56:2900-3.

Frenkel, S, Barzel, I, Levy, J, Lin, AY, Bartsch, DU, Majumdar, D, Folberg, R and Pe'er, J (2007) Demonstrating circulation in vasculogenic mimicry patterns of uveal melanoma by confocal indocyanine green angiography. Eye doi:10.1038/sj.eye.6702783.

Giambernardi, TA, Sakaguchi, AY, Gluhak, J, Pavlin, D, Troyer, DA, Das, G, Rodeck, U and Klebe, RJ (2001) Neutrophil collagenase (MMP-8) is expressed during early development in neural crest cells as well as in adult melanoma cells. Matrix Biol 20:577-87.

Gies, P (2003) Australia has more than enough solar UV radiation. Clin Experimen Optom 86:71-73.

Godfrey, DG, Waldron, RG and Capone, A, Jr. (1999) Transpupillary thermotherapy for small choroidal melanoma. Am J Ophthalmol 128:88-93.

Goldberg, GI, Strongin, A, Collier, IE, Genrich, LT and Marmer, BL (1992) Interaction of 92-kDa type IV collagenase with the tissue inhibitor of metalloproteinases prevents dimerization,

complex formation with interstitial collagenase, and activation of the proenzyme with stromelysin. J Bio Chem 267:4583-91.

Gomez, DE, Alonso, DF, Yoshiji, H and Thorgeirsson, UP (1997) Tissue inhibitors of metalloproteinases: structure, regulation and biological functions. Eur J Cell Biol 74:111-22.

Gragoudas, ES, Egan, KM, Seddon, JM, Glynn, RJ, Walsh, SM, Finn, SM, Munzenrider, JE and Spar, MD (1991) Survival of patients with metastases from uveal melanoma. Ophthalmology. 98:383-9.

Gunduz, K, Shields, CL, Shields, JA, Cater, J, Freire, JE and Brady, LW (1999) Radiation retinopathy following plaque radiotherapy for posterior uveal melanoma. Arch Ophthalmol 117:609-14.

Guo, L, Hussain, AA, Limb, GA and Marshall, J (1999) Age-dependent variation in metalloproteinase activity of isolated human Bruch's membrane and choroid. Invest Ophthalmol Vis Sci 40:2676-82.

Haass, NK, Smalley, KS, Li, L and Herlyn, M (2005) Adhesion, migration and communication in melanocytes and melanoma. Pigment Cell Res 18:150-9.

Handsley, MM and Edwards, DR (2005) Metalloproteinases and their inhibitors in tumor angiogenesis. Int J Cancer 115:849-60.

Hargreaves, PG, Wang, F, Antcliff, J, Murphy, G, Lawry, J, Russell, RG and Croucher, PI (1998) Human myeloma cells shed the interleukin-6 receptor: inhibition by tissue inhibitor of metalloproteinase-3 and a hydroxamate-based metalloproteinase inhibitor. Br J Haematol 101:694-702.

Hashizume, H, Baluk, P, Morikawa, S, McLean, JW, Thurston, G, Roberge, S, Jain, RK and McDonald, DM (2000) Openings between defective endothelial cells explain tumor vessel leakiness. Am J Pathol 156:1363-80.

Hayashita-Kinoh, H, Kinoh, H, Okada, A, Komori, K, Itoh, Y, Chiba, T, Kajita, M, Yana, I and Seiki, M (2001) Membrane-type 5 matrix metalloproteinase is expressed in differentiated neurons and regulates axonal growth. Cell Growth & Differentiation 12:573-80.

Heimberger, AB, McGary, EC, Suki, D, Ruiz, M, Wang, H, Fuller, GN and Bar-Eli, M (2005) Loss of the AP-2alpha transcription factor is associated with the grade of human gliomas. Clin Cancer Res 11:267-72.

Hendrix, MJ, Seftor, EA, Hess, AR and Seftor, RE (2003) Vasculogenic mimicry and tumour-cell plasticity: lessons from melanoma. Nat Rev Cancer 3:411-21.

Hernandez-Barrantes, S, Shimura, Y, Soloway, PD, Sang, QA and Fridman, R (2001) Differential roles of TIMP-4 and TIMP-2 in pro-MMP-2 activation by MT1-MMP. Biochem Biophys Res Commun 281:126-30.

Hiraoka, N, Allen, E, Apel, IJ, Gyetko, MR and Weiss, SJ (1998) Matrix metalloproteinases regulate neovascularization by acting as pericellular fibrinolysins. Cell 95:365-77.

Hofmann, UB, Westphal, JR, Van Muijen, GN and Ruiter, DJ (2000) Matrix metalloproteinases in human melanoma. J Invest Dermatol 115:337-44.

Holly, EA, Aston, DA, Char, DH, Kristiansen, JJ and Ahn, DK (1990) Uveal melanoma in relation to ultraviolet light exposure and host factors. Cancer Res 50:5773-7.

Horsman, DE and White, VA (1993) Cytogenetic analysis of uveal melanoma. Consistent occurrence of monosomy 3 and trisomy 8q. Cancer 71:811-9.

Hu, DN, Savage, HE and Roberts, JE (2002) Uveal melanocytes, ocular pigment epithelium, and Muller cells in culture: in vitro toxicology. Int J Toxicol 21:465-72.

Hu, DN, Yu, GP, McCormick, SA, Schneider, S and Finger, PT (2005) Population-based incidence of uveal melanoma in various races and ethnic groups. Am J Ophthalmol 140:612-7.

Hughes, S, Damato, BE, Giddings, I, Hiscott, PS, Humphreys, J and Houlston, RS (2005) Microarray comparative genomic hybridisation analysis of intraocular uveal melanomas identifies distinctive imbalances associated with loss of chromosome 3. Br J Cancer 93:1191-6.

Hungerford, JL (1995) Management of ocular melanoma. Br Med Bull 51:694-716.

Hurst, EA, Harbour, JW and Cornelius, LA (2003) Ocular melanoma: a review and the relationship to cutaneous melanoma. Arch Dermatol 139:1067-73.

Iida, J and McCarthy, JB (2007) Expression of collagenase-1 (MMP-1) promotes melanoma growth through the generation of active transforming growth factor-beta. Melanoma Res 17:205-13.

Inoue, T, Yashiro, M, Nishimura, S, Maeda, K, Sawada, T, Ogawa, Y, Sowa, M and Chung, KH (1999) Matrix metalloproteinase-1 expression is a prognostic factor for patients with advanced gastric cancer. Int J Mol Med 4:73-7.

Jager, MJ, Niederkorn, JY and Ksander, BR (2004) Uveal Melanoma: a Model for Exploring Fundamental Cancer Biology. Taylor & Francis Group plc, The Netherlands, Lisse.

Jaworski, DM (2000) Developmental regulation of membrane type-5 matrix metalloproteinase (MT5-MMP) expression in the rat nervous system. Brain Res 860:174-7.

Jean, D, Gershenwald, JE, Huang, S, Luca, M, Hudson, MJ, Tainsky, MA and Bar-Eli, M (1998) Loss of AP-2 results in up-regulation of MCAM/MUC18 and an increase in tumor growth and metastasis of human melanoma cells. J Biol Chem 273:16501-8.

Jodele, S, Blavier, L, Yoon, JM and Declerck, YA (2006) Modifying the soil to affect the seed: role of stromal-derived matrix metalloproteinases in cancer progression. Cancer Metastasis Rev 25:35-43.

Johnson, JP (1994) Identification of molecules associated with the development of metastasis in human malignant melanoma. Invasion Metastasis 14:123-30.

Kadekaro, AL, Kavanagh, RJ, Wakamatsu, K, Ito, S, Pipitone, MA and Abdel-Malek, ZA (2003) Cutaneous photobiology. The melanocyte vs. the sun: who will win the final round? Pigment Cell Res 16:434-47.

Kan-Mitchell, J, Mitchell, MS, Rao, N and Liggett, PE (1989) Characterization of uveal melanoma cell lines that grow as xenografts in rabbit eyes. Invest Ophthalmol Vis Sci 30:829-34.

Kanekura, T, Chen, X and Kanzaki, T (2002) Basigin (CD147) is expressed on melanoma cells and induces tumor cell invasion by stimulating production of matrix metalloproteinases by fibroblasts. Int J Cancer 99:520-8.

Kanski, JJ (1994) Clinical Ophthalmology: A Systematic Approach. Butterworth Heinemann, Oxford.

Kanski, JJ, Milewski, SA, Damato, BE and Tanner, V (2005) Diseases of the Ocular Fundus. Elsevier Mosby, United Kingdom.

Karlen, S and Braathen, LR (1999) Regulation of the melanoma cell adhesion molecule gene in melanoma: modulation of mRNA synthesis by cyclic adenosine monophosphate, phorbol ester, and stem cell fFactor/c-kKit signaling. J Invest Dermatol 113:711-9.

Karlen, S and Braathen, LR (2000) Role of the initiator element in the regulation of the melanoma cell adhesion molecule gene. J Invest Dermatol 115:668-73.

Keilholz, U, Scheibenbogen, C, Brado, M, Georgi, P, Maclachlan, D, Brado, B and Hunstein, W (1994) Regional adoptive immunotherapy with interleukin-2 and lymphokine-activated killer (LAK) cells for liver metastases. Eur J Cancer 30A:103-5.

Kikuchi, E, Yamazaki, K, Torigoe, T, Cho, Y, Miyamoto, M, Oizumi, S, Hommura, F, Dosaka-Akita, H and Nishimura, M (2007) HLA class I antigen expression is associated with a favorable prognosis in early stage non-small cell lung cancer. Cancer Sci 98:1424-30.

Kilic, E, van Gils, W, Lodder, E, Beverloo, HB, van Til, ME, Mooy, CM, Paridaens, D, de Klein, A and Luyten, GP (2006) Clinical and cytogenetic analyses in uveal melanoma. Invest Ophthalmol Vis Sci 47:3703-7.

Kojima, S, Itoh, Y, Matsumoto, S, Masuho, Y and Seiki, M (2000) Membrane-type 6 matrix metalloproteinase (MT6-MMP, MMP-25) is the second glycosyl-phosphatidyl inositol (GPI)-anchored MMP. FEBS Letters 480:142-6.

Kolb, C, Mauch, S, Krawinkel, U and Sedlacek, R (1999) Matrix metalloproteinase-19 in capillary endothelial cells: expression in acutely, but not in chronically, inflamed synovium. Exp Cell Res 250:122-30.

Koshiba, T, Hosotani, R, Wada, M, Fujimoto, K, Lee, JU, Doi, R, Arii, S and Imamura, M (1997) Detection of matrix metalloproteinase activity in human pancreatic cancer. Surg Today 27:302-4.

Kraus, A, Masat, L and Johnson, JP (1997) Analysis of the expression of intercellular adhesion molecule-1 and MUC18 on benign and malignant melanocytic lesions using monoclonal antibodies directed against distinct epitopes and recognizing denatured, non-glycosylated antigen. Melanoma Res 7 Suppl 2:S75-81.

Krengel, S, Alexander, M, Brinckmann, J and Tronnier, M (2002) MMP-2, TIMP-2 and MT1-MMP are differentially expressed in lesional skin of melanocytic nevi and their expression is modulated by UVB-light. J Cutan Pathol 29:390-6.

Krishnakumar, S, Abhyankar, D, Lakshmi, SA, Pushparaj, V, Shanmugam, MP and Biswas, J (2004) HLA expression in choroidal melanomas: correlation with clinicopathological features. Curr Eye Res 28:409-16.

Kroll, AJ (1969) Secondary retinal detachment: elctron microscopy of retina and pigment epithelium. Am J Ophthalmol 68:223-237.

Kumar, R, Yoneda, J, Bucana, CD and Fidler, IJ (1998) Regulation of distinct steps of angiogenesis by different angiogenic molecules. Int J Oncol 12:749-57.

Lafleur, MA, Forsyth, PA, Atkinson, SJ, Murphy, G and Edwards, DR (2001) Perivascular cells regulate endothelial membrane type-1 matrix metalloproteinase activity. Biochemical & Biophysical Research Communications 282:463-73.

Lai, K (2002) Distribution of Metalloproteinases (MMPs) and Tissue Inhibitors of Metalloproteinases (TIMPs) in Uveal Melanoma. Honours Thesis B.MedSci, The University of Sydney.

Lai, K, Conway, RM, Crouch, R, Jager, MJ and Madigan, MC (2007) Expression and Distribution of MMPs and TIMPs in Human Uveal Melanoma. Submiited to Exp Eye Res.

Lambert, E, Dasse, E, Haye, B and Petitfrere, E (2004) TIMPs as multifacial proteins. Crit Rev Oncol Hematol 49:187-98.

Lane, AM, Egan, KM, Yang, J, Saornil, MA, Alroy, J, Albert, D and Gragoudas, ES (1997) An evaluation of tumour vascularity as a prognostic indicator in uveal melanoma. Melanoma Res 7:237-42.

Laver, NV (2002) Uveal malignant melanoma and tissue metalloproteinase profiles. Ophthalmol Vis. Sci. 43(suppl):1118(nr).

Lawry, J, Currie, Z, Smith, MO and Rennie, IG (1999) The correlation between cell surface markers and clinical features in choroidal malignant melanomas. Eye 13 (Pt 3a):301-8.

Lehmann, JM, Holzmann, B, Breitbart, EW, Schmiegelow, P, Riethmuller, G and Johnson, JP (1987) Discrimination between benign and malignant cells of melanocytic lineage by two novel antigens, a glycoprotein with a molecular weight of 113,000 and a protein with a molecular weight of 76,000. Cancer Res 47:841-5.

Lehmann, JM, Riethmuller, G and Johnson, JP (1989) MUC18, a marker of tumor progression in human melanoma, shows sequence similarity to the neural cell adhesion molecules of the immunoglobulin superfamily. Proc Natl Acad Sci U S A 86:9891-5.

Lerman, S (1980) Radiant energy and the eye. Macmillan Publishing Co., Inc, New York.

Leslie, MC and Bar-Eli, M (2005) Regulation of gene expression in melanoma: new approaches for treatment. J Cell Biochem 94:25-38.

Leslie, MC, Zhao, YJ, Lachman, LB, Hwu, P and Bar-Eli, M (2007) Immunization against MUC18/MCAM, a novel antigen that drives melanoma invasion and metastasis. Gene Ther 14:316-23.

Leu, ST, Batni, S, Radeke, MJ, Johnson, LV, Anderson, DH and Clegg, DO (2002) Drusen are Cold Spots for Proteolysis: Expression of Matrix Metalloproteinases and Their Tissue Inhibitor Proteins in Age-related Macular Degeneration. Exp Eye Res 74:141-54.

Li, W, Judge, H, Gragoudas, ES, Seddon, JM and Egan, KM (2000) Patterns of tumor initiation in choroidal melanoma. Cancer Res 60:3757-60.

Limb, GA, Daniels, JT, Pleass, R, Charteris, DG, Luthert, PJ and Khaw, PT (2002) Differential expression of matrix metalloproteinases 2 and 9 by glial Muller cells: response to soluble and extracellular matrix-bound tumor necrosis factor-alpha. Am J Pathol 160:1847-55.

Lin, AY, Maniotis, AJ, Valyi-Nagy, K, Majumdar, D, Setty, S, Kadkol, S, Leach, L, Pe'er, J and Folberg, R (2005) Distinguishing fibrovascular septa from vasculogenic mimicry patterns. Arch Pathol Lab Med 129:884-92.

Lindegaard, J, Isager, P, Prause, JU and Heegaard, S (2007) Optic nerve invasion of uveal melanoma. APMIS 115:1-16.

Liu, Q, Yan, X, Li, Y, Zhang, Y, Zhao, X and Shen, Y (2004) Pre-eclampsia is associated with the failure of melanoma cell adhesion molecule (MCAM/CD146) expression by intermediate trophoblast. Lab Invest 84:221-8.

Llano, E, Pendas, AM, Freije, JP, Nakano, A, Knauper, V, Murphy, G and Lopez-Otin, C (1999) Identification and characterization of human MT5-MMP, a new membrane-bound activator of progelatinase a overexpressed in brain tumors. Cancer Res 59:2570-6.

Lohi, J, Lehti, K, Valtanen, H, Parks, WC and Keski-Oja, J (2000) Structural analysis and promoter characterization of the human membrane-type matrix metalloproteinase-1 (MT1-MMP) gene. Gene 242:75-86.

Ma, D, Luyten, GP, Luider, TM and Niederkorn, JY (1995) Relationship between natural killer cell susceptibility and metastasis of human uveal melanoma cells in a murine model. Invest Ophthalmol Vis Sci 36:435-41.

Makitie, T, Summanen, P, Tarkkanen, A and Kivela, T (1999) Microvascular density in predicting survival of patients with choroidal and ciliary body melanoma. Invest Ophthalmol Vis Sci 40:2471-80.

Makitie, T, Summanen, P, Tarkkanen, A and Kivela, T (2001) Tumor-infiltrating macrophages (CD68(+) cells) and prognosis in malignant uveal melanoma. Invest Ophthalmol Vis Sci 42:1414-21.

Maniotis, AJ, Folberg, R, Hess, A, Seftor, EA, Gardner, LM, Pe'er, J, Trent, JM, Meltzer, PS and Hendrix, MJ (1999) Vascular channel formation by human melanoma cells in vivo and in vitro: vasculogenic mimicry. Am J Pathol 155:739-52.

Marchenko, GN, Ratnikov, BI, Rozanov, DV, Godzik, A, Deryugina, EI and Strongin, AY (2001) Characterization of matrix metalloproteinase-26, a novel metalloproteinase widely expressed in cancer cells of epithelial origin. Biochem J 356:705-18.

Marchenko, ND, Marchenko, GN, Weinreb, RN, Lindsey, JD, Kyshtoobayeva, A, Crawford, HC and Strongin, AY (2004) Beta-catenin regulates the gene of MMP-26, a novel metalloproteinase expressed both in carcinomas and normal epithelial cells. Int J Biochem Cell Biol 36:942-56.

Marnitz, S, Hoecht, S and Hinkelbein, W (2006) The role of radiotherapy in the management of malignant melanoma. Front Radiat Ther Oncol 39:140-8.

McCarty, CA, Nanjan, MB and Taylor, HR (2000) Attributable risk estimates for cataract to prioritize medical and public health action. Invest Ophthalmol Vis Sci 41:3720-5.

McDonald, DM, Munn, L and Jain, RK (2000) Vasculogenic mimicry: how convincing, how novel, and how significant? Am J Pathol 156:383-8.

McGary, EC, Heimberger, A, Mills, L, Weber, K, Thomas, GW, Shtivelband, M, Lev, DC and Bar-Eli, M (2003) A fully human antimelanoma cellular adhesion molecule/MUC18 antibody inhibits spontaneous pulmonary metastasis of osteosarcoma cells in vivo. Clin Cancer Res 9:6560-6.

McLean, IW (1993) The biology of haematogenous metastasis in human uveal malignant melanoma. Virchows Arch A Pathol Anat Histopathol 422:433-7.

McLean, IW, Foster, WD and Zimmerman, LE (1982) Uveal melanoma: location, size, cell type, and enucleation as risk factors in metastasis. Human Pathol. 13:123-32.

McLean, IW, Keefe, KS and Burnier, MN (1997) Uveal melanoma. Comparison of the prognostic value of fibrovascular loops, mean of the ten largest nucleoli, cell type, and tumor size. Ophthalmology 104:777-80.

McLean, IW, Saraiva, VS and Burnier, MN, Jr. (2004) Pathological and prognostic features of uveal melanomas. Can J Ophthalmol 39:343-50.

McLean, MJ, Foster, WD and Zimmerman, LE (1977) Prognostic factors in small malignant melanomas of choroid and ciliary body. Arch Ophthalmol 95:48-58.

Meier, F, Schittek, B, Busch, S, Garbe, C, Smalley, K, Satyamoorthy, K, Li, G and Herlyn, M (2005) The RAS/RAF/MEK/ERK and PI3K/AKT signaling pathways present molecular targets for the effective treatment of advanced melanoma. Front Biosci 10:2986-3001.

Melnikova, VO and Bar-Eli, M (2006) Bioimmunotherapy for melanoma using fully human antibodies targeting MCAM/MUC18 and IL-8. Pigment Cell Res 19:395-405.

Mino, N, Takenaka, K, Sonobe, M, Miyahara, R, Yanagihara, K, Otake, Y, Wada, H and Tanaka, F (2007) Expression of tissue inhibitor of metalloproteinase-3 (TIMP-3) and its prognostic significance in resected non-small cell lung cancer. J Surg Oncol 95:250-7.

Mintz-Weber, CS and Johnson, JP (2000) Identification of the elements regulating the expression of the cell adhesion molecule MCAM/MUC18. Loss of AP-2 is not required for MCAM expression in melanoma cell lines. J Biol Chem 275:34672-80.

Missotten, GS, Notting, IC, Schlingemann, RO, Zijlmans, HJ, Lau, C, Eilers, PH, Keunen, JE and Jager, MJ (2006) Vascular endothelial growth factor a in eyes with uveal melanoma. Arch Ophthalmol 124:1428-34.

Mitchell, DL, Jen, J and Cleaver, JE (1991) Relative induction of cyclobutane dimers and cytosine photohydrates in DNA irradiated in vitro and in vivo with ultraviolet-C and ultraviolet-B light. Photochem Photobiol 54:741-6.

Miyake, H, Hara, I, Gohji, K, Yamanaka, K, Hara, S, Arakawa, S, Nakajima, M and Kamidono, S (1999) Relative expression of matrix metalloproteinase-2 and tissue inhibitor of metalloproteinase-2 in mouse renal cell carcinoma cells regulates their metastatic potential. Clin Cancer Res 5:2824-9.

Mosmann, T (1983) Rapid colorimetric assay for cellular growth and survival: application to proliferation and cytotoxicity assays. J Immunol Methods 65:55-63.

Mueller, AJ, Bartsch, DU, Folberg, R, Mehaffey, MG, Boldt, HC, Meyer, M, Gardner, LM, Goldbaum, MH, Pe'er, J and Freeman, WR (1998) Imaging the microvasculature of choroidal melanomas with confocal indocyanine green scanning laser ophthalmoscopy. Arch Ophthalmol 116:31-9.

Murphy, AN, Unsworth, EJ and Stetler-Stevenson, WG (1993) Tissue inhibitor of metalloproteinases-2 inhibits bFGF-induced human microvascular endothelial cell proliferation. J Cell Physiol 157:351-8.

Murray, GI, Duncan, ME, O'Neil, P, McKay, JA, Melvin, WT and Fothergill, JE (1998) Matrix metalloproteinase-1 is associated with poor prognosis in oesophageal cancer. J Pathol 185:256-61.

Murray, GI, Duncan, ME, O'Neil, P, Melvin, WT and Fothergill, JE (1996) Matrix metalloproteinase-1 is associated with poor prognosis in colorectal cancer. Nature Medicine 2:461-2.

Mylona, E, Magkou, C, Giannopoulou, I, Agrogiannis, G, Markaki, S, Keramopoulos, A and Nakopoulou, L (2006) Expression of tissue inhibitor of matrix metalloproteinases (TIMP)-3 protein in invasive breast carcinoma: relation to tumor phenotype and clinical outcome. Breast Cancer Res 8:R57.

Nagase, H and Frederick Woessner, J, J. (1999) Matrix metalloproteinases. J Biol Chem 274:21491-21494.

Nagase, H, Visse, R and Murphy, G (2006) Structure and function of matrix metalloproteinases and TIMPs. Cardiovasc Res 69:562-73.

Nareyeck, G, Zeschnigk, M, von der Haar, D, Schilling, H, Bornfeld, N and Anastassiou, G (2005) Differential expression of tissue inhibitor of matrix metalloproteinases 3 in uveal melanoma. Ophthalmic Res 37:23-8.

Naumann, G, Yanoff, M and Zimmerman, LE (1966) Histogenesis of malignant melanomas of the uvea. I. Histopathologic characteristics of nevi of the choroid and ciliary body. Arch Ophthalmol 76:784-96.

Neidhart, M, Wehrli, R, Bruhlmann, P, Michel, BA, Gay, RE and Gay, S (1999) Synovial fluid CD146 (MUC18), a marker for synovial membrane angiogenesis in rheumatoid arthritis. Arthritis Rheum 42:622-30.

Newman, E and Reichenbach, A (1996) The Muller cell: a functional element of the retina. Trends Neurosci 19:307-12.

Nguyen, M, Arkell, J and Jackson, CJ (2000) Activated protein C directly activates human endothelial gelatinase A. J Biol Chem 275:9095-8.

Nguyen, M, Arkell, J and Jackson, CJ (2001) Human endothelial gelatinases and angiogenesis. International J Biochem Cell Biol 33:960-70.

Nikkola, J, Vihinen, P, Vlaykova, T, Hahka-Kemppinen, M, Kahari, VM and Pyrhonen, S (2001) High collagenase-1 expression correlates with a favourable chemoimmunotherapy response in human metastatic melanoma. Melanoma Res 11:157-66.

Nordlund, JJ (1989) The lives of pigment cells. Clin Geriatr Med 5:91-108.

Notting, IC, Missotten, GS, Sijmons, B, Boonman, ZF, Keunen, JE and van der Pluijm, G (2006) Angiogenic profile of uveal melanoma. Curr Eye Res 31:775-85.

O'Neill, PA, Butt, M, Eswar, CV, Gillis, P and Marshall, E (2006) A prospective single arm phase II study of dacarbazine and treosulfan as first-line therapy in metastatic uveal melanoma. Melanoma Res 16:245-8.

Oh, J, Takahashi, R, Kondo, S, Mizoguchi, A, Adachi, E, Sasahara, RM, Nishimura, S, Imamura, Y, Kitayama, H, Alexander, DB, Ide, C, Horan, TP, Arakawa, T, Yoshida, H, Nishikawa, S, Itoh, Y, Seiki, M, Itohara, S, Takahashi, C and Noda, M (2001) The membrane-anchored MMP inhibitor RECK is a key regulator of extracellular matrix integrity and angiogenesis. Cell 107:789-800.

Onken, MD, Lin, AY, Worley, LA, Folberg, R and Harbour, JW (2005) Association between microarray gene expression signature and extravascular matrix patterns in primary uveal melanomas. Am J Ophthalmol 140:748-9.

Onken, MD, Worley, LA, Ehlers, JP and Harbour, JW (2004) Gene expression profiling in uveal melanoma reveals two molecular classes and predicts metastatic death. Cancer Res 64:7205-9.

Onoue, S, Kobayashi, T, Takemoto, Y, Sasaki, I and Shinkai, H (2003) Induction of matrix metalloproteinase-9 secretion from human keratinocytes in culture by ultraviolet B irradiation. J Dermatol Sci 33:105-11.

Ooto, S, Akagi, T, Kageyama, R, Akita, J, Mandai, M, Honda, Y and Takahashi, M (2004) Potential for neural regeneration after neurotoxic injury in the adult mammalian retina. Proc Natl Acad Sci U S A 101:13654-9.

Ozerdem, U, Mach-Hofacre, B, Varki, N, Folberg, R, Mueller, AJ, Ochabski, R, Pham, T, Appelt, K and Freeman, WR (2002) The effect of prinomastat (AG3340), a synthetic inhibitor of matrix metalloproteinases, on uveal melanoma rabbit model. Curr Eye Res 24:86-91.

Pacifico, MD, Grover, R, Richman, PI, Daley, FM, Buffa, F and Wilson, GD (2005) Development of a tissue array for primary melanoma with long-term follow-up: discovering melanoma cell adhesion molecule as an important prognostic marker. Plast Reconstr Surg 115:367-75.

Pane, AR and Hirst, LW (2000) Ultraviolet light exposure as a risk factor for ocular melanoma in Queensland, Australia. Ophthalmic Epidemiol 7:159-67.

Pap, T, Shigeyama, Y, Kuchen, S, Fernihough, JK, Simmen, B, Gay, RE, Billingham, M and Gay, S (2000) Differential expression pattern of membrane-type matrix metalloproteinases in rheumatoid arthritis. Arthritis & Rheumatism 43:1226-32.

Papp, AM, Nyilas, R, Szepesi, Z, Lorincz, ML, Takacs, E, Abraham, I, Szilagyi, N, Toth, J, Medveczky, P, Szilagyi, L, Juhasz, G and Juhasz, G (2007) Visible light induces matrix metalloproteinase-9 expression in rat eye. J Neurochem 103:2224-33.

Pardo, M, Garcia, A, Thomas, B, Pineiro, A, Akoulitchev, A, Dwek, RA and Zitzmann, N (2005) Proteome analysis of a human uveal melanoma primary cell culture by 2-DE and MS. Proteomics 5:4980-93.

Pardo, M, Garcia, A, Thomas, B, Pineiro, A, Akoulitchev, A, Dwek, RA and Zitzmann, N (2006) The characterization of the invasion phenotype of uveal melanoma tumour cells shows the presence of MUC18 and HMG-1 metastasis markers and leads to the identification of DJ-1 as a potential serum biomarker. Int J Cancer 119:1014-22.

Pavloff, N, Staskus, PW, Kishnani, NS and Hawkes, SP (1992) A new inhibitor of metalloproteinases from chicken: ChIMP-3. A third member of the TIMP family. J Biol Chem 267:17321-6.

Pei, D (1999) Identification and characterization of the fifth membrane-type matrix metalloproteinase MT5-MMP. J Biol Chem 274:8925-32.

Pei, D (1999) Leukolysin/MMP25/MT6-MMP: a novel matrix metalloproteinase specifically expressed in the leukocyte lineage. Cell Res 9:291-303.

Pendas, AM, Knauper, V, Puente, XS, Llano, E, Mattei, MG, Apte, S, Murphy, G and Lopez-Otin, C (1997) Identification and characterization of a novel human matrix metalloproteinase with unique structural characteristics, chromosomal location, and tissue distribution. J Biol Chem 272:4281-6.

Pepper, MS, Montesano, R, Mandriota, SJ, Orci, L and Vassalli, JD (1996) Angiogenesis: a paradigm for balanced extracellular proteolysis during cell migration and morphogenesis. Enzyme Protein 49:138-62.

Peters, S, Voelter, V, Zografos, L, Pampallona, S, Popescu, R, Gillet, M, Bosshard, W, Fiorentini, G, Lotem, M, Weitzen, R, Keilholz, U, Humblet, Y, Piperno-Neumann, S, Stupp, R and Leyvraz, S (2006) Intra-arterial hepatic fotemustine for the treatment of liver metastases from uveal melanoma: experience in 101 patients. Ann Oncol 17:578-83.

Peyman, GA, Raichand, M and Zeimer, RC (1984) Ocular effects of various laser wavelengths. Surv Ophthalmol 28:391-404.

Pfohler, C, Cree, IA, Ugurel, S, Kuwert, C, Haass, N, Neuber, K, Hengge, U, Corrie, PG, Zutt, M, Tilgen, W and Reinhold, U (2003) Treosulfan and gemcitabine in metastatic uveal melanoma patients: results of a multicenter feasibility study. Anticancer Drugs 14:337-40.

Pickl, WF, Majdic, O, Fischer, GF, Petzelbauer, P, Fae, I, Waclavicek, M, Stockl, J, Scheinecker, C, Vidicki, T, Aschauer, H, Johnson, JP and Knapp, W (1997) MUC18/MCAM (CD146), an activation antigen of human T lymphocytes. J Immunol 158:2107-15.

Prescher, G, Bornfeld, N and Becher, R (1990) Nonrandom chromosomal abnormalities in primary uveal melanoma. J Natl Cancer Inst 82:1765-9.

Prescher, G, Bornfeld, N, Friedrichs, W, Seeber, S and Becher, R (1995) Cytogenetics of twelve cases of uveal melanoma and patterns of nonrandom anomalies and isochromosome formation. Cancer Genet Cytogenet 80:40-6.

Prescher, G, Bornfeld, N, Hirche, H, Horsthemke, B, Jockel, KH and Becher, R (1996) Prognostic implications of monosomy 3 in uveal melanoma. Lancet 347:1222-5.

Puusaari, I, Damato, B and Kivela, T (2007) Transscleral local resection versus iodine brachytherapy for uveal melanomas that are large because of tumour height. Graefes Arch Clin Exp Ophthalmol 245:522-33.

Qi, JH, Ebrahem, Q, Moore, N, Murphy, G, Claesson-Welsh, L, Bond, M, Baker, A and Anand-Apte, B (2003) A novel function for tissue inhibitor of metalloproteinases-3 (TIMP3): inhibition of angiogenesis by blockage of VEGF binding to VEGF receptor-2. Nat Med 9:407-15.

Raffetto, JD and Khalil, RA (2008) Matrix metalloproteinases and their inhibitors in vascular remodeling and vascular disease. Biochem Pharmacol 75:346-59.

Ramos, MC, Steinbrenner, H, Stuhlmann, D, Sies, H and Brenneisen, P (2004) Induction of MMP-10 and MMP-1 in a squamous cell carcinoma cell line by ultraviolet radiation. Biol Chem 385:75-86.

Rao, RA, Stoleru, MA, Laver, NV and McLean, IW (2004) Matrix metalloproteinases in uveal malignant melanoma: computer-based morphometric analysis (E abstract) Invest Ophthalmol Vis Sci 45, 1198.

Reichenbach, A, Wurm, A, Pannicke, T, Iandiev, I, Wiedemann, P and Bringmann, A (2007) Muller cells as players in retinal degeneration and edema. Graefes Arch Clin Exp Ophthalmol 245:627-36.

Rietschel, P, Panageas, KS, Hanlon, C, Patel, A, Abramson, DH and Chapman, PB (2005) Variates of survival in metastatic uveal melanoma. J Clin Oncol 23:8076-80.

Rittie, L and Fisher, GJ (2002) UV-light-induced signal cascades and skin aging. Ageing Res Rev 1:705-20.

Ruiz, M, Troncoso, P, Bruns, C and Bar-Eli, M (2001) Activator protein 2alpha transcription factor expression is associated with luminal differentiation and is lost in prostate cancer. Clin Cancer Res 7:4086-95.

Rummel, MM, Sers, C and Johnson, JP (1996) Phorbol ester and cyclic AMP-mediated regulation of the melanoma-associated cell adhesion molecule MUC18/MCAM. Cancer Res 56:2218-23.

Rummelt, V, Mehaffey, MG, Campbell, RJ, Pe'er, J, Bentler, SE, Woolson, RF, Naumann, GO and Folberg, R (1998) Microcirculation architecture of metastases from primary ciliary body and choroidal melanomas. Am J Ophthalmol 126:303-5.

Saarialho-Kere, UK, Crouch, EC and Parks, WC (1995) Matrix metalloproteinase matrilysin is constitutively expressed in adult human exocrine epithelium. J Invest Dermatol 105:190-6.

Sachdev, NH, Di Girolamo, N, Nolan, TM, McCluskey, PJ, Wakefield, D and Coroneo, MT (2004) Matrix metalloproteinases and tissue inhibitors of matrix metalloproteinases in the human lens: implications for cortical cataract formation. Invest Ophthalmol Vis Sci 45:4075-82.

Sahin, A, Kiratli, H, Tezel, GG, Soylemezoglu, F and Bilgic, S (2007) Expression of vascular endothelial growth factor a, matrix metalloproteinase 9 and extravascular matrix patterns in iris and ciliary body melanomas. Ophthalmic Res 39:40-4.

Salzmann, J, Limb, GA, Khaw, PT, Gregor, ZJ, Webster, L, Chignell, AH and Charteris, DG (2000) Matrix metalloproteinases and their natural inhibitors in fibrovascular membranes of proliferative diabetic retinopathy. Br J Ophthalmol 84:1091-6.

Sandinha, MT, Farquharson, MA and Roberts, F (2004) Identification of monosomy 3 in choroidal melanoma by chromosome in situ hybridisation. Br J Ophthalmol 88:1527-32.

Sato, H, Takino, T, Okada, Y, Cao, J, Shinagawa, A, Yamamoto, E and Seiki, M (1994) A matrix metalloproteinase expressed on the surface of invasive tumour cells. Nature 370:61-5.

Sato, T, Terai, M and Huandong, Y (2002) Systemic immune response after immunoembolization of liver metastasis with granulocyte-macrophage colony stimulating factor (GM-CSF) (abstract). Proc Am Assoc Cancer Res 43.

Satyamoorthy, K, Muyrers, J, Meier, F, Patel, D and Herlyn, M (2001) Mel-CAM-specific genetic suppressor elements inhibit melanoma growth and invasion through loss of gap junctional communication. Oncogene 20:4676-84.

Saunders, WB, Bohnsack, BL, Faske, JB, Anthis, NJ, Bayless, KJ, Hirschi, KK and Davis, GE (2006) Coregulation of vascular tube stabilization by endothelial cell TIMP-2 and pericyte TIMP-3. J Cell Biol 175:179-91.

Schmittel, A, Scheulen, ME, Bechrakis, NE, Strumberg, D, Baumgart, J, Bornfeld, N, Foerster, MH, Thiel, E and Keilholz, U (2005) Phase II trial of cisplatin, gemcitabine and treosulfan in patients with metastatic uveal melanoma. Melanoma Res 15:205-7.

Scholes, AG, Damato, BE, Nunn, J, Hiscott, P, Grierson, I and Field, JK (2003) Monosomy 3 in uveal melanoma: correlation with clinical and histologic predictors of survival. Invest Ophthalmol Vis Sci 44:1008-11.

Schwartz, LH, Ferrand, R, Boelle, PY, Maylin, C, D'Hermies, F and Virmont, J (1997) Lack of correlation between the location of choroidal melanoma and ultraviolet-radiation dose distribution. Radiat Res 147:451-6.

Seddon, J, Egan, K and Gragoudas, E (1994) Epidemiology of Uveal Melanoma. Retina 1:717-23.

Seddon, JM, Gragoudas, ES, Glynn, RJ, Egan, KM, Albert, DM and Blitzer, PH (1990) Host factors, UV radiation, and risk of uveal melanoma. A case-control study. Arch Ophthalmol 108:1274-80.

Seftalioglu, A and Karakoc, L (2000) Expression of CD146 adhesion molecules (MUC18 or MCAM) in the thymic microenvironment. Acta Histochem 102:69-83.

Seftor, EA, Meltzer, PS, Kirschmann, DA, Margaryan, NV, Seftor, RE and Hendrix, MJ (2006) The epigenetic reprogramming of poorly aggressive melanoma cells by a metastatic microenvironment. J Cell Mol Med 10:174-96.

Seftor, EA, Meltzer, PS, Kirschmann, DA, Pe'er, J, Maniotis, AJ, Trent, JM, Folberg, R and Hendrix, MJ (2002) Molecular determinants of human uveal melanoma invasion and metastasis. Clin Exp Metastasis 19:233-46.

Seftor, RE, Seftor, EA and Hendrix, MJ (1999) Molecular role(s) for integrins in human melanoma invasion. Cancer & Metastasis Reviews 18:359-75.

Seftor, RE, Seftor, EA, Koshikawa, N, Meltzer, PS, Gardner, LM, Bilban, M, Stetler-Stevenson, WG, Quaranta, V and Hendrix, MJ (2001) Cooperative interactions of laminin 5 gamma2 chain, matrix metalloproteinase-2, and membrane type-1-matrix/metalloproteinase are required for mimicry of embryonic vasculogenesis by aggressive melanoma. Cancer Res 61:6322-7.

Sekine-Aizawa, Y, Hama, E, Watanabe, K, Tsubuki, S, Kanai-Azuma, M, Kanai, Y, Arai, H, Aizawa, H, Iwata, N and Saido, TC (2001) Matrix metalloproteinase (MMP) system in brain: identification and characterization of brain-specific MMP highly expressed in cerebellum. European Journal of Neuroscience 13:935-48.

Sers, C, Riethmuller, G and Johnson, JP (1994) MUC18, a melanoma-progression associated molecule, and its potential role in tumor vascularization and hematogenous spread. Cancer Res 54:5689-94.

Shah, CP, Weis, E, Lajous, M, Shields, JA and Shields, CL (2005) Intermittent and chronic ultraviolet light exposure and uveal melanoma: a meta-analysis. Ophthalmology 112:1599-607.

Shellman, YG, Makela, M and Norris, DA (2006) Induction of secreted matrix metalloproteinase-9 activity in human melanoma cells by extracellular matrix proteins and cytokines. Melanoma Res 16:207-11.

Sheu, BC, Lien, HC, Ho, HN, Lin, HH, Chow, SN, Huang, SC and Hsu, SM (2003) Increased expression and activation of gelatinolytic matrix metalloproteinases is associated with the progression and recurrence of human cervical cancer. Cancer Res 63:6537-42.

Shields, CL, Shields, JA, Materin, M, Gershenbaum, E, Singh, AD and Smith, A (2001) Iris melanoma: risk factors for metastasis in 169 consecutive patients. Ophthalmology 108:172-8.

Shields, JA and Shields, CL (1999) Atlas of intraocular tumors. Lippincott Williams & Wilkins, Philadelphia.

Shields, JA, Shields, CL and Donoso, LA (1991) Management of posterior uveal melanoma. Surv Ophthalmol 36:161-95.

Shih, IM (1999) The role of CD146 (Mel-CAM) in biology and pathology. J Pathol 189:4-11.

Shih, IM, Elder, DE, Hsu, MY and Herlyn, M (1994) Regulation of Mel-CAM/MUC18 expression on melanocytes of different stages of tumor progression by normal keratinocytes. Am J Pathol 145:837-45.

Shih, IM, Elder, DE, Speicher, D, Johnson, JP and Herlyn, M (1994) Isolation and functional characterization of the A32 melanoma-associated antigen. Cancer Res 54:2514-20.

Shih, IM, Nesbit, M, Herlyn, M and Kurman, RJ (1998) A new Mel-CAM (CD146)-specific monoclonal antibody, MN-4, on paraffin-embedded tissue. Mod Pathol 11:1098-106.

Shih, IM, Speicher, D, Hsu, MY, Levine, E and Herlyn, M (1997) Melanoma cell-cell interactions are mediated through heterophilic Mel-CAM/ligand adhesion. Cancer Res 57:3835-40.

Shih, LM, Hsu, MY, Palazzo, JP and Herlyn, M (1997) The cell-cell adhesion receptor Mel-CAM acts as a tumor suppressor in breast carcinoma. Am J Pathol 151:745-51.

Singh, AD, Boghosian-Sell, L, Wary, KK, Shields, CL, De Potter, P, Donoso, LA, Shields, JA and Cannizzaro, LA (1994) Cytogenetic findings in primary uveal melanoma. Cancer Genet Cytogenet 72:109-15.

Singh, AD, Shields, CL and Shields, JA (2001) Prognostic factors in uveal melanoma. Melanoma Res 11:255-63.

Singh, AD, Sisley, K, Xu, Y, Li, J, Faber, P, Plummer, SJ, Mudhar, HS, Rennie, IG, Kessler, PM, Casey, G and Williams, BG (2007) Reduced Expression of Autotaxin Predicts Survival in Uveal Melanoma. Br J Ophthalmol doi:10.1136/bjo.2007.116947:

Sisley, K, Cottam, DW, Rennie, IG, Parsons, MA, Potter, AM, Potter, CW and Rees, RC (1992) Non-random abnormalities of chromosomes 3, 6, and 8 associated with posterior uveal melanoma. Genes Chromosomes Cancer 5:197-200.

Sisley, K, Rennie, IG, Cottam, DW, Potter, AM, Potter, CW and Rees, RC (1990) Cytogenetic findings in six posterior uveal melanomas: involvement of chromosomes 3, 6, and 8. Genes Chromosomes Cancer 2:205-9.

Sisley, K, Rennie, IG, Parsons, MA, Jacques, R, Hammond, DW, Bell, SM, Potter, AM and Rees, RC (1997) Abnormalities of chromosomes 3 and 8 in posterior uveal melanoma correlate with prognosis. Genes Chromosomes Cancer 19:22-8.

Sivak, JM and Fini, ME (2002) MMPs in the eye: emerging roles for matrix metalloproteinases in ocular physiology. Prog Retin Eye Res 21:1-14.

Sliney, DH (2002) How light reaches the eye and its components. Int J Toxicol 21:501-9.

Smith, MR, Kung, H, Durum, SK, Colburn, NH and Sun, Y (1997) TIMP-3 induces cell death by stabilizing TNF-alpha receptors on the surface of human colon carcinoma cells. Cytokine 9:770-80.

Solovey, AN, Gui, L, Chang, L, Enenstein, J, Browne, PV and Hebbel, RP (2001) Identification and functional assessment of endothelial P1H12. J Lab Clin Med 138:322-31.

Soulen, MC (1994) Chemoembolization of hepatic malignancies. Oncology (Williston Park) 8:77-84.

Spurbeck, WW, Ng, CY, Vanin, EF and Davidoff, AM (2003) Retroviral vector-producer cell-mediated in vivo gene transfer of TIMP-3 restricts angiogenesis and neuroblastoma growth in mice. Cancer Gene Ther 10:161-7.

St Croix, B, Rago, C, Velculescu, V, Traverso, G, Romans, KE, Montgomery, E, Lal, A, Riggins, GJ, Lengauer, C, Vogelstein, B and Kinzler, KW (2000) Genes expressed in human tumor endothelium. Science 289:1197-202.

Stamenkovic, I (2000) Matrix metalloproteinases in tumor invasion and metastasis. Seminars in Cancer Biol 10:415-33.

Stracke, JO, Fosang, AJ, Last, K, Mercuri, FA, Pendas, AM, Llano, E, Perris, R, Di Cesare, PE, Murphy, G and Knauper, V (2000) Matrix metalloproteinases 19 and 20 cleave aggrecan and cartilage oligomeric matrix protein (COMP). FEBS Lett 478:52-6.

Sun, J and Hemler, ME (2001) Regulation of MMP-1 and MMP-2 production through CD147/extracellular matrix metalloproteinase inducer interactions. Cancer Res 61:2276-81.

Suomela, S, Kariniemi, AL, Impola, U, Karvonen, SL, Snellman, E, Uurasmaa, T, Peltonen, J and Saarialho-Kere, U (2003) Matrix metalloproteinase-19 is expressed by keratinocytes in psoriasis. Acta Derm Venereol 83:108-14.

Tang, A, Eller, MS, Hara, M, Yaar, M, Hirohashi, S and Gilchrest, BA (1994) E-cadherin is the major mediator of human melanocyte adhesion to keratinocytes in vitro. J Cell Sci 107 (Pt 4):983-92.

Tellez, C and Bar-Eli, M (2003) Role and regulation of the thrombin receptor (PAR-1) in human melanoma. Oncogene 22:3130-7.

Tschentscher, F, Husing, J, Holter, T, Kruse, E, Dresen, IG, Jockel, KH, Anastassiou, G, Schilling, H, Bornfeld, N, Horsthemke, B, Lohmann, DR and Zeschnigk, M (2003) Tumor classification based on gene expression profiling shows that uveal melanomas with and without monosomy 3 represent two distinct entities. Cancer Res 63:2578-84.

Tschentscher, F, Prescher, G, Horsman, DE, White, VA, Rieder, H, Anastassiou, G, Schilling, H, Bornfeld, N, Bartz-Schmidt, KU, Horsthemke, B, Lohmann, DR and Zeschnigk, M (2001) Partial deletions of the long and short arm of chromosome 3 point to two tumor suppressor genes in uveal melanoma. Cancer Res 61:3439-42.

Tschentscher, F, Prescher, G, Zeschnigk, M, Horsthemke, B and Lohmann, DR (2000) Identification of chromosomes 3, 6, and 8 aberrations in uveal melanoma by microsatellite analysis in comparison to comparative genomic hybridization. Cancer Genet Cytogenet 122:13-7.

Tucker, MA, Shields, JA, Hartge, P, Augsburger, J, Hoover, RN and Fraumeni, JF, Jr. (1985) Sunlight exposure as risk factor for intraocular malignant melanoma. N Engl J Med 313:789-92.

Vaisanen, A, Kallioinen, M, von Dickhoff, K, Laatikainen, L, Hoyhtya, M and Turpeenniemi-Hujanen, T (1999) Matrix metalloproteinase-2 (MMP-2) immunoreactive protein--a new prognostic marker in uveal melanoma? J Pathol 188:56-62.

Vajdic, CM, Kricker, A, Giblin, M, McKenzie, J, Aitken, J, Giles, GG and Armstrong, BK (2001) Eye color and cutaneous nevi predict risk of ocular melanoma in Australia. Int J Cancer 92:906-12.

Vajdic, CM, Kricker, A, Giblin, M, McKenzie, J, Aitken, J, Giles, GG and Armstrong, BK (2002) Sun exposure predicts risk of ocular melanoma in Australia. Int J Cancer 101:175-82.

Vajdic, CM, Kricker, A, Giblin, M, McKenzie, J, Aitken, J, Giles, GG and Armstrong, BK (2003) Incidence of ocular melanoma in Australia from 1990 to 1998. Int J Cancer. 105:117-22.

Vajdic, CM, Kricker, A, Giblin, M, McKenzie, J, Aitken, JF, Giles, GG and Armstrong, BK (2004) Artificial ultraviolet radiation and ocular melanoma in Australia. Int J Cancer 112:896-900.

van der Velden, PA, Zuidervaart, W, Hurks, MH, Pavey, S, Ksander, BR, Krijgsman, E, Frants, RR, Tensen, CP, Willemze, R, Jager, MJ and Gruis, NA (2003) Expression profiling reveals that methylation of TIMP3 is involved in uveal melanoma development. Int J Cancer 106:472-9.

van Duinen, SG, Ruiter, DJ, Broecker, EB, van der Velde, EA, Sorg, C, Welvaart, K and Ferrone, S (1988) Level of HLA antigens in locoregional metastases and clinical course of the disease in patients with melanoma. Cancer Res 48:1019-25.

Velasco, G, Cal, S, Merlos-Suarez, A, Ferrando, AA, Alvarez, S, Nakano, A, Arribas, J and Lopez-Otin, C (2000) Human MT6-matrix metalloproteinase: identification, progelatinase A activation, and expression in brain tumors. Cancer Res 60:877-82.

Visse, R and Nagase, H (2003) Matrix metalloproteinases and tissue inhibitors of metalloproteinases: structure, function, and biochemistry. Circ Res 92:827-39.

Vogl, T, Eichler, K, Zangos, S, Herzog, C, Hammerstingl, R, Balzer, J and Gholami, A (2006) Preliminary experience with transarterial chemoembolization (TACE) in liver metastases of uveal malignant melanoma: local tumor control and survival. J Cancer Res Clin Oncol 133: 177-84.

Vogl, TJ, Muller, PK, Mack, MG, Straub, R, Engelmann, K and Neuhaus, P (1999) Liver metastases: interventional therapeutic techniques and results, state of the art. Eur Radiol 9:675-84.

Vranka, JA, Johnson, E, Zhu, X, Shepardson, A, Alexander, JP, Bradley, JM, Wirtz, MK, Weleber, RG, Klein, ML and Acott, TS (1997) Discrete expression and distribution pattern of TIMP-3 in the human retina and choroid. Curr Eye Res 16:102-10.

Waas, ET, Lomme, RM, DeGroot, J, Wobbes, T and Hendriks, T (2002) Tissue levels of active matrix metalloproteinase-2 and -9 in colorectal cancer. Br J Cancer 86:1876-83.

Wang, S, Coleman, EJ, Pop, LM, Brooks, KJ, Vitetta, ES and Niederkorn, JY (2006) Effect of an anti-CD54 (ICAM-1) monoclonal antibody (UV3) on the growth of human uveal melanoma cells transplanted heterotopically and orthotopically in SCID mice. Int J Cancer 118:932-41.

Ward, RV, Atkinson, SJ, Slocombe, PM, Docherty, AJ, Reynolds, JJ and Murphy, G (1991) Tissue inhibitor of metalloproteinases-2 inhibits the activation of 72 kDa progelatinase by fibroblast membranes. Biochimica et Biophysica Acta 1079:242-6.

Watson-Hurst, K and Becker, D (2006) The role of N-cadherin, MCAM and beta3 integrin in melanoma progression, proliferation, migration and invasion. Cancer Biol Ther 5:1375-82.

Weber, BH, Vogt, G, Pruett, RC, Stohr, H and Felbor, U (1994) Mutations in the tissue inhibitor of metalloproteinases-3 (TIMP3) in patients with Sorsby's fundus dystrophy. Nat Genet 8:352-6.

Webster, L, Chignell, AH and Limb, GA (1999) Predominance of MMP-1 and MMP-2 in epiretinal and subretinal membranes of proliferative vitreoretinopathy. Exp Eye Res 68:91-8.

Wenczl, E, Van der Schans, GP, Roza, L, Kolb, RM, Timmerman, AJ, Smit, NP, Pavel, S and Schothorst, AA (1998) (Pheo)melanin photosensitizes UVA-induced DNA damage in cultured human melanocytes. J Invest Dermatol 111:678-82.

West, SK, Duncan, DD, Munoz, B, Rubin, GS, Fried, LP, Bandeen-Roche, K and Schein, OD (1998) Sunlight exposure and risk of lens opacities in a population-based study: the Salisbury Eye Evaluation project. 280:714-8.

Whelchel, JC, Farah, SE, McLean, IW and Burnier, MN (1993) Immunohistochemistry of infiltrating lymphocytes in uveal malignant melanoma. Invest Ophthalmol Vis Sci 34:2603-6.

White, VA, Chambers, JD, Courtright, PD, Chang, WY and Horsman, DE (1998) Correlation of cytogenetic abnormalities with the outcome of patients with uveal melanoma. Cancer 83:354-9.

Williamson, RA, Marston, FA, Angal, S, Koklitis, P, Panico, M, Morris, HR, Carne, AF, Smith, BJ, Harris, TJ and Freedman, RB (1990) Disulphide bond assignment in human tissue inhibitor of metalloproteinases (TIMP). Biochem J 268:267-74.

Wiltshire, RN, Elner, VM, Dennis, T, Vine, AK and Trent, JM (1993) Cytogenetic analysis of posterior uveal melanoma. Cancer Genet Cytogenet 66:47-53.

Wlaschek, M, Heinen, G, Poswig, A, Schwarz, A, Krieg, T and Scharffetter-Kochanek, K (1994) UVA-induced autocrine stimulation of fibroblast-derived collagenase/MMP-1 by interrelated loops of interleukin-1 and interleukin-6. Photochem Photobiol 59:550-6.

Woll, E, Bedikian, A and Legha, SS (1999) Uveal melanoma: natural history and treatment options for metastatic disease. Melanoma Res 9:575-81.

Woodward, JK, Rennie, IG, Elshaw, SR, Burn, JL and Sisley, K (2005) Invasive and noninvasive uveal melanomas have different adhesive properties. Eye 19:342-8.

Wu, CS, Yu, CL, Lan, CC and Yu, HS (2004) Narrow-band ultraviolet-B stimulates proliferation and migration of cultured melanocytes. Exp Dermatol 13:755-63.

Wu, GJ, Varma, VA, Wu, MW, Wang, SW, Qu, P, Yang, H, Petros, JA, Lim, SD and Amin, MB (2001) Expression of a human cell adhesion molecule, MUC18, in prostate cancer cell lines and tissues. Prostate 48:305-15.

Wu, GJ, Wu, MW, Wang, SW, Liu, Z, Qu, P, Peng, Q, Yang, H, Varma, VA, Sun, QC, Petros, JA, Lim, SD and Amin, MB (2001) Isolation and characterization of the major form of human MUC18 cDNA gene and correlation of MUC18 over-expression in prostate cancer cell lines and tissues with malignant progression. Gene 279:17-31.

Xie, S, Luca, M, Huang, S, Gutman, M, Reich, R, Johnson, JP and Bar-Eli, M (1997) Expression of MCAM/MUC18 by human melanoma cells leads to increased tumor growth and metastasis. Cancer Res 57:2295-303.

Xu, H, Sta Iglesia, DD, Kielczewski, JL, Valenta, DF, Pease, ME, Zack, DJ and Quigley, HA (2007) Characteristics of progenitor cells derived from adult ciliary body in mouse, rat, and human eyes. Invest Ophthalmol Vis Sci 48:1674-82.

Yan, X, Lin, Y, Yang, D, Shen, Y, Yuan, M, Zhang, Z, Li, P, Xia, H, Li, L, Luo, D, Liu, Q, Mann, K and Bader, BL (2003) A novel anti-CD146 monoclonal antibody, AA98, inhibits angiogenesis and tumor growth. Blood 102:184-91.

Yanoff, M and Zimmerman, LE (1967) Histogenesis of malignant melanomas of the uvea. II. Relationship of uveal nevi to malignant melanomas. Cancer 20:493-507.

Young, T, Burgess, BL, Rao, NP, Gorin, MB and Straatsma, BR (2007) High-density genome array is superior to fluorescence in-situ hybridization analysis of monosomy 3 in choroidal melanoma fine needle aspiration biopsy. Mol Vis 13:2328-2333.

Yu, AE, Hewitt, RE, Kleiner, DE and Stetler-Stevenson, WG (1996) Molecular regulation of cellular invasion--role of gelatinase A and TIMP-2. Biochem Cell Biol 74:823-31.

Yu, WH, Yu, S, Meng, Q, Brew, K and Woessner, JF, Jr. (2000) TIMP-3 binds to sulfated glycosaminoglycans of the extracellular matrix. J Biol Chem 275:31226-32.

Zhang, H (2005) Survivin protein in UVB induced apoptosis of melanoma cells and in melanoma progression. Oncol Rep 13:1121-6.

Zhang, H and Rosdahl, I (2003) Ultraviolet A and B differently induce intracellular protein expression in human skin melanocytes--a speculation of separate pathways in initiation of melanoma. Carcinogenesis 24:1929-34.

Zimmerman, LE and McLean, IW (1979) An evaluation of enucleation in the management of uveal melanomas. Am J Ophthalmol 87:741-60.